A Doctoral Thesis

Regulation of DNA replication origins by chromatin structures

Makoto Hayashi

Department of Biology

Graduate School of Science

Osaka University

November 2008

A Doctoral Thesis

Regulation of DNA replication origins by chromatin structures

Makoto Hayashi

Department of Biology

Graduate School of Science

Osaka University

November 2008

博士論文

Regulation of DNA replication origins by chromatin structures

（クロマチン構造による複製開始点の制御機構の解析）

林　眞理

大阪大学大学院理学研究科　生物科学専攻

２００８年１１月

Contents

ABSTRACT

DNA replication initiates at numbers of discrete loci, called replication origins, on the eukaryotic chromosomes. Distribution and regulation of origins are important for complete duplication of the genome. To elucidate control mechanisms of initiation of DNA replication, I determined location of proteins that binds to origins as well as actual DNA synthesis using the whole genome tiling-chip of fission yeast. Replication origins distribute throughout the chromosomes. However, only subset of origins is activated in early S phase. Early and late origins tend to distribute separately in large chromosome regions. Heterochromatin in the pericentromere and the silent mating-type (*mat*) locus replicates in early S phase. This seemed paradoxical because heterochromatin was proposed to be a structurally compacted region where initiation of replication is inactivated. Further analysis revealed that Swi6, a fission yeast homolog of heterochromatin protein 1 (HP1), is required for early replication specifically at the pericentromere and the *mat* locus. Loading of Sld3 to replication origin, which depends on Dfp1 (Dbf4)-dependent kinase (DDK), is stimulated by Swi6. An HP1-binding motif within Dfp1 is required for *in vitro* interaction with Swi6 and for early replication of the pericentromere and the *mat* locus. Tethering of Dfp1 to the pericentromere and the *mat* locus in swi6 deficient cells restores early replication of these loci. These results demonstrate the novel mechanism that a heterochromatin protein positively regulates initiation of replication by recruiting a regulatory kinase to replication origins in heterochromatic regions.

GENERAL INTRODUCTION

Cell cycle regulation of DNA replication

Accurate and complete DNA replication is crucial for the maintenance of the genetic integrity of all organisms. To ensure that a complete set of the eukaryotic genome is precisely duplicated during the limited period of S phase in every cell cycle, DNA replication initiates at a number of chromosomal elements called replication origins (Bell and Dutta, 2002; Gilbert, 2001a). The basic mechanism of initiation occurs in several steps and results in bidirectional replication from the origin (Sclafani and Holzen, 2007). (A) First, origin sequence is recognized by origin recognition complex (ORC), which is composed of six subunits Orc1-6. ORC binds to the origin throughout the cell cycle, although localization of its subunits is regulated in cell cycle-dependent manner in some organisms (Diffley, 2004). (B) Second, the ORC-bound origin is "licensed" by loading of mini-chromosome maintenance (MCM) complex composed of six subunits Mcm2-7 in G1 phase of the cell cycle, resulting in the formation of pre-replicative complex (pre-RC) (Bell and Dutta, 2002; Diffley et al., 1994). (C) Third, at the beginning of S phase, pre-RC is activated by recruitment of several factors dependent on two conserved kinases, cyclin-dependent kinase (CDK) and Dbf4-dependent kinase (DDK), and finally, the replisome including DNA polymerase and single-stranded DNA binding protein (SSB) (or replication protein A: RPA) are loaded onto the unwound origin DNA and bidirectional replication initiates.

A) Origin recognition by ORC

Although ORC is conserved among eukaryotes, the nucleotide sequences of replication origins are very diverse among organisms (Gilbert, 2001a), mainly due to differences in DNA binding properties of ORCs. In budding yeast, the ORC recognizes the specific sequences called the ARS consensus sequence (ACS). In contrast, no clear consensus sequence has been found in origins in fission yeast, *Schizosaccharomyces pombe* (Clyne and Kelly, 1995; Dubey et al., 1996; Okuno et al., 1999), although AT-rich sequences to which ORC preferentially binds are required (Chuang and Kelly, 1999). Requirements for specific sequences become less clear in multicellular organisms such as metazoans, and ORC exhibits

little sequence specificity in DNA binding *in vitro* (Remus et al., 2004; Vashee et al., 2003). In other words, it is difficult to predict the precise location of origins from cis-sequences and it is important to determine the locations of ORC binding for identification of origins.

B) Formation of pre-RC

Recruitment of MCM and resultant pre-RC formation depend on ORC, as well as two other factors, cdc10 target gene 1 (Cdt1) and cell division cycle 6 (Cdc6, in fission yeast Cdc18). The formation of pre-RC is strictly regulated to occur in late M and G1 phase of the cell cycle, when the CDK activity is relatively low. This mechanism ensures inhibition of the second-round pre-RC formation in the same cell cycle and consequent re-replication (Machida et al., 2005). Growing evidence strongly support a role for MCM as a replicative DNA helicase in replication fork (Labib and Diffley, 2001). Although pre-RC formation is essential for initiation of replication, it is not in itself sufficient.

C) Activation of pre-RC

Origin activation at the onset of S phase is regulated by two conserved protein kinases, CDK and DDK. These kinases are required for assembly of several other protein factors including Sld3, GINS and Cdc45 onto pre-RCs. The precise role of each factor in initiation of replication is not fully understood. However, appropriate sequential recruitment of these factors results in the activation of MCM helicase and origin DNA unwinding, and the replication machinery is established through assembly of RPA and DNA polymerases onto single-stranded DNA (Bell and Dutta, 2002).

Although both CDK and DDK are highly active after S phase entry, not all pre-RCs are activated at the onset of S phase simultaneously. It is well documented in budding yeast that activation of pre-RC occurs in temporal order, suggesting regulation of the initiation timing (Weinreich et al., 2004). When progression of DNA replication is impaired in the presence of inhibitory chemicals, initiation of replication from late origin, which normally fires in late S phase, is blocked by checkpoint kinases, Mec1, a homologue of ATR, and Rad53, a homologue of CHK2. (Santocanale and Diffley, 1998; Shirahige et al., 1998). The ATM/ATR-mediated checkpoint has been proposed to regulate origin initiation even in unperturbed metazoan cells (Shechter et al., 2004). However, even if the checkpoint pathway acts to suppress late and inefficient origins in normal S phase, the temporal order of

each origin firing is determined before the checkpoint regulation. The underlying molecular mechanism for such temporal regulation is largely unclear, although the involvement of chromatin structures is suggested.

Regulation of replication in chromatin context

As described above, the time at which replication origin initiates replication within S phase is a characteristic of each origin. In general, transcriptionally active euchromatin tends to replicate in early S phase, while silent heterochromatin replicates in late S phase. Recent genome-wide approaches agree with this notion, showing that chromosomal regions that are gene-rich, and rich in GC sequences replicate earlier, whereas gene-poor regions and heterochromatin tend to replicate late (MacAlpine and Bell, 2005). Since localization and activation of origins are regulated by several actions of replication factors on the chromosome, they must be affected by the surrounding chromatin structures. It is well accepted that the transcriptional activity is modulated by the chromatin structure around the promoter region. Using analogy of the transcriptional regulation, it has been proposed that chromatin structures surrounding origins regulate replication timing; replication factors have easier access to DNA in open chromatin (Gilbert, 2002). Histone acetylation is linked to opening chromatin for gene activation. Notably, mutation of the histone deacetylase (HDAC) Rpd3 induced genome-wide hyperacetylation and a redistribution of ORC2, a subunit of ORC, in *Drosophila* follicle cells (Aggarwal and Calvi, 2004), suggesting that ORC localization is determined by chromatin structure. The study in *Xenopus* extracts, however, suggested that histone acetylation specify the site of origin after ORC binding (Danis et al., 2004). In budding yeast, deletion of Rpd3 or its interacting partner Sin3 caused early activation of late origins at internal chromosomal loci but did not alter the initiation timing of early origins or a late-firing, telomere-proximal origin (Aparicio et al., 2004). These studies suggest that different steps in origin activation have potential to be targeted by chromatin structures and that there is distinct regulation in different chromosomal loci. Although growing evidences suggest that compact chromatin structure is suppressive to origin activation, not all regions of chromosomes follow this trend. There are early-replicating heterochromatin and highly transcribed but late-replicating regions (Hiratani et al., 2004; White et al., 2004), showing significant flexibility in regulation of replication timing. Therefore, it remains to be

unraveled experimentally how origins are regulated in different chromatin contexts. The especially interesting topics are the underlying molecular mechanism(s) of the regulation and the step(s) at which initiation is regulated by the specific chromatin structure.

Fission yeast as a model to study the link between DNA replication and chromatin

Replication factors are well conserved among species, but the cis-acting sequences of origin are diverse. As described, fission yeast ORC prefers AT-rich sequence, yet there is no consensus sequence, which is similar property with metazoan organisms. One of the advantages of using fission yeast to study replication is well-defined nature of initiation steps (Yabuuchi et al., 2006), providing the clues to dissect the molecular mechanism of regulation by chromatin. Completion of genomic sequencing of fission yeast predicted the presence of highly conserved chromo-domain proteins involved in formation of higher order chromatin structures (Wood et al., 2002). Consistent with this prediction, fission yeast has three major heterochromatic loci: pericentromere, the silent mating-type locus and subtelomeric region. Intensive molecular genetic analysis unlabeled the involvement of the higher conserved chromo-domain proteins in heterochromatin formation in fission yeast, which is absent from budding yeast but well conserved in higher eukaryotic species (Grewal and Jia, 2007). Furthermore, the structures of functional chromosomal loci, such as centromeres and telomeres, of fission yeast have similar properties with those of metazoans. These characteristics of fission yeast with powerful genetics provide a great advantage to study the molecular link between DNA replication and chromatin structures.

Aim of experiments

Although lots of efforts have been concentrated on the dissection of assemblies of replication factors at origins, the knowledge about the molecular mechanism of their regulation by chromatin structures is limited. To understand this issue, it is necessary to identify replication origins along different chromosomal regions.

In this thesis, I examined the distribution of pre-RC in G1 phase and their activity in S phase along whole fission yeast genome to identify replication origins. I further focused on the molecular mechanism underlying regulation of replication in heterochromatic loci. From the results, I propose a model for regulation of replication by a component of heterochromatin structure.

Part I: Genome-wide localization of pre-RC sites and identification of replication origins in fission yeast

INTRODUCTION

Since each chromosome region replicates in a specific period within S phase, timing of origin activation must be regulated. Although we have a growing understanding of protein factors involved in initiation and elongation of replication, the mechanisms of origin activation at the chromosome level have yet to be clarified in detail. Thus it is important to determine locations of all replication origins on chromosomes. However, only small numbers of replication origins have so far been identified in most organisms other than budding yeast *Saccharomyces cerevisiae* (MacAlpine and Bell, 2005).

Genome-wide analyses of replication kinetics and distribution of ORC and MCM proteins using DNA microarrays have been performed in budding yeast (Raghuraman et al., 2001; Wyrick et al., 2001). The majority of proposed ARS (pro-ARS) sites identified by ChIP-based analysis exhibit ARS activity, and the correlation with actual initiation sites has been demonstrated (Feng et al., 2006). On the other hand, replication timing analyses using microarrays with human, mouse and *Drosophila* chromosomes have suggested links between early replication timing and active transcription in large chromatin domains (MacAlpine and Bell, 2005). However, because of difficulties in genome-wide analysis of replication factor binding sites in metazoans, it has not been possible to clarify the relation between pre-RC sites and selection of active origins. Fission yeast is a suitable model organism to study genome-wide regulation of chromosome replication, because both the structures of replication origins and the chromatin configuration have similarities with those in metazoan organisms.

In fission yeast, due to preferred binding of ORC to AT-rich sequences (Chuang and Kelly, 1999) and the requirement of multiple ORC binding sites for origin activity (Takahashi et al., 2003), replication origins have been predicted to be "A+T-rich islands" located preferentially in intergenic regions (Segurado et al., 2003). Locations of single stranded DNA regions under nucleotide depleting conditions are consistent with this prediction (Feng et al., 2006). Because the ARS activity of intergenic regions correlates

with the AT content and the length, it has been proposed that replication origins fire stochastically in fission yeast (Dai et al., 2005). Single molecule analyses using DNA combing also support the stochastic model (Patel et al., 2006). However, due to the lack of information on genome-wide distribution of pre-RC sites, it has remained an open question whether all the pre-RCs are activated or only a subset of origins is selected to fire.

In this study, I conducted high-resolution mapping of Orc1 and Mcm6 binding sites in G1 phase, using a tiling array covering almost the entire genome of fission yeast, to identify pre-RC sites precisely on the whole genome. Mapping of nascent DNA in the presence of HU in wild type and checkpoint deficient *cds1*Δ cells allowed to identify early-firing replication origins and late-firing and/or inefficient origins. Replication timing is coordinated in large chromosome regions. The pericentromere, kinetochore, the silent mating-type (*mat*) locus and subtelomeric heterochromatin behaved differently, suggesting distinct regulation in functional chromatin domains.

RESULTS

Mapping of pre-replicative complexes, pre-RCs, on fission yeast chromosomes

Initiation of DNA replication in eukaryotic cells requires the ordered assembly of replication factors at specific sites on the chromosome. To determine the site of pre-replicative complex (pre-RC) formation on fission yeast chromosomes, DNA immunoprecipitated with Orc1 and Mcm6 in G1-arrested cells (Ogawa et al., 1999; Takahashi et al., 2003) was analyzed with a tiling array that covers almost the entire genome of fission yeast at 250 base pair (bp) resolution except for telomeres and rDNA repeats. Both Orc1 and Mcm6 were located exclusively at intergenic regions, and 84% of Orc1 binding sites co-localized with Mcm6 (Fig. I-1, Supplementary Table I-S1; data of the tiling array analysis are available online, see materials and methods). A total of 460 pre-RC sites, where peaks of Orc1 and Mcm6 co-localized, were identified (black triangles in Fig. I-1 and Table I-S1). The pre-RC sites were distributed throughout the chromosomes with an average separation of 26.7 kb and enriched at the centromeres and the subtelomeric regions. Enrichment at the subtelomeric regions was not observed on chromosome III, where both ends of the array were flanked with rDNA repeats. I confirmed localization of Orc4, another component of ORC complex in logarithmically growing cells were highly colocalized with those of Orc1 (>90%; Fig. I-2 and Supplementary Table I-S1). This result indicates that peaks of Orc1 represent the binding sites of ORC complex,.

Identification of early replication origins that incorporate BrdU in the presence of HU

For identification of active replication origins, it is crucial to label newly synthesized DNA around replication origins. I labeled newly synthesized DNA by incorporation of 5-bromo-2'-deoxyuridine (BrdU), a heavy-density nucleotide analogue. Because fission yeast cells do not normally intake BrdU due to lack of thymidine kinase activity, the herpes simplex virus thymidine kinase gene was expressed from the inducible promoter. The experimental scheme is shown in Fig. I-3. Fission yeast cells expressing thymidine kinase were synchronously released from the G2/M boundary in the presence of BrdU and hydroxyurea (HU) that depletes dNTPs. BrdU-labeled DNA was separated in an equilibrium gradient of CsCl by centrifugation. To confirm that BrdU was selectively incorporated around replication origins, the amounts of BrdU-DNA for the *ars2004* locus, an early replication

Figure I-1

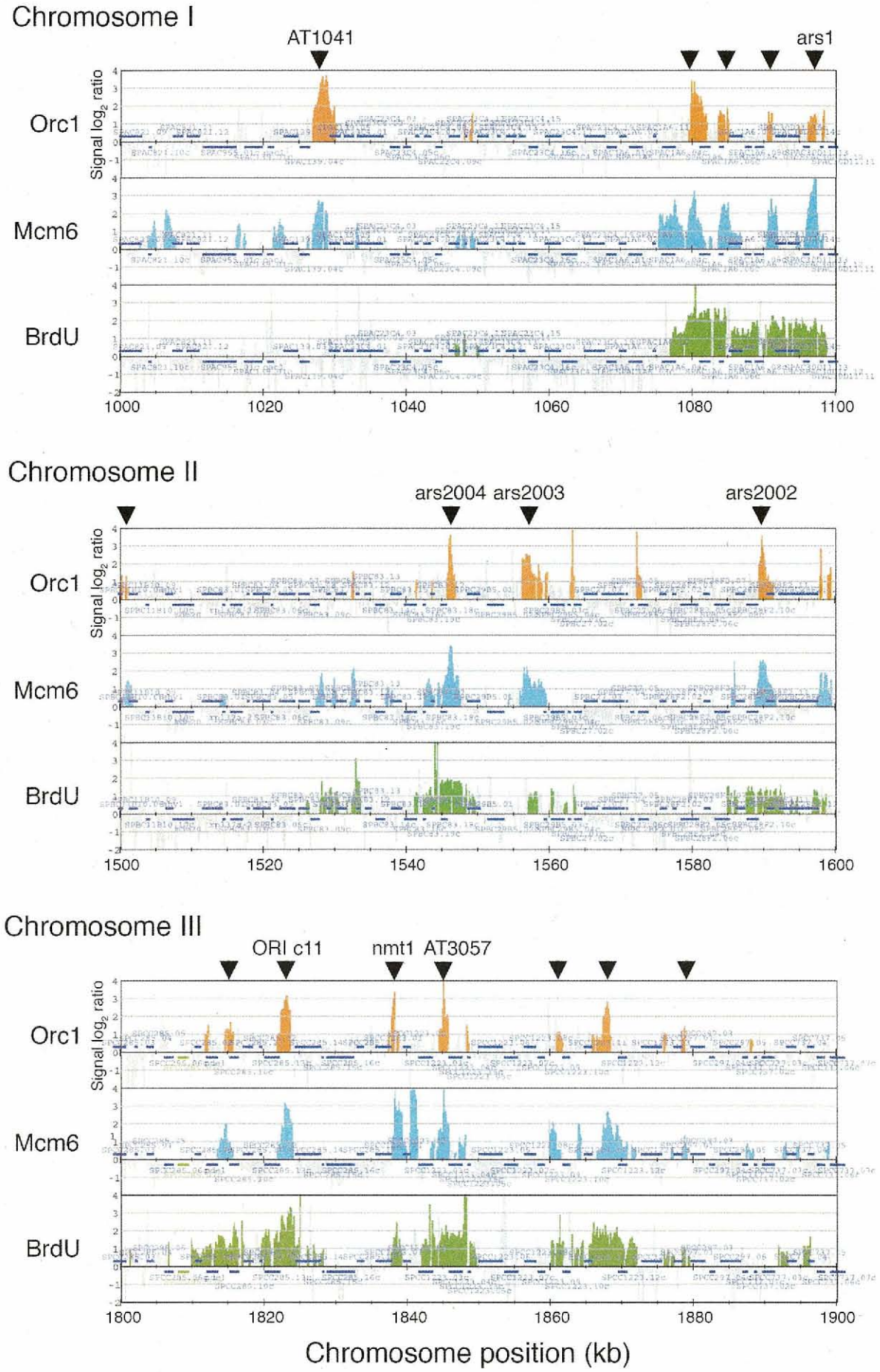
Chromosome I
AT1041
ars1
Orc1
Mcm6
BrdU
Signal log2 ratio
1000
1020
1040
1060
1080
1100
Chromosome II
ars2004 ars2003
ars2002
Orc1
Mcm6
BrdU
Signal log2 ratio
1500
1520
1540
1560
1580
1600
Chromosome III
ORI c11
nmt1 AT3057
Orc1
Mcm6
BrdU
Signal log2 ratio
1800
1820
1840
1860
1880
1900
Chromosome position (kb)

Fig. I-1. Locations of Orc1 and Mcm6 binding sites and BrdU incorporation sites were highly colocalized on fission yeast chromosomes. For mapping of Orc1 and Mcm6 localization sites, HM568 (*h- nda3-KM311 cdc10-129 ura4-D18 leu1-32 orp1-5flag* / pREP82-cdc18 pREP81-cdt1) cells expressing Cdc18 and Cdt1 were arrested at the *cdc10* arrest point in G1 phase and used for ChIP. The orange and blue vertical bars represent the binding ratios of loci showing enrichment of ChIP fractions with anti-Flag-Orc1 (top panels) and anti-Mcm6 (middle panels) antibodies, respectively, for regions 1000-1100 kb on chromosome I, 1500-1600 kb on chromosme II and 1800-1900 kb on chromosome III. For mapping of nascent DNA synthesis, HM668 (h- *cdc25-22 nmt1-TK*) cells arrested at the G2/M boundary were released at 25°C for 90 min in the presence of 10 mM HU and 200 μM BrdU. Cellular DNA was digested with *Hae*III and centrifuged in a CsCl gradient. The experimental scheme is shown in Fig. I-3. Relative enrichment of BrdU-labeled DNA compared to the control whole cell DNA is presented (bottom panels, green bars). Black triangles indicate pre-RC sites identified as colocalization sites of Orc1 and Mcm6, which were programmatically picked up (Supplementary Table I-S1, and online materials). Names of known replication origins colocalized with pre-RCs are shown. Horizontal bars show open reading frames. The scale of the vertical axis is $\log_2$.

Figure I-2

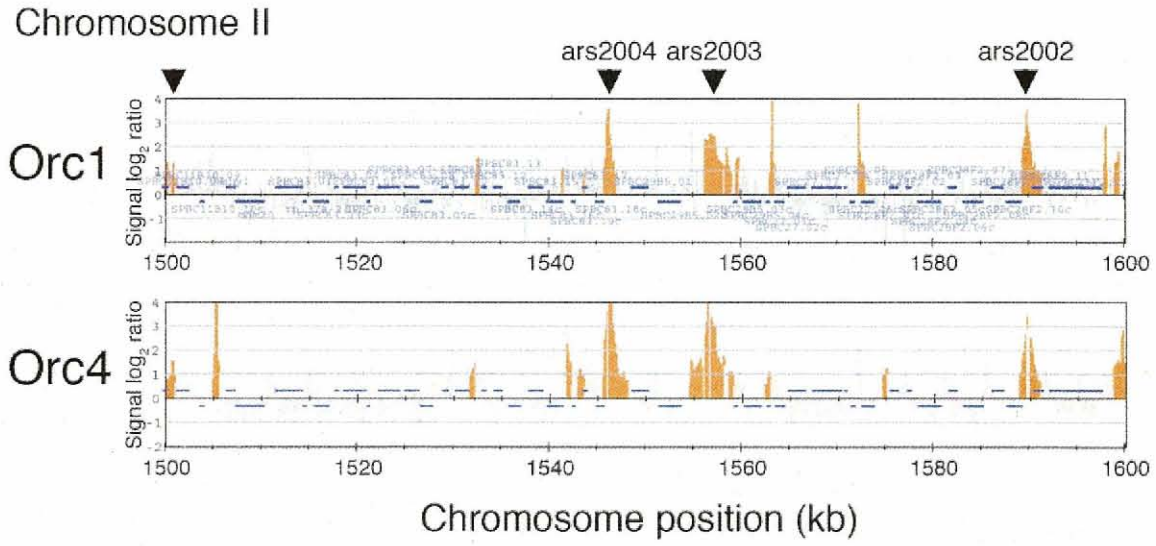

Fig. I-2. Peaks of Orc4 binding sites are highly colocalized with those of Orc1 binding sites. ChIP was performed against Orc4 from logarithmically growing cells and recovered DNA was analyzed as described in Fig. I-1. A representative region around ars2004 is shown. Yellow bar represents significant signal of Orc1 (upper panel) and Orc4 (lower panel).

Figure I-3

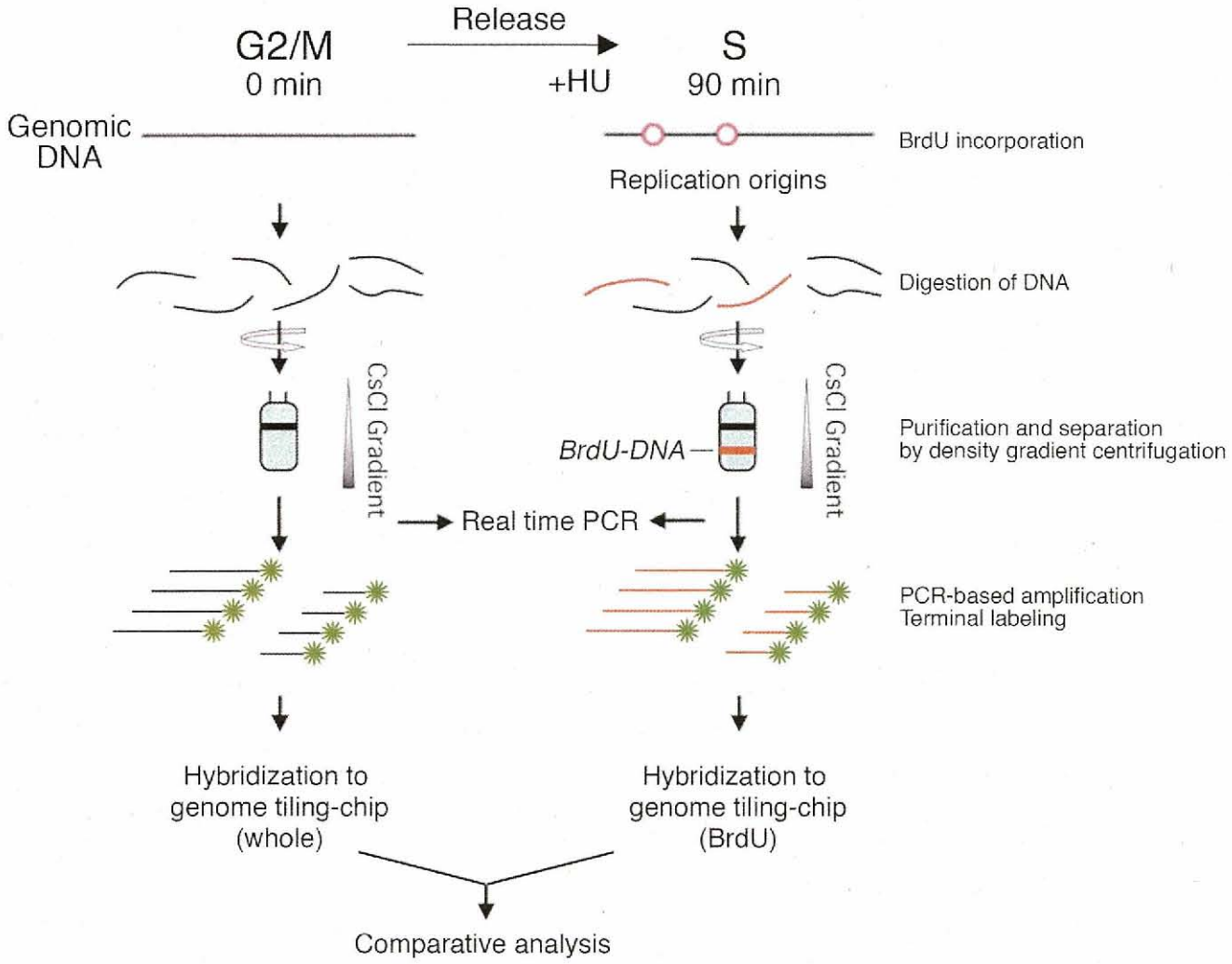

Fig. I-3. A scheme to localize nascent DNA strands in early S phase. HM668 (*h-cdc25-22 nmt1-TK*) cells were synchronized and labeled with BrdU in the presence of HU as described in Fig I-1. Cellular DNA at 0 and 90 min after release from G2/M block was digested with *Hae*III and centrifuged in a CsCl gradient. Fractions collected from the top were dialyzed and recovery of DNA in each fraction was analyzed by real time PCR with ars2004 and non-ARS primers (see Fig. I-4). DNA in the HL-density fractions was pooled and used for tiling-array analysis. For discrimination of positive and negative signals for BrdU incorporation, HL-density fractions at 90 min (early S phase) were compared with LL-density fractions at 0 min (G2/M phase).

origin (Okuno et al., 1999), and a non-ARS (non-origin) region about 30 kb distant from the origin were analyzed by real time PCR. After 90 min of BrdU-labeling in the presence of HU, about 50% of the *ars2004* region was recovered in the heavy-light density fractions, while the non-ARS fragment remained in the light-light density (Fig. I-4), indicating that BrdU was incorporated selectively around the origin. I also confirmed that both *ars2004* and non-ARS regions were fully substituted with BrdU in HU-free conditions (Fig. I-5), excluding the possibility that selective incorporation of BrdU around the *ars2004* was due to a shortage of BrdU. Since recovery of the nascent DNA by the method was verified, the heavy-light DNA fractions were pooled and subjected to the whole-genome analysis (Fig. I-3).

The results of the tiling array analysis showed that BrdU-labeled DNA was co-localized with Orc1 and Mcm6 at a very high frequency (Fig. I-1, green bars in bottom panels and Supplementary Table I-S1). At the *ars2004* origin locus, BrdU-labeled DNA spanned about 10 kb around the intergenic region where Orc1 and Mcm6 were confined (Fig. I-1, middle set of panels). This is consistent with bidirectional DNA synthesis initiated from the origin in early S phase (Okuno et al., 1997; Takahashi et al., 2003). The colocalization sites of Orc1, Mcm6 and BrdU, a total of 307 loci, 119, 107 and 81, on chromosomes I, II and III, respectively, were defined as early replication origins that fired in the presence of HU (red squares in Fig. I-6, and Supplementary Table I-S1). In contrast, 153 Orc1-Mcm6 colocalization sites, 88, 62 and 3, on chromosomes I, II and III, respectively, did not incorporate BrdU in the presence of HU. Although it is not distinguished whether BrdU-negative origins fire in late S phase and/or at a low efficiency, they are collectively designated as late origins below (blue squares in Fig. I-6, and Supplementary Table I-S1).

Among 36 origins previously identified by two-dimensional gel electrophoresis, 28 coincide with the early origins identified here, while 2 match to the late origins (Fig. I-6) (Dubey et al., 1994; Gomez and Antequera, 1999; Okuno et al., 1997; Sanchez et al., 1998; Segurado et al., 2003; Segurado et al., 2002; Smith et al., 1995; Wohlgemuth et al., 1994). At the remaining 6 known origin loci, Orc1 signals were below the standard, although at least either BrdU or Mcm6 signals were detected. When the replication origins identified in this study were compared with those obtained in the previous genome-wide analyses, 189 out of 307 early origins (62%) and 69 out of 153 late origins (45%) coincide precisely with the origins (A+T-rich islands) predicted from AT content calculation (Segurado et al., 2003) (Supplementary Table I-S1). On the other hand, the early origins are colocalized at a high

Figure I-4

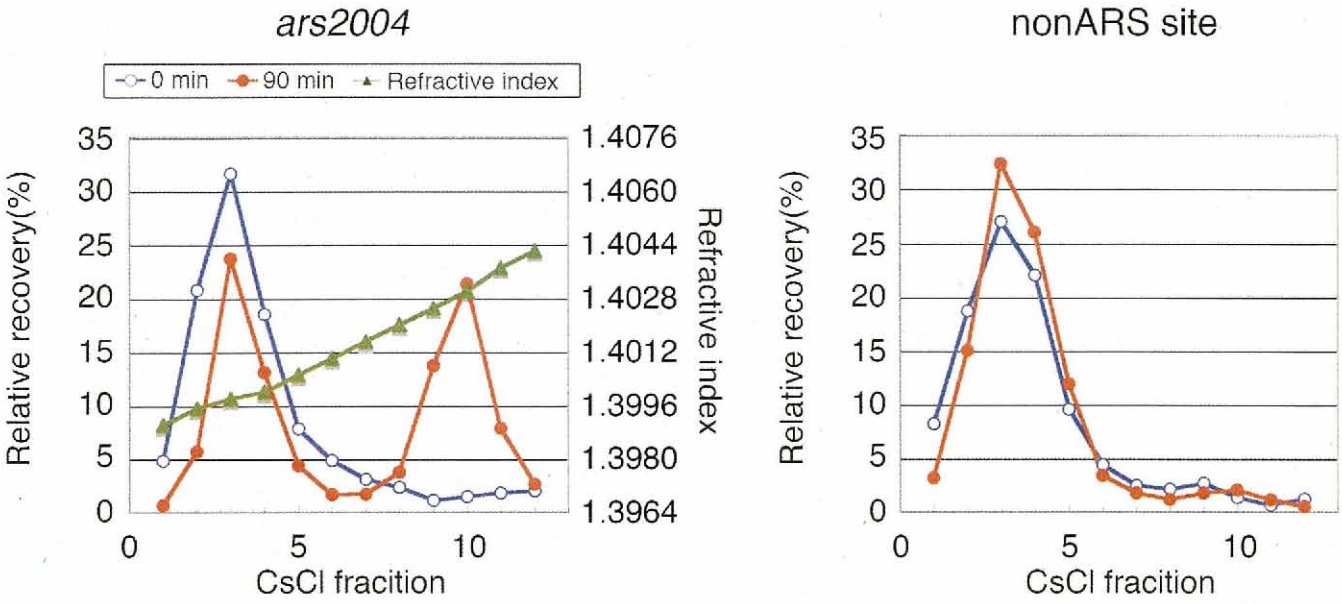

Fig. I-4. BrdU is incorporated preferentially into origin proximal regions. DNA in each fraction at 0 min (blue open circles) and 90 min (red filled circles) was analyzed by real time PCR using primers for ars2004 (left) and non-ARS (right) regions. Relative recovery (%) among total DNA recovered is presented together with the refractive index (green triangles). For the whole genomic analysis, the heavy-light density fractions 8-12 of 90 min (BrdU-DNA) and light fractions 1-6 of 0 min (Whole DNA) were pooled and used for comparative analysis with the tiling array.

Figure I-5

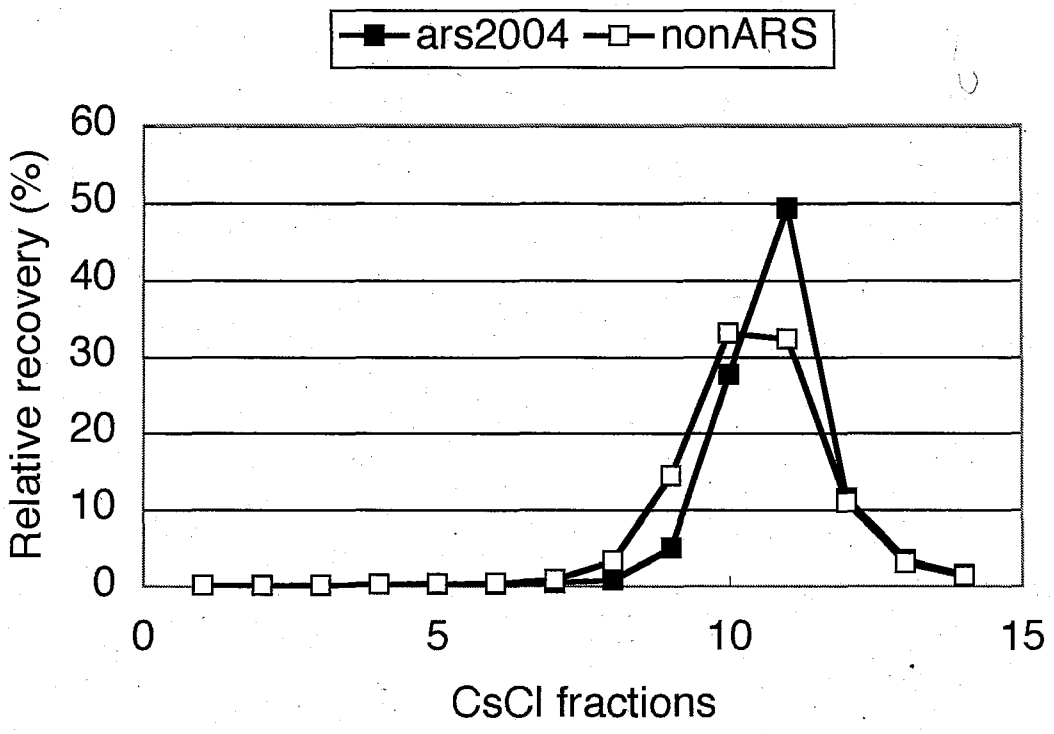

Fig. I-5. The ars2004 locus as well as the nonARS locus fully incorporate BrdU in the absence of HU. HM668 cells released from G2/M were labeled with BrdU for 160 min as described in Fig. I-1 and I-3, except that HU was not added. DNA in each fraction after CsCl centrifugation was analyzed by real time PCR using primers for the ars2004 (filled square) and the nonARS (open square).

Figure I-6

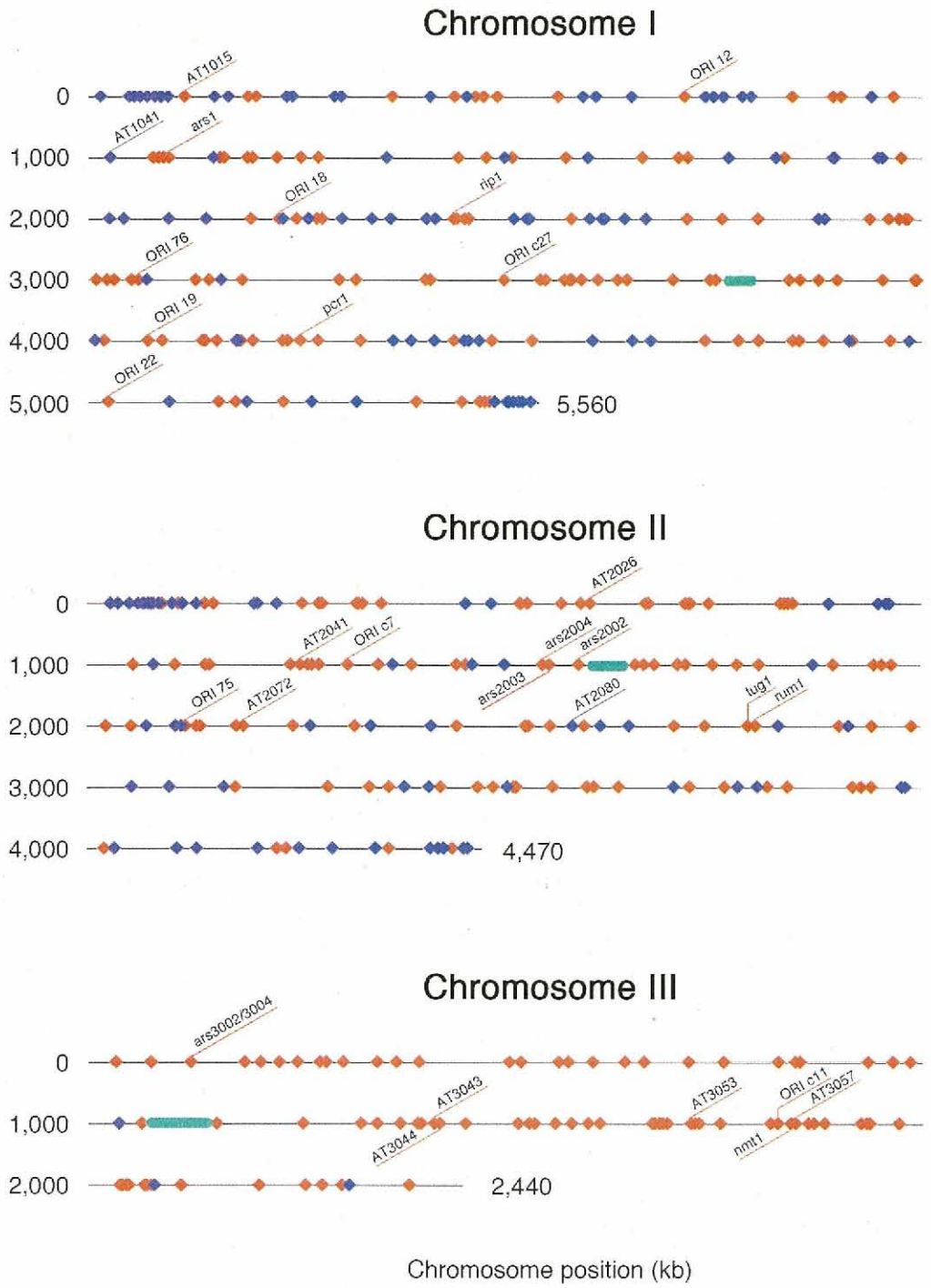

Fig. I-6. Distributions of early and late replication origins. Locations of the early origins (red squares) and those of the late and/or inefficient origins (blue squares) are shown on chromosomes I, II and III. Positions of known replication origins are shown. Positions of centromeres are shown by green ellipses.

frequency (239 origins, 78%) with the origins identified as peaks of DNA content increase, while the late origins coincide at a lower frequency (34 origins, 22%) (Heichinger et al., 2006). In comparison with the origins identified as the center of single-stranded DNA formed in the presence of HU (Feng et al., 2006), 50% (154 loci) of the early origins and 16% (24 loci) of the late origins match with the previously identified origins (Supplementary Table I-S1).

Early origins clustered in narrow regions

It should be noted that Orc1-Mcm6 colocalization sites are frequently clustered within a broad BrdU-labeled region extending 20-30 kb, such as at positions 510-530 of chromosome II (Fig. I-7A). The presence of multiple peaks of BrdU-labeled DNA corresponding to Orc1-Mcm6 binding sites is consistent with the initiation from closely located several origins, although the possibility that DNA synthesis extended from a unique origin remains. To distinguish these possibilities, I first examined whether each of Orc1-Mcm6 colocalization sites exhibited the ARS activity. Among 11 fragments derived from the region, five generated transformants at a high frequency (Fig. I-7B), indicating that the ARS fragments are clustered.

Next, I examined whether these ARS's are active on the chromosome. Chromosomal DNA of cells synchronously released from G2/M in the presence of HU was analyzed by two-dimensional gel electrophoresis. The results presented in Fig. I-7C show that bubble arcs, which are indicative of initiation of replication from the fragments, were detected for fragments 3, 7, 8 and 11 (black triangles in Fig. I-7C). Fragments 7, 8 and 11 correspond to *ori2031E*, *2032E*, *2033E*, respectively (Supplementary Table I-S1). Another early origin exists in fragment 3, although the origin was not identified by genome-wide analysis due to weak Orc1 signal (Supplementary Fig. I-S1). These results demonstrate that clustered pre-RC sites act as early-firing origins. Initiation of replication from closely located origins has been reported for the *ura4*$^+$ locus on chromosome III by 2D-gel and DNA combing analyses (Dubey et al., 1994; Patel et al., 2006), and it seems to be common on fission yeast chromosome.

Repression of late firing origins by checkpoint kinase Cds1

Late replication origins in budding yeast are repressed by checkpoint pathway under replication stress such as depletion of nucleotide by HU (Feng et al., 2006; Santocanale and

Figure I-7

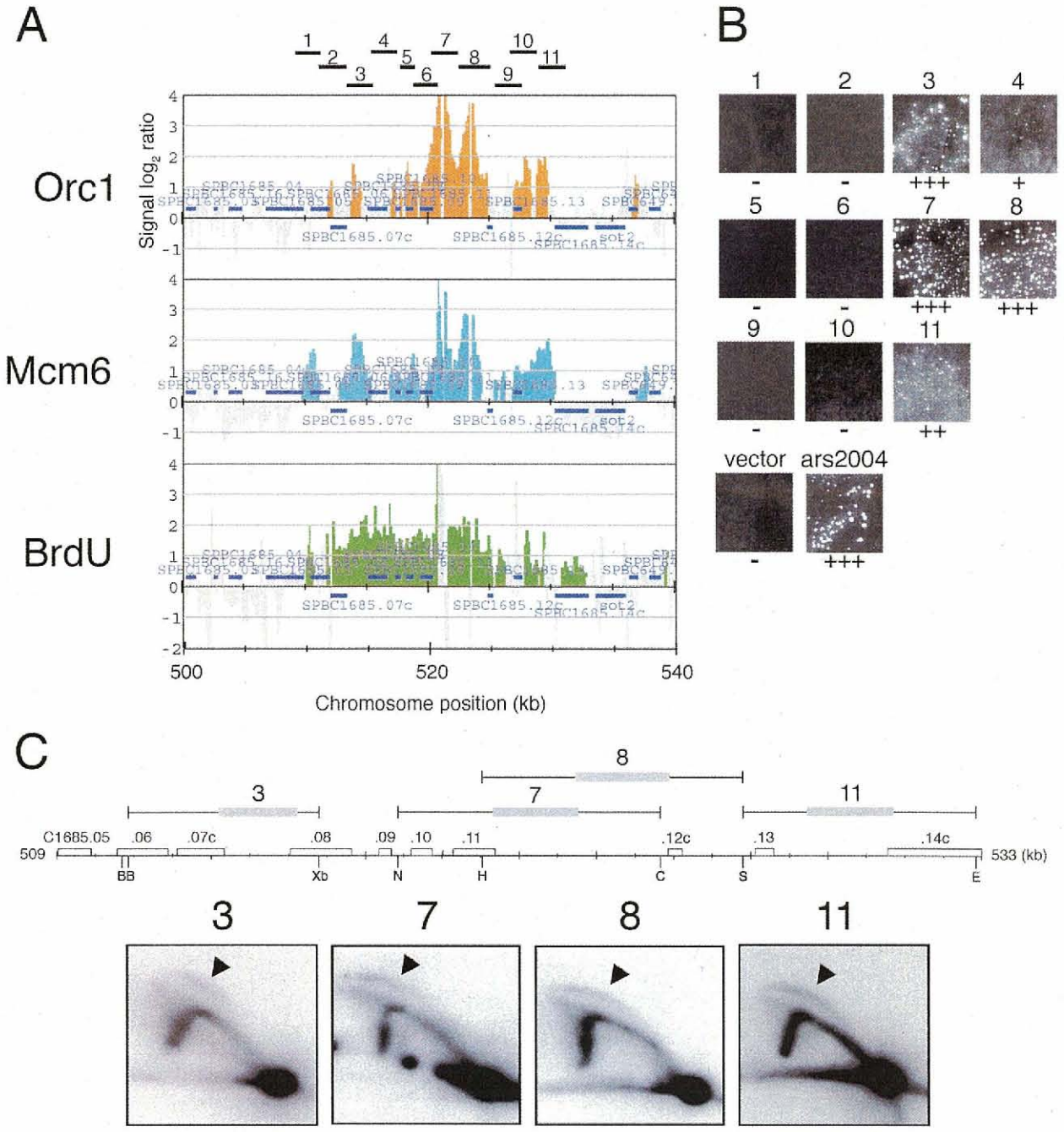

Fig. I-7. Clustered pre-RC sites act as early replication origins. (A) Locations of Orc1 (orange, top panel), Mcm6 (blue, middle panel) and BrdU-labeled DNA (green, bottom panel) in the 500-540 kb region of chromosome II are presented. (B) Eleven fragments containing intergenic regions, shown by horizontal lines in (A) were cloned into the pYC11 vector and used for transformation of HM123 (*h- leu1-32*). Transformants formed on minimum media plates after 4 days at 30°C are presented. Vector alone and the ars2004 plasmid were used as controls. Plus signs, +++, ++ and + below panels represent large, middle and small colony size, respectively, while a minus sign shows absence of any visible colony. (C) HM668 (*h- cdc25-22 nmt1-TK*) cells released from the G2/M block were cultured at 25°C for 90 min in the presence of 10 mM HU and replication intermediates were analyzed by neutral-neutral 2D gel electrophoresis. Locations of the restriction fragments analyzed by 2D-gel methods are shown above the map of open reading frames and the relevant restriction enzyme sites: B, *Bam*HI; Xb, *Xba*I; N, *Nde*I; H, *Hind*III; C, *Cla*I; S, *Spe*I; E, *Eco*RI. Positions of the hybridization probes, which correspond to the fragments used for the ARS assay in (B), are shown as gray bars.

Diffley, 1998). Mapping of single-stranded DNA in the HU-arrested fission yeast cells has suggested that similar regulation exists in fission yeast (Feng et al., 2006). On the other hand, Rad3, the ATR homologue in fission yeast, affects initiation from a small number of origins (Heichinger et al., 2006). I tested whether the late origins identified in this study might be activated in the absence of replication checkpoint kinase Cds1/Chk2. Wild type and *cds1*Δ cells were synchronously released from G2/M block and labeled with BrdU in the presence of HU for 150 min. The BrdU DNA purified by CsCl centrifugation was analyzed by the tiling array. The results of wild type at 150 min were very similar to those at 90 min, except that BrdU DNA extended further than those at 90 min, which is consistent with slow DNA synthesis in the presence of HU (top panels in Fig. I-8). In contrast, small but significant BrdU incorporation was detected in the subtelomeric regions of chromosomes I and II specifically in *cds1*Δ cells, although BrdU DNA did not form peaks at most of late origins (middle panels in Fig. I-8). These results suggest that the majority of late origins do not fire at a comparable efficiency of early origins even in *cds1*Δ mutant. However, when the ratio of BrdU DNA in *cds1*Δ to that in wild type was calculated, *cds1*Δ-specific BrdU incorporation was observed at subtelomeric regions and at the late origin loci but not at the early origin loci (brown bars in bottom panels of Fig. I-8). BrdU incorporation was increased at 90 late origin loci (59% of the late origins) and at 10 early origin loci (3% of the early origins), showing specific firing of late origins in *cds1*Δ cells. To confirm the tiling array result, I examined replication kinetics in wild type and *cds1*Δ cells in the presence of HU using real time PCR. Figure I-9 shows that BrdU incorporation increased in *cds1*Δ cells compared to those in wild type at the late origin *AT2080* and at the subtelomere locus but not at the early origin or non-ARS locus. These results suggest that a subset of late origins in the arm and the subtelomeric regions are repressed in the presence of HU in part by replication checkpoint regulation.

Coordinated distribution of early and late origins in large chromatin regions

In figure I-6, the early and late origins tend to cluster separately, spanning several hundred kilo-bases on chromosome I and on the left arm of chromosome II. This distribution could result from either random or coordinated choice of pre-RCs. The distribution of inter-pre-RC distances fitted well to an exponential curve (Fig. I-10), suggesting that pre-RCs themselves are randomly distributed along chromosomes (Patel et al., 2006). Then, I asked

Figure I-8

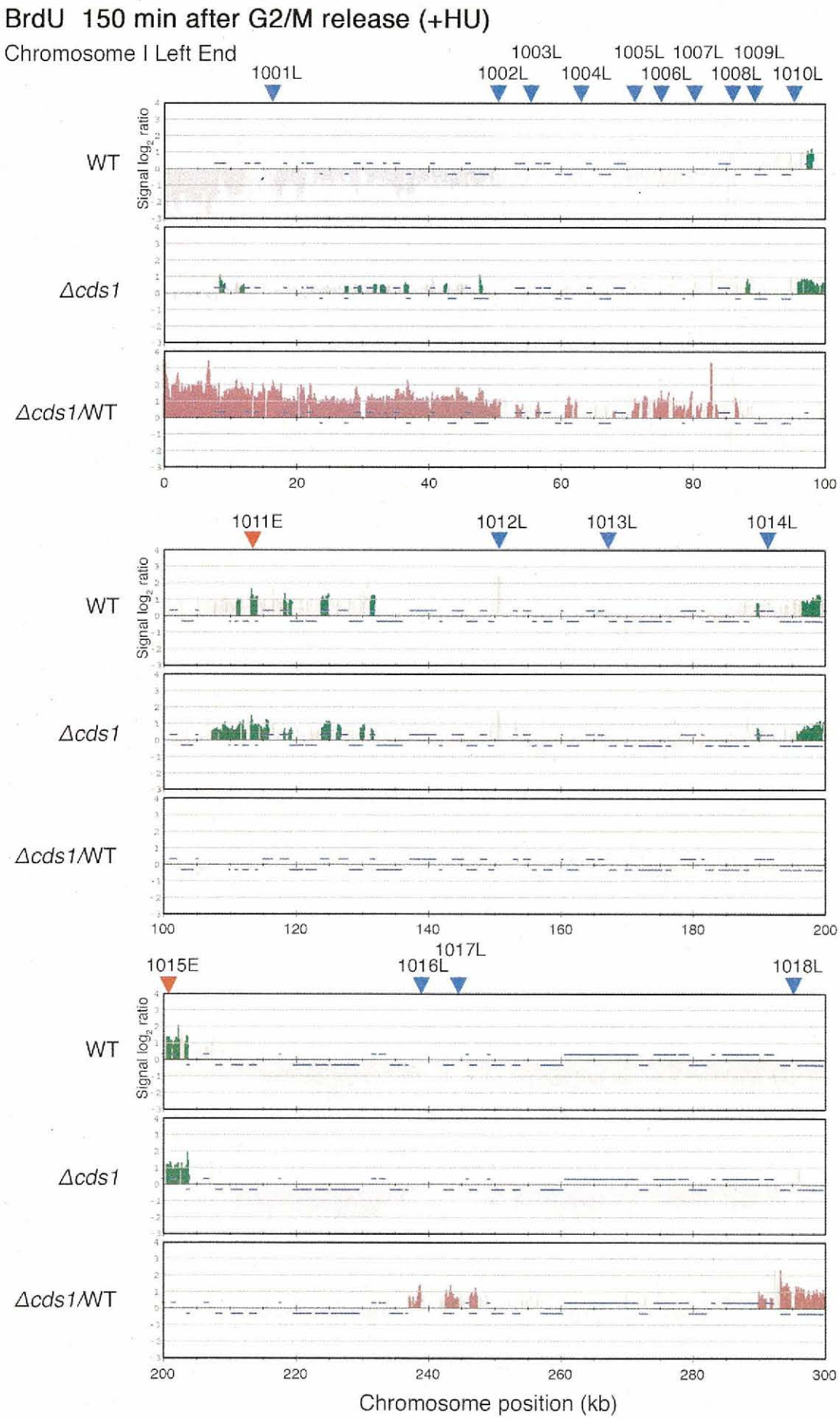
BrdU 150 min after G2/M release (+HU)
Chromosome I Left End
1001L
1002L
1003L
1004L
1005L
1006L
1007L
1008L
1009L
1010L
1011E
1012L
1013L
1014L
1015E
1016L
1017L
1018L
WT
Δcds1
Δcds1/WT
Signal log2 ratio
0
20
40
60
80
100
120
140
160
180
200
220
240
260
280
300
Chromosome position (kb)

Fig. I-8. Incorporation of BrdU increases at late origins in subtelomere and chromosome arms in *cds1Δ* cells. HM668 (*h- cdc25-22 nmt1-TK*) and HM1405 (*h- cdc25-22 nmt1-TK cds1Δ::kanMX6*) were released from G2/M block and labeled with BrdU for 150 min at 25°C in the presence of HU and the genomic DNA was analyzed with the tiling array as described in Fig. I-1. Green vertical bars represent relative enrichment of BrdU-incorporated DNA in wild type (top panels) and in *cds1Δ* (middle panels) in 300 kb region from the left end of chromosome I. The bottom panels show ratios of enrichment of BrdU DNA in *cds1Δ* to that in wild type (brown vertical bars). Red and blue triangles above panels show locations of the early and late origins identified in this work, respectively. Horizontal bars show open reading frames. The scale of the vertical axis is $\log_2$.

Figure I-9

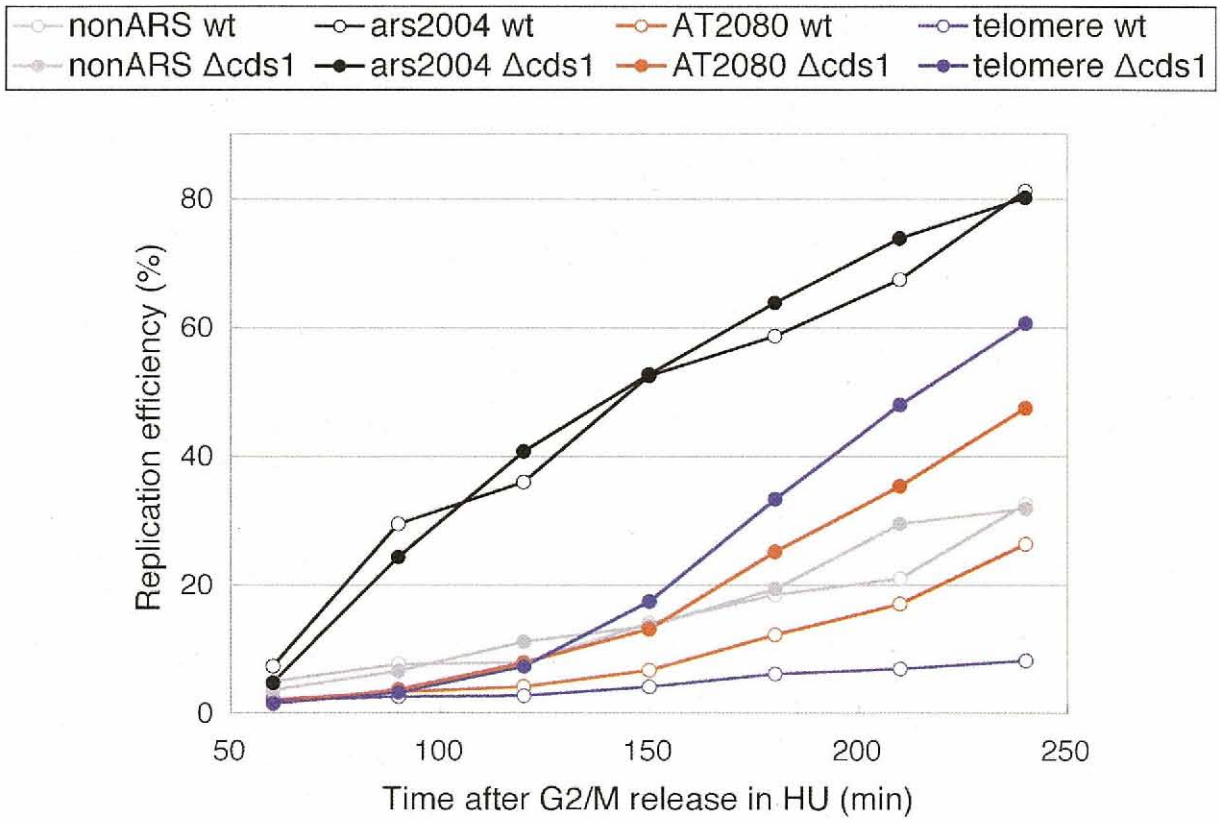

Fig. I-9. BrdU incorporation at the subtelomere and late origin loci gradually increases in the absence of *cds1*. HM668 (*h- cdc25-22 nmt1-TK*) and HM1405 (*h- cdc25-22 nmt1-TK cds1Δ::kanMX6*) were labeled with BrdU from 60 min to 240 min after release in the presence of HU. The genomic DNA from wild type (open circle) and *cds1Δ* (filled circle) at each time point was prepared as described in Fig. I-1. DNA in the heavy-light and light-light fractions was analyzed by real time PCR using primers for ars2004 (black), non-ARS (gray), AT2080 (red), and right subtelomere 2 (telo2R-203)(purple). The replication efficiency (Re %) was obtained by the equation, Re = [(HL/2)/(LL+HL/2)] x 100. The heavy-light fractions at 150 min were used for DNA microarray analysis (Fig. I-8 and online materials)

Figure I-10

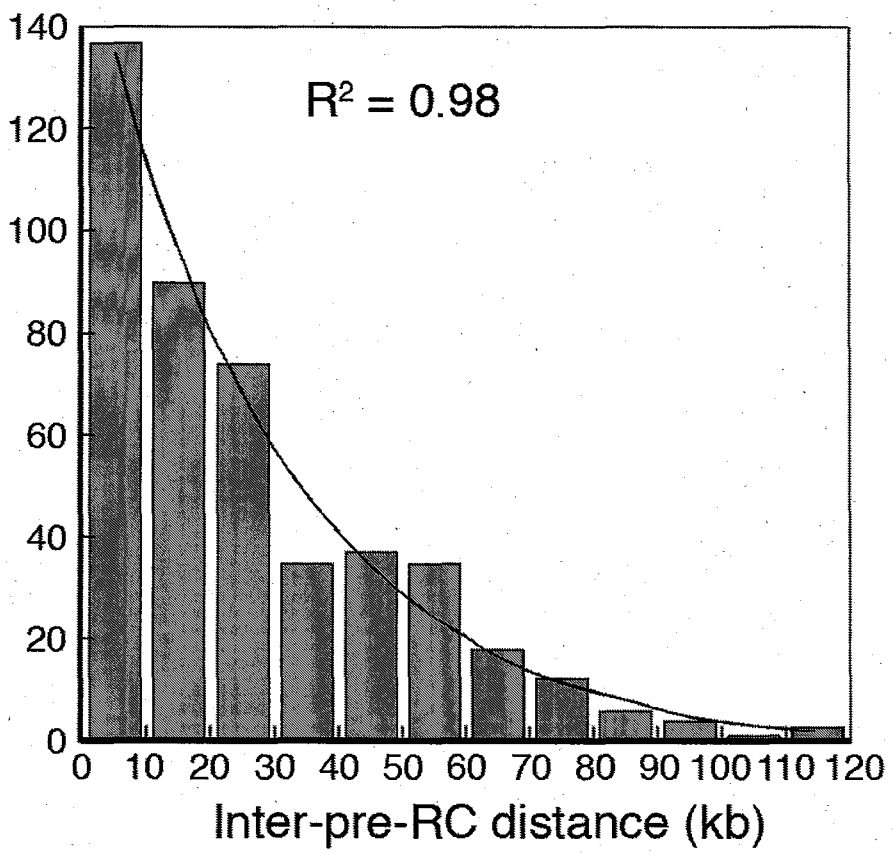

Fig. I-10. Pre-RCs distribute randomly on fission yeast chromosomes. Distribution of inter-pre-RC distances are shown. Best-fit exponential curve and associated R2 value for the distribution of inter pre-RC distance were calculated by using KaleidaGraph 4.0J for Mac (Synergy Software, HULINKS Inc.). The exponential nature of this distribution indicates that pre-RC sites are randomly distributed along fission yeast chromosomes (Patel et al., 2006).

Table I-1

The z statistic for distribution of the early origins and late origins on each chromosome arm.

		OriE	OriL	pre-RCs	run	mean (μ)	variance (σ^2)	test statistic (z)
Chr I	Left arm	78	63	141	48	70.7	35.0	-3.88
	Right arm	41	25	66	22	32.1	15.8	-2.65
Chr II	Left arm	47	25	72	20	33.6	17.3	-3.58
	Right arm	60	37	97	36	46.8	23.7	-2.33
Chr III	Left arm	30	1	31	3	NA	NA	NA
	Right arm	51	2	53	5	NA	NA	NA
	Whole	307	153	460	131	221.0	105.0	-8.78

Early and late origins were symbolized as E and L, respectively, to perform Wald-Wolfowitz runs test (see Materials and methods). To test the coordinateness of origins on whole genome, the three chromosomes were considered to be one sequence. Centromeres were neglected, while runs were divided at each telomeric end. NA: not applicable.

whether a pre-RC is chosen to be an early origin independently from the neighboring origins or a subset of pre-RCs are coordinately chosen. To examine these possibilities, a statistical analysis, Wald-Wolfowitz run test (Chang, 2000), was carried out against a null hypothesis that a pre-RC is randomly chosen to be an early origin (Table I-1 and Materials and methods). The actual distribution of early origins does not likely result from randomness on chromosome I and on the left arm of chromosome II ($P < 0.01$), while randomness was not rejected on the right arm of chromosome II ($P = 0.0198$; $\alpha = 0.01$). The analysis was not applied on chromosome III, where only a few late origins exist. These results suggest that activation of pre-RCs tends to occur coordinately in large chromosome regions.

Initiation of replication is differently regulated in centromeres, the silent mating-type locus and subtelomeric heterochromatin

It is of interest how initiation of replication is regulated in specific chromosomal loci, such as centromeres and telomeres, because these loci contain heterochromatic regions, which have been reported to replicate generally in late S phase in higher eukaryotes (Jeon et al., 2005; Woodfine et al., 2004). In fission yeast, three regions, centromere, subtelomere and the silent mating-type (*mat*) locus, are known to form constitutive heterochromatin structures. In 100-250 kb subtelomeric regions from the ends of chromosomes I and II, BrdU incorporation was rare despite of the existence of highly clustered pre-RCs (Fig. I-6 and Fig. I-11A), suggesting that they were not activated at least in early S phase. In order to investigate replication origins near the chromosome ends, where the tiling array does not cover, I used ChIP-qPCR method and examined the pre-RC formation near the very end of chromosome II (0.3-21 kb from the end), where expression of ectopic *ura4*$^+$ marker is inactivated (Kanoh et al., 2005). ChIP against Orc4 and Mcm6 were performed, followed by real time PCR analysis (Fig. I-11B). The result shows that Orc4 and Mcm6 are highly enriched at the following sites: 3 kb, 6.5 kb, 9 kb and 21 kb from the right end of chromosome II. This demonstrates that pre-RCs are formed near the telomeric ends. These pre-RCs are likely to be suppressed to fire in early S phase because I failed to detect Ssb2 (a component of RPA) binding in HU-arrested cells (Fig. I-11B). It is worth noting that Mcm6 is absent from the very end (0.3 kb) despite the localization of Orc4. Binding of MCM might be restricted by the telomere specific components that bind telomeric repeats.

Fission yeast centromeres are composed of two functional domains, the unique

Figure I-11

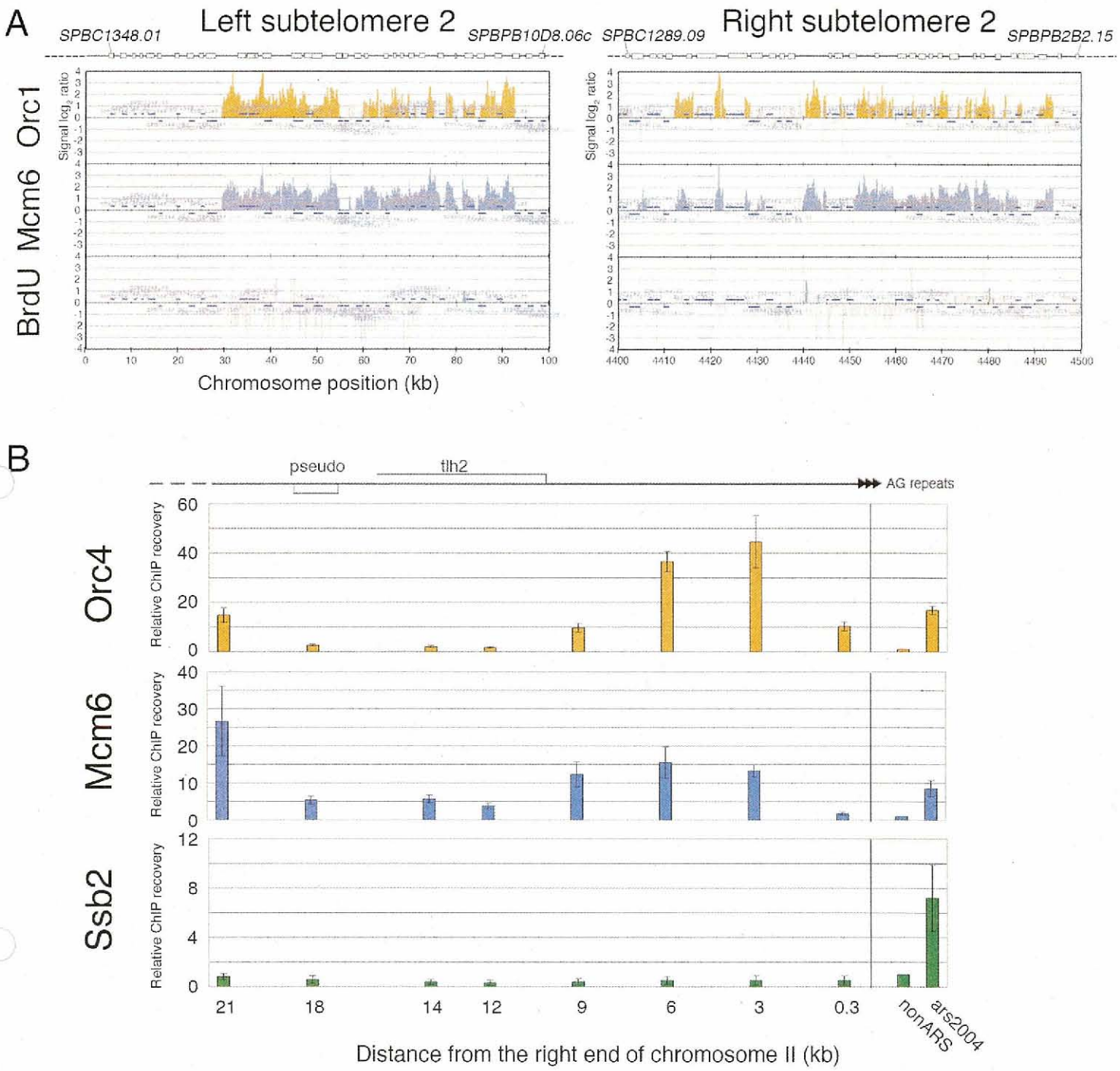

Fig. I-11. Potential origins are clustered in the subtelomeric regions. (A) Locations of Orc1 (orange bars, top), Mcm6 (blue bars, middle) and BrdU incorporation (green bars, bottom) in left and right subtelomeric regions on chromosome II in wild type HM668 (*h-cdc25-22 nmt1-TK*) are presented. Note that the tiling array does not contain telomere-proximal regions because they share highly homologous sequences. White boxes above the panels denote open reading frames. Signals are absent in gray-shaded regions because of the presence of homologous sequences. (B) Locations of Orc4 (top), Mcm6 (middle) and Ssb2 (bottom) in the right end of chromosome II. HM1182 (h^{90} *cdc25-22 nmt1-TK*) cells were arrested in early S phase by HU after G2/M synchronization. ChIP samples were quantified by real time PCR with telomeric primers (Kanoh et al., 2005), and recovery was normalized to the nonARS locus. Note that all telomeres contain sequences homologous to this region. White boxes above the panels denote open reading frames. Black triangles represent telomeric repeats. Error bar indicates standard deviation.

central core region (*cnt*), where the kinetochore complex is formed, and the inverted repeats (*imr*) and the outer centromeric repeats (*otr*), where heterochromatin is formed (Pidoux and Allshire, 2004). It is remarkable that all BrdU, Orc1 and Mcm6 signals were detected at the *otr*, indicative of efficient initiation from the *otr* in early S phase (Fig. I-12A). In contrast, the inner centromere *cnt2* region did not replicate in the presence of HU (Fig. I-12A). Surprisingly, Mcm6 was not localized at the *cnt2* region despite enriched binding of Orc1 (Fig. I-12A). Localization of Orc1 without Mcm6 or BrdU incorporation at the *cnt* was common property on all the chromosomes (online data and data not shown). Since I anticipated that epitopes in Mcm6 could be sequestered from antibody in *cnt*-specific protein complex, DNA samples chromatin-immunoprecipitated with polyclonal antibodies against Mcm2 and Orc4 in addition to Orc1 and Mcm6 in G1-arrested cells (Takahashi et al, 2002) were analyzed by real time PCR. The *cnt2* DNA was recovered by Orc1-IP and Orc4-IP at a higher efficiency than the *ars2004* and the *otr* DNA (Fig. I-12B). In contrast, recoveries of the *cnt2* DNA by Mcm2-IP and Mcm6-IP were about one-tenth of those of the *ars2004* and the *otr* DNA (Fig. I-12B). These results show that Mcm2 nor Mcm6 is efficiently located at *cnt2*, which is consistent with the results of the tiling array. Thus, initiation of replication is differently regulated in the inner and outer centromere domains.

At the *mat* region, a 20-kb domain containing the *mat2* and *mat3*, which serve as recombinational donor for the *mat1* locus; and the interval between them, known as the K-locus, are subject to heterochromatin-mediated silencing (Nakayama et al., 2000). In order to examine replication origins in the *mat* K-locus I performed ChIP-qPCR analysis against Orc4 and Mcm6 to locate pre-RCs because the tiling array does not cover the *mat* K-locus. Although Orc4 signals in HU-arrested cells are relatively low in the *mat* K-locus, they are significantly high around the *mat2* and *mat3* loci (16, 17, 20, 23, 29, 33, 34 and 36 kb from the *mat1* locus) compared to surrounding euchromatic regions as well as the nonARS locus (Fig. I-13; Orc4). Consistent with this observation, Mcm6 signals are highly enriched around the *mat2* and *mat3* loci (Fig. I-13; Mcm6), indicating enriched localization of replication origins in the *mat* heterochromatic region. To examine the property of these origins, I performed ChIP against Ssb2 using HU-arrested early S phase cells. Ssb2 signals at these origins are comparable to that at the ars2004 (Fig. I-13; Ssb2), suggesting these origins act as early replication origins.

Figure I-12

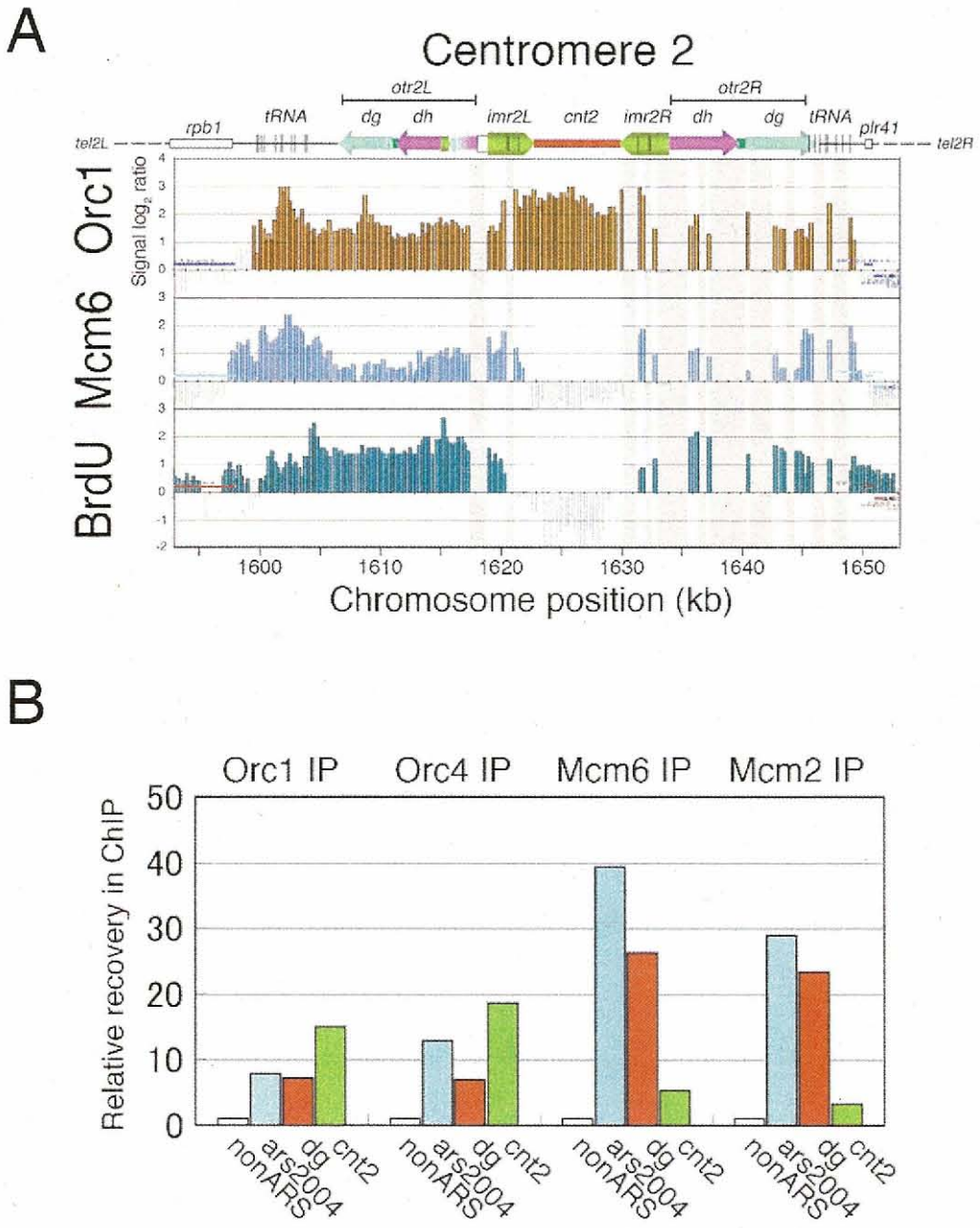

Fig. I-12. Replication is distinctly regulated in centromeric domains. (A) Locations of Orc1, Mcm6 and BrdU incorporation at centromere on chromosome II are shown. The physical map of fission yeast cen2 above the panels denotes *otr* comprised of *dg* and *dh* elements, *imr* and *cnt*. Vertical lines indicate *tRNA* genes. Signals are not present in gray-shaded regions at *imr2R* and *otr2R* because of the presence of identical sequences with *imr2L* and *otr2L*, respectively. (B) Orc1 and Orc4 but not of Mcm6 and Mcm2 localize at *cnt2*. ChIP with Orc1-5Flag, Orc4, Mcm6 and Mcm2 was carried out from G1 arrested cells as described in Fig. I-1. DNA recovered in ChIP was analyzed by real time PCR using primers amplifying nonARS, ars2004, *dg* and *cnt2* regions and relative recovery normalized to nonARS region is presented.

Figure I-13

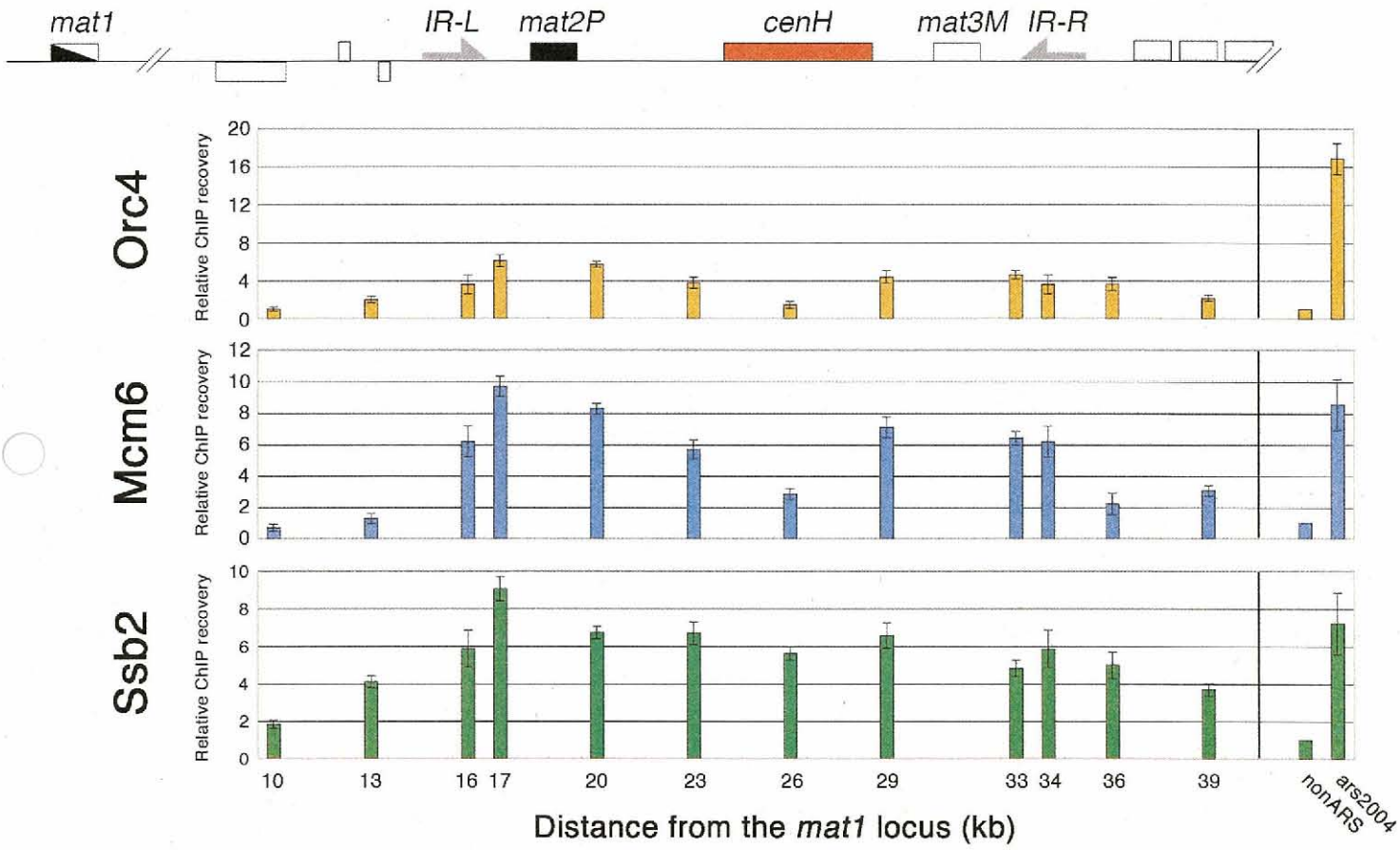

Fig. I-13. Early origins clustere in the silent mating-type locus. Locations of Orc4 (yellow), Mcm6 (blue) and Ssb2 (green) in the silent mating-type K-locus. A diagram of the *mat* locus is shown on top. IR-L and IR-R indicate heterochromatin boundary elements. The *mat2P* and *mat3M* are the silent donor loci for the *mat1* locus . Red box represent *cenH* sequence homologous to the pericentromeric repeats. White boxes indicate open reding frames. HM1182 (h^{90} *cdc25-22 nmt1-TK*) cells were arrested in early S phase by HU after G2/M synchronization. ChIP samples were quantified by real time PCR, and recovery was normalized to the nonARS locus. The ars2004 is an euchromatic early origin control. Error bar indicates standard deviation.

DISCUSSION

In this study, high-resolution whole-genome mapping of Orc1 and Mcm6 binding sites allowed to identify precise locations of 460 pre-RC sites on *S. pombe* chromosomes. I found that 307 pre-RC sites acted as early origins that initiated DNA synthesis in the presence of HU, whereas the rest of pre-RCs were considered as late and/or inefficient origins (called collectively as late origins) (Fig. I-6). Interestingly, pericentromeric heterochromatin and the silent *mat* locus replicated in the presence of HU, while the inner centromeres or subtelomeric regions did not, suggesting specific regulation of replication in these specialized functional chromatin regions (Fig. I-11 and I-12).

Distribution and regulation of replication origins in chromosomal arm regions

Because more than 80% of Orc1 binding sites were colocalized with Mcm6, the majority of ORC binding sites serve for pre-RC assembly. The pre-RCs are formed exclusively in long and AT-rich intergenic regions as described previously (Dai et al., 2005; Gomez and Antequera, 1999). Pre-RCs are distributed randomly along the entire chromosomes (Fig. I-10) except for enriched localization at pericentromere, the *mat* locus and subtelomeric regions (Fig. I-11, I-12 and I-13). However, only a subset of pre-RCs is activated in early S phase. When the early origin *ars2004* and the late origin *AT2080* fragments were mutually exchanged, *AT2080* became early origin while *ars2004* became late one, suggesting that timing of firing is not intrinsic to ARS fragment but dependent on the context of the locus (Hayashi et al., 2007). Furthermore, the results of statistical analysis suggest that distribution of the early and late origins does not result from random choice of pre-RCs at least in chromosome I and in the left arm of chromosome II (Table I-1). These results are consistent with the idea that replication origins are coordinately regulated in broad chromosome regions, such as chromatin domains, which has been documented in higher eukaryotes (Schwaiger and Schubeler, 2006).

In metazoan organisms, different chromatin structures representing chromatin-banding patterns replicate with different timing in S phase (Takebayashi et al., 2005). Growing evidence suggests coordinated regulation of replication timing and transcriptional activity in chromatin domains (MacAlpine et al., 2004; Schubeler et al., 2002; Schwaiger and Schubeler, 2006; Woodfine et al., 2004). Various histone modifications could be involved

in regulation of chromatin activities. Histone deacetylase inhibitors alter replication timing in mammalian cells (Bickmore and Carothers, 1995). In budding yeast, the Rpd3-Sin3 histone deacetylase affects replication timing of origins, which is independent of its role in transcription (Aparicio et al., 2004). Thus, it is of interest whether histone-modifications are involved in regulation of replication timing on fission yeast chromosomes and, if this is the case, whether the regulation of replication correlates with transcriptional regulation.

I showed that the late origins in subtelomeric and arm regions incorporated BrdU in HU-arrested late S phase in *cds1*Δ mutant (Fig. I-8 and I-9). These results are consistent with the finding that single stranded DNA accumulates at subtelomeric regions and other chromosome loci in HU-arrested *cds1*Δ cells (Feng et al, 2006). It should be noted, however, *cds1*Δ-specific BrdU incorporation at the late origins was much less efficient than those at the early origins (Fig. I-8), suggesting that replication initiation occurs only in small population of cells. This is consistent with the report that deletion of Rad3 does not significantly change the number of origins identified by DNA content increase (Heichinger et al., 2006). Therefore, both checkpoint-dependent and checkpoint-independent regulations may account for suppression of initiation from the late origins.

Distribution and regulation of replication origins in functional genomic loci

Using the tiling array and ChIP-qPCR method, overall replication profiles of centromere, telomere and the *mat* locus in fission yeast were shown in this study. Unlike euchromatic arm regions, pre-RCs are highly abundant in constitutive heterochromatic regions. Interestingly, those origins in heterochromatic regions behave distinctly in each locus. The origns in subtelomeric regions are not activated in early S phase (Fig. I-11), while those in pericentromere and the silent *mat* K-locus replicate in early S phase (Figs. I-12 and I-13). Consistent with these observations, a part of the early origins in pericentromere and the silent *mat* locus and late replication of subtelomere were reported previously (Kim et al., 2003; Kim and Huberman, 2001; Smith et al., 1995). The activation of origins in pericentromere and the silent *mat* K-locus will be analyzed and discussed farther in ***Part II***.

In budding yeast, mutations in Sir3 result in both increased gene expression (Wyrick et al., 1999) and firing of silent replication origins in subtelomeric regions (Stevenson and Gottschling, 1999). In fission yeast, Swi6, a fission yeast homologue of heterochromatin protein 1 (HP1), is required for repression of transcription by

heterochromatin structures extending from the telomere ends (Kanoh et al., 2005), although it is not likely that Swi6 is involved in repression of the subtelomeric late origin firing (see ***Part II***). On the other hand, I showed that, in the absence of Cds1, BrdU incorporation increased at subtelomeric regions after prolonged incubation with HU (Fig. I-9), suggesting that Cds1 has an important role in repression of subtelomere replication under replication stress. Progression of replication fork at subtelomeric region may be particularly sensitive to replication stress and this may be avoided by strict suppression of initiation. Highly clustered pre-RCs in the subtelomeric regions might be required for efficient replication in very late S phase. Alternatively, they might play some role in telomere maintenance.

The results of this study clearly demonstrated distinct replication profiles at centromere; replication initiates at the pericentromeric repeats (*otr*) but not at the core regions (*cnt*) (Fig. I-12). Although the *cnt1* and *cnt2* fragments cloned on plasmids exhibit ARS activity, these replicators do not fire in the native centromere (Smith et al., 1995; Takahashi et al., 1992). Remarkably, Mcm6 or Mcm2 was not localized at the core regions on all three chromosomes despite of Orc1 and Orc4 enrichment (Fig. I-12B). It should be noted that suppression of pre-RC formation onto ORC bound origins was observed in the core centromere and the telomeric end, suggesting that interactions of ORC with pre-RC components might be interfered by centromeric core and telomere specific proteins, respectively. Since ORC but not MCM is allowed to bind to these sites, it would be possible that ORC is involved in kinetochore and/or telomere functions. Possible involvement of ORC in many different cellular functions including cytokinesis has been suggested in different species (Prasanth et al., 2004; Sasaki and Gilbert, 2007).

Early replication at the pericentromeric repeats and the absence of initiation at the centromeric cores may ensure establishment of cohesion at pericentromeric heterochromatin before kinetochore re-assembly on duplicated *cnt*. Thus, distinct replication patterns of centromeric subdomains might be important for centromere functions. Earlier replication of pericentromeric heterochromatin (major satellite) than kinetochore-forming minor satellite on mouse chromosomes has been reported (Guenatri et al., 2004; Hollo et al., 1996).

Since replication is likely to be coupled with various chromatin functions such as sister chromatid cohesion, condensation, DNA repair, checkpoint and chromatin structures, the data on replication machinery assembly sites and direction of replication fork progression will help to identify locations and movement of relevant proteins.

MATERIALS AND METHODS

Yeast strains and genetics

All *S. pombe* strains used are listed in Table I-2. Fission yeast strains were cultured in complete YE medium (0.5% yeast extract and 3% glucose) and Edinburgh minimal medium (Moreno et al., 1991). All solid media contain 2% agar. Transformation of *S. pombe* was performed by electroporation and lithium acetate method (Forsburg, 2003).

Construction of yeast cells expressing thymidine kinase gene

A fission yeast strain expressing the herpes simplex virus thymidine kinase gene (*TK*) was obtained as below. For integration of *TK-ura4*$^+$ fragment into *ura4* locus, PCR-amplified upstream (-1078 to -579 bp) and downstream (+1244 to +1594 bp) locus of *ura4*$^+$ gene was cloned into *Bam*HI site of pBluescript II SK(+) by using primers 5'-AAAGGATCCTGCAGGCATGAAGAATTGGTTATCC-3' and 5'-AAAGGATCCAAGCTTCTGTCAAAGTTTAAC-3', and 5'-AAAGGATCCGCGGCCGCTAGTATACTTTTTCTCGGAG-3' and 5'-AAAGGATCCTCGAGCCTGCAGGAGACGGTTCA-3', respectively, resulting in pBS-ura4up (pMH9) and pBS-ura4dw (pMH10). To obtain pMH2, a *Hin*dIII and *Sse*I8387 fragment of pMH9 was cloned into modified pBluescript II, where *Xho*I-*Not*I fragment was replaced with a fragment carrying *Xho*I-*Not*I-*Cla*I-*Hin*dIII-*Sse*I8387 recognition sites. A 1.8 kb *ura4*$^+$ fragment was inserted at *Hin*dIII site of the pMH2 generating pMH3, and then both the *Xho*I-*Not*I fragment of pMH10 and *Not*I fragment of pUC-nmt-Not were cloned into *Xho*I-*Not*I site of pMH3, resulting in pMH5. The *TK* gene was re-cloned from the pGAD-*TK* plasmid (Katou et al., 2003) into the *Bam*HI site between the *nmt1* promoter and terminator sequences (Maundrell, 1993) on pMH5 to create pMH6. pMH6 was digested by *Sse*I8387 and used for transformation of HM52 (*h*$^+$ *ura4-D18 leu1-32*).

Chromatin immunoprecipitation (ChIP) assay

ChIP assay was performed essentially as described previously (Takahashi et al., 2003). For examination of pre-RC localization at *cnt* and ChIP on chip analysis, I used ChIP samples previously prepared by Dr. Tatsuro Takahashi (Takahashi et al., 2003). In brief, HM568 (*h*$^-$ *nda3-KM311 cdc10-129 orp1::orp1-5flag ura4-D18 leu1-32*) cells harboring pREP82-cdc18

and pREP81-cdt1 were cultured at 28°C for 16 hr to express Cdc18 and Cdt1 from inducible *nmt1* promoters and then at 20°C for 4 hr for M-phase arrest. Cells synchronously reentering the cell cycle were incubated at 36°C, the restrictive temperature for the *cdc10-129*, for 3hr to arrest them in G1 phase. Cell extracts were used for ChIP assays with mouse anti-Flag (Sigma-Aldrich), rabbit anti-Orc4, rabbit anti-Mcm2 or rabbit anti-Mcm6 antibodies as described earlier (Takahashi et al., 2003). To analyze localization of pre-RC and RPA in the subtelomere and the silent *mat* locus, HM1182 (h^{90} *cdc25-22 nmt1-TK*) cells were arrested in early S phase by HU at 25°C for 80 min after G2/M synchronization (36°C, 3 hr). Cell extract was used for ChIP assays with rabbit anti-Orc4, rabbit anti-Mcm6 or rabbit anti-Ssb2 antibodies. Recovery of DNA was quantified by real time PCR using primers amplifying subtelomeric region (Kanoh et al., 2005) and the silent *mat* K-locus (Table I-3).

BrdU incorporation

HM668 (h^- *cdc25-22 ura4-D18::ura4*$^+$*nmt1-TK*$^+$) cells grown in EMM medium lacking thiamine to induce transcription of the *TK* gene at 25°C for 18 hr to 1 x 10^7 cells/ml were arrested at the G2/M boundary for 3 hr at 36°C and then released for 90 min at 25°C in the presence of 200 μM 5-bromodeoxyuridine (BrdU) and 10 mM hydroxyurea (HU). Cells (1 x 10^8) were fixed with cold water containing 0.1% sodium azide and the total cellular DNA was purified as described (Raghuraman et al., 2001). DNA was digested with *Hae*III and centrifuged in 1.7 ml of the CsCl solution containing 10 mM Tris-HCl (pH 7.4), 1 mM EDTA and 150 mM NaCl (the refractive index at 25°C adjusted to 1.4030) in a Hitachi RP120VT rotor at 80,000 rpm for 14 hr at 20°C. Fractions (120 μl each) collected from the top were dialyzed using the Micro Dialysis System (GIBCO BRL) and recovery of DNA in each fraction was analyzed after PCR-amplification with *ars2004* and nonARS primers. DNA in the HL-density fractions was pooled and used for the tiling-array analysis as described below. For quantitative analysis, DNA in each fraction was analyzed by real time PCR using SYBR Green I in 7300 Real Time PCR System (Applied Biosystems). Primers used for real time PCR are listed in Table I-3.

Tiling array (chip) analysis

S. pombe chromosomes II-III high-density oligonucleotide tiling-arrays and whole chromosome tiling-arrays were produced by Affymetrix Custom Express Service

(S_pombea520106F, P/N 550106; pombeAlla520099, P/N 520099). Sequences and positions of oligonucleotides on the array are available from Affymetrix. Amplification of chromatin-immunoprecipitated and total DNA, labeling with biotin-N6-ddATP, hybridization and primary data analyses were performed by Dr. Yuki Katou and Dr. Takehiko Itoh as described (Katou et al., 2003). For discrimination of positive and negative signals, the ChIP fraction or BrdU DNA in heavy-light fractions from early S phase cells was compared with total cellular DNA without immunoprecipitation or total DNA from G2/M phase cells, respectively, using three criteria. First, reliability of the strength of signals was judged by the detection *P*-value for each locus ($P \leq 0.025$). Second, reliability of binding ratios was judged by change in *P*-values ($P \leq 0.025$). Third, clusters consisting of at least three contiguous loci that fulfilled the above two criteria were selected. All data of the tiling array analysis are accessible at the website (http://www.nature.com/emboj/journal/v26/n5/suppinfo/7601585a.html).

ARS assay

Intergenic regions of the indicated locus were PCR amplified and cloned into pYC11, a derivative of pBluescript II SK(-) carrying the *LEU2* gene (Okuno et al., 1997), resulting in pMH12, 13, 14, 15, 16, 17, 18, 19,, 20, 21 and 22, and used for transformation of HM123 (h^- *leu1-32*). After 4 days incubation on EMM plates at 30°C, ARS plasmids yielded visible transformants at a high frequency.

Two-dimensional gel electrophoresis

HM668 cells arrested at G2/M block were released at 25°C for 90 min in the presence of 10 mM HU. DNA was prepared and digested with indicated restriction enzymes in agarose plugs (Arcangioli, 1998). Fractions enriched for replication intermediates were obtained by melting the agarose plugs as described below (Dr. Kanji Furuya, personal communication). Following 2 h digestion of genomic DNA with restriction enzymes (40 U/plug), the plugs were incubated at 70°C for 10 min, and then incubated at 37°C for 1 h with the restriction enzymes (40 U/plug), B-Agarase I (2 U/plug, New England Bio Labs Inc.) and RNaseA (1 μg/plug, Sigma-Aldrich Inc.). Supernatant was collected after centrifugation at 13,000 r.p.m. for 10 min and DNA was precipitated with isopropanol. The replication intermediates were analyzed by neutral/neutral 2D gel electrophoresis as described previously (Brewer and

Fangman, 1987).

Statistical analysis

To test the randomness of distribution of the early and late origins, I used Wald-Wolfowitz runs test (Chang, 2000). A 'run' means a sequence of adjacent equal symbols. For example, the sequence "EEELLLELLLLLEELE" is divided in seven runs: four of them are made of 'E' and the others are made of 'L'. If the two symbols are generated randomly, an expected number of runs, μ, and the variance, σ^2, are given as $\mu = 1 + (2N_E N_L) / N$ and $\sigma^2 = 2N_E N_L(2N_E N_L - N) / N^2(N - 1) = (\mu - 1)(\mu - 2) / (N - 1)$, respectively, where N_E is the number of E, N_L that of L, and $N = N_E + N_L$. The z statistic is given by $z = (Ra - \mu) / \sqrt{\sigma^2}$, where Ra is the actual number of runs in the pattern. If the z statistic is negative, the actual number of runs is smaller than the expected number of runs, which means that each symbol has tendency to be clustered. I set the significance level, α, as 0.01 in the analysis and calculated the z statistic for the distribution of the early and late origins on the left and right arms of each chromosome except for chromosome III, where the number of late origins is too small for valid statistics. All the values of z were negative and I could successfully reject null hypothesis that the distribution pattern of the early and late origins is random on the whole chromosome I and on the left arm of chromosome II ($P < 0.01$), whereas the randomness was not rejected in the right arm of chromosome II ($P = 0.0198$).

Table I-2 ***S. pombe*** **strains used in this study**

Strain	Genotype		Figures I
HM52	h^+	*ura4-D18 leu1-32*	used for transformation
HM123	h^-	*leu1-32*	7B
HM568	h^-	*ura4-D18 leu1-32 nda3-KM311 cdc10-129 orp1::5FLAG-orp1*	1, 2, 7A, 11A, 12A, 12B
HM654	h^+	*ura4-D18::ura4+nmt1-TK+ leu1-32*	transformant
HM668	h^-	*cdc25-22 ura4-D18::ura4+nmt1-TK*$^+$	1, 4, 5, 7A, 7C, 8, 9, 11A, 12A
HM1182	h^{90}	*cdc25-22 ura4-D18::ura4+nmt1-TK*$^+$ *his2 Kint2::ura4*$^+$	11B, 13
HM1405	h^-	*cdc25-22 cds1 Δ::kanMX6 ura4-D18::ura4+nmt1-TK*$^+$	8, 9

Table I-3 Primers used in this study

Locus	Name	Sequence	Source
ars2004	ars2004-66-F	5'-CGGATCCGTAATCCCAACAA-3'	This study
	ars2004-66-R	5'-TTTGCTTACATTTTCGGGAACTTA-3'	
nonARS	nonARS-70-F	5'-TACGCGACGAACCTTGCATAT-3'	This study
	nonARS-70-R	5'-TTATCAGACCATGGAGCCCATT-3'	
AT2080	AT2080-71-F	5'-CGAACAACAGGCTTGGTTAGAA-3'	This study
	AT2080-71-R	5'-GAAGTACGGACTTGTTTCGATTCC-3'	
dg	dg-108-F	5'-TCCAAATGTCGCATGAACACTC-3'	This study
	dg-108-R	5'-CTTTTTTGGGAATACATTGGGTTT-3'	
cnt2	cnt2-211-F	5'-GGTTTTATGATTTTGGCGAAGTG-3'	This study
	cnt2-211-R	5'-CGACAAGCGTGGATTTATTTTATG-3'	
subtelomere	telo2R-203-F	5'-GACTACAGCCACAAGCTA-3'	This study
	telo2R-203-R	5'-CATTATGACTTCCAATCCCT-3'	
subtelomere	TEL-59-F	5'-CAGAAGAGACTACAGAGGCGGTTT-3'	This study
	TEL-59-R	5'-GGATGCCTTATCTGCGACCA-3'	
subtelomere	jk682 (18K-#1)	5'-AATTTCAGTTGCCAAGGGACA-3'	Kanoh *et al.*, 2005
	jk683 (18K-#2)	5'-GGGTCAAAACCTGCGCATAA-3'	
subtelomere	jk386 (14K-#1)	5'-TTCCAAGTATGCCAGCTTATCATC-3'	Kanoh *et al.*, 2005
	jk387 (14K-#2)	5'-CATCAGCAACGTCGCCAACT-3'	
subtelomere	jk384 (12K-#1)	5'-GCTCTCGACAAAGCCGTTCT-3'	Kanoh *et al.*, 2005
	jk385 (12K-#2)	5'-CAGCATTAACCAACAGTGGTCTTC-3'	
subtelomere	jk620 (E-9K-#1)	5'-TTCTTAATCATTATCAAGTATTCATTGCAA-3'	Kanoh *et al.*, 2005
	jk621 (E-9K-#2)	5'-ACAGTAAACTATGATCGCTTTTGAAGAC-3'	
subtelomere	jk618 (D-6.5K-#1)	5'-GCCTACCGCTTGCAGTTGTT-3'	Kanoh *et al.*, 2005
	jk619 (D-6.5K-#2)	5'-GGTTTGAGCATCTGTCAGAGGTAA-3'	
subtelomere	jk614 (A-3K-#1)	5'-GTCTCGTTGCTCGCTTCACA-3'	Kanoh *et al.*, 2005
	jk615 (A-3K-#2)	5'-GGAGGATGGGAAATTTTGAGGAT-3'	
subtelomere	jk380 (TEL-0.3K-#1)	5'-TATTTCTTTATTCAACTTACCGCACTTC-3'	Kanoh *et al.*, 2005
	jk381 (TEL-0.3K-#2)	5'-CAGTAGTGCAGTGTATTATGATAATTAAAATGG-3'	
mat K-locus	matK-L(-8k)-113-F	5'-AATGCGATAGCGGCATAAGG-3'	This study
	matK-L(-8k)-113-R	5'-GGTCTCGTGGCTCTCGGTT-3'	
mat K-locus	matK-L(-5k)-71-F	5'-TACCCGATACGGTGCTGGAT-3'	This study
	matK-L(-5k)-71-R	5'-AACTTTTAAGGACACCCGGCTA-3'	
mat K-locus	matK-IR-60-F	5'-CAGAAGAGACTACAGAGGCGGTTT-3'	This study
	matK-IR-60-R	5'-CCCAGGACCCCAAACCAT-3'	
mat K-locus	matK-L(-2k)-65-F	5'-CATGTAGGCATCGAGAAAGCTG-3'	This study
	matK-L(-2k)-65-R	5'-ATAACTATTGGGAAGTGAACGTGATG-3'	

mat K-locus	RT-matK108-F	5'-TCTTCCCTGCGTTGGACTTC-3'	This study
	RT-matK108-R	5'-CACCCTACCATCCGTGTTACCT-3'	
mat K-locus	matK(4k)-83-F	5'-ACGGGATTAGTGCTGCAAATG-3'	This study
	matK(4k)-83-R	5'-GTTCATGGGATCCGTCACATT-3'	
mat K-locus	matK(7k)-62-F	5'-TCGTCGATGTCTAAGAAGGATCTAAG-3'	This study
	matK(7k)-62-R	5'-TGTTTGTTTTGCTGATCTGTTTTCT-3'	
mat K-locus	matK(10k)-65-F	5'-CTGGAAAATCAAAGTGCGCTAA-3'	This study
	matK(10k)-65-R	5'-GCTTCCTCGCCTGCTTACAT-3'	
mat K-locus	matK-R(2.5k)-174-F	5'-ATCCCAAGCACCAAGCTTTG-3'	This study
	matK-R(2.5k)-174-R	5'-TCCTGCCGAAGTTTCTAAATGAG-3'	
mat K-locus	matK-R(6k)-90-F	5'-GATACGGGTTATTGTCGACTTGAA-3'	This study
	matK-R(6k)-90-R	5'-CGTGTCGTTGGTAGTCTTAGCATT-3'	
mat K-locus	matK-R(9k)-68-F	5'-ATTAACAAGTGCCCAGCTTCTGA-3'	This study
	matK-R(9k)-68-R	5'-CATCACGAAGATGGCACTTTCTAA-3'	

Part II: The heterochromatin protein Swi6/HP1 activates replication origins at pericentromeres and the silent mating-type locus

INTRODUCTION

Heterochromatin is highly condensed chromosomal regions throughout the cell cycle. In many cases heterochromatin replicates in late S phase and hardly contains transcriptionally active genes. Epigenetic inactivation of ectopic genes in heterochromatic loci provided the notion that a highly condensed chromatin is inaccessible to trans-acting factors. A molecular mechanism underlying such function has been explained by the presence of conserved heterochromatin protein, HP1, which binds to methylated Lys 9 on histone H3 (H3K9Me) with its chromo-domain (Nakayama et al., 2001b). HP1 also dimerizes through its chromoshadow-domain, which probably gives a basis for higher order chromatin structure at heterochromatin. However, the situation is not so simple. Growing evidences indicate that heterochromatin is not so an inert and inaccessible domain but rather has a dynamic and plastic feature (Maison and Almouzni, 2004). Previous study in fission yeast has shown that, among its major constitutive heterochromatin, the pericentromere, the silent mating-type (*mat*) locus and the subtelomere, the pericentromere and the *mat* locus contain active replication origins that fire in early S phase (Kim et al., 2003; Kim and Huberman, 2001)(see also ***Part I***). This phenomenon also argues against considering heterochromatin as an inactive and static domain and suggests an active regulation of replication in heterochromatin, yet the molecular basis for activation of heterochromatic replication remained elusive.

Recent studies in fission yeast indicate that Swi6, a fission yeast homologue of HP1, serves as a molecular platform to recruit a variety of effectors, such as factors involved in transcriptional silencing, modifications of histones, chromosome segregation and even in transcriptional activation (Grewal and Jia, 2007), shedding light on dynamic feature of heterochromatin (Zofall and Grewal, 2006). Moreover, Swi6 has been shown to interact with replication factors, such as Polα, a primase at replication fork (Ahmed et al., 2001; Nakayama et al., 2001a), and Dfp1, a regulatory subunit of Dbf4-dependent kinase (DDK) essential for replication initiation (Bailis et al., 2003). However, these interactions have been considered

to represent participation in heterochromatin maintenance and cohesin localization, respectively, and thus involvement of Swi6 in regulation of replication has remained unclear.

Initiation of replication proceeds in stepwise manner: formation of pre-replicative complex (pre-RC) in G1 phase and activation of pre-RC in the following S phase (Bell and Dutta, 2002). In fission yeast, loading of Sld3 is the furthest upstream reaction in activation of pre-RC depending on DDK; then GINS is recruited depending on CDK, followed by Cdc45 loading (Yabuuchi et al., 2006). Assembly of DNA polymerases and RPA, a single strand binding protein, follows the activation of MCM, resulting in initiation of replication. Each step has a potential to be influenced by chromatin context and thus may become a target of heterochromatin specific regulation of replication.

Here I show that Swi6 activates heterochromatic replication origins in pericentromere and the *mat* locus, which results in early replication of these loci. In swi6 deletion mutant, efficiency of replication initiation reduced in these heterochromatic loci, resulting in retardation of replication kinetics specifically at the pericentromere and the *mat* locus. ChIP-qPCR analysis shows that Swi6 stimulates Sld3 loading at heterochromatin. Point mutations at a putative chromoshadow-domain binding (HP1-binding) motif at C terminal region of Dfp1 abrogate interaction between Swi6 and Dfp1 *in vitro* and early replication of Swi6-bound heterochromatin *in vivo*. Furthermore, tethering Dfp1-chromodomain fusion protein to heterochromatin in the absence of Swi6 restored early replication. These results strongly suggest that Swi6 recruits DDK through the interaction with Dfp1, which results in loading of Sld3 and activation of replication origins in hardly accessible heterochromatic region.

RESULTS

Swi6 activates replication origins specifically at the pericentromeres and the silent *mat* locus

To elucidate the role of Swi6 in replication of heterochromatin, I examined the replication kinetics of heterochromatin loci in wild type and *swi6Δ* cells. The heavy analogue 5-bromo-2'-deoxyuridine (BrdU) was incorporated into the newly synthesized DNA for various periods of the synchronous cell cycle and replicated DNA with heavy-light density was separated from non-replicated DNA by CsCl density gradient centrifugation. Replication efficiencies were calculated by real-time PCR for replication origins in the pericentromere (Smith et al., 1995), the *mat* locus (*matK*: 20 kb from the *mat1* locus, see ***Part I***)(Olsson et al., 1993) and the subtelomere (21 kb from the telomeric end, see ***Part I***)(Fig. II-1A; red, orange, purple lollipops, respectively), as well as an early replication origin in the euchromatic region (*ars2004*)(Fig. II-1A; black lollipop) and a non-origin locus (*nonARS*) located at about 30 kb from the *ars2004* origin (Fig. II-1A; white lollipop). All origins including the subtelomeric origin have autonomously replicating activity (ARS activity) when cloned on a plasmid (Fig. II-1B). In the wild type, *ars2004* replicated earlier than the *nonARS* locus by about 10 min (Fig. II-2). The replication kinetics of the pericentromere and *matK* were similar to those of *ars2004*, showing early replication of these heterochromatic loci, whereas the subtelomeric origin (subtelomere) replicated much later than the *nonARS* locus. Moreover, the telomere-proximal locus (TEL-0.3K; dark red lollipop in Fig. II-1A) replicated even later than the subtelomeric origin, suggesting passive replication of the subtelomeric region by a replication fork from telomere-distal side. In *swi6Δ* cells, the profiles of the *ars2004* and the *nonARS* loci were similar to those of the wild type (Fig. II-2). The replication kinetics of the subtelomere and the TEL-0.3K did not change (Fig. II-2), suggesting that the subtelomeric origin does not fire efficiently in early S phase in the absence of Swi6. Surprisingly, however, replication of the pericentromere and *matK* was delayed as late as that of the *nonARS* locus (Fig. II-2), indicating that Swi6 is required for early replication of the pericentromere and the silent *mat* locus. To examine whether this role of Swi6 is dependent on its localization at these heterochromatic loci, I introduced a chromo-domain mutation, *swi6-W104A*, which impairs the interaction of *Dorosophila* HP1 with H3K9me (Jacobs and Khorasanizadeh, 2002). The mutation caused defect in silencing of a reporter *ura4*$^{+}$ gene

Figure II-1

A

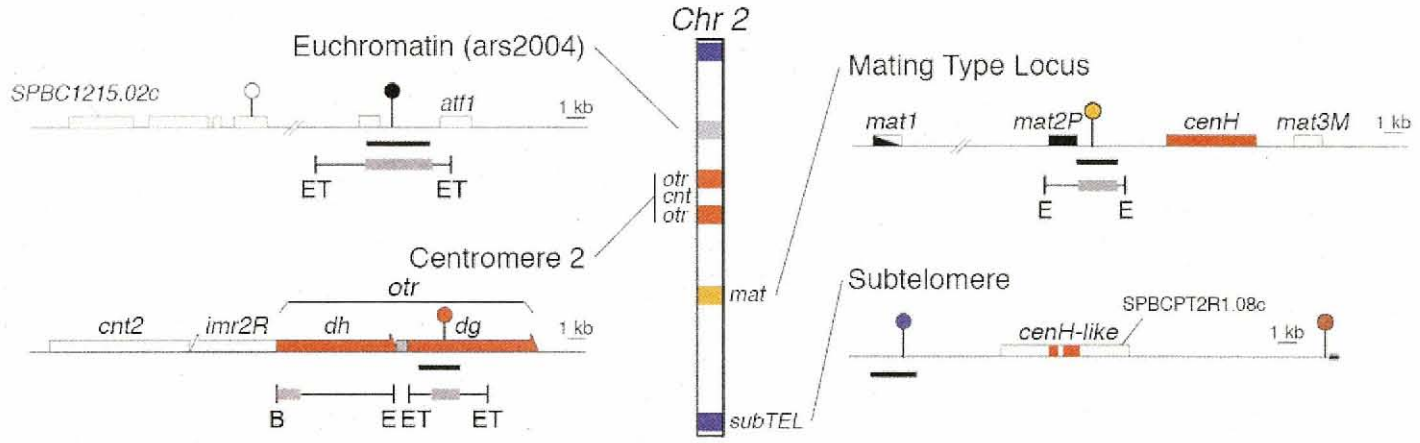

B

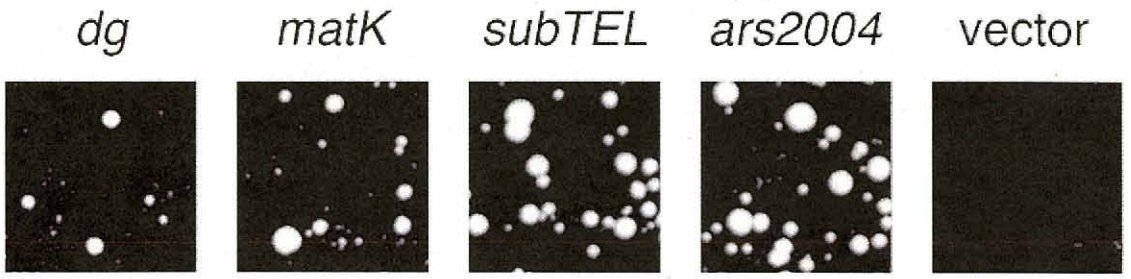

Fig. II-1. All heterochromatic loci contain autonomously replicating sequence (ARS). (A) Schematic representation of fission yeast euchromatic (ars2004) and heterochromatic (centromere, the silent mating type locus and subtelomere) loci. The central vertical box represents a whole view of chromosome 2 along with the locations of ars2004 (gray); *otr*, pericentromeric heterochromatin (red) flanking the central core region (*cnt*); mat, the mating type locus (orange); and *subTEL*, subtelomeric heterochromatin (purple). Maps of relevant regions are shown. The *dh* and *dg* repeats at the outer centromere, *cenH* in the silent mating type locus and *cenH-like* in subtelomere contain sequences involved in the establishment of heterochromatin through an RNAi-dependent mechanism (red boxes on each map). A black bar below the map denotes the fragment used for ARS analysis. Relevant restriction fragments (ET, *Eco*T22I; B, *Bam*HI; E, *Eco*RI) and probes (gray box) used for two-dimensional gel electrophoresis and southern hybridization are shown below the maps (Fig. II-4B). Lollipops represent positions of the segment analyzed by quantitative real-time PCR. (B) To examine the ARS activity of heterochromatic replication origins, fragments corresponding to ars3.0K (Smith et al., 1995) in the pericentromere (*dg*) and ars2PR (Olsson et al., 1993) in the *mat* locus, which had been previously described, were PCR-cloned into pYC11 carrying *LEU2* gene. For the subtelomeric replication origin, a fragment that contains multiple AT-stretches characteristic in fission yeast replication origins at 21 kb from the right telomere of chromosome 2 was PCR-cloned into pYC11. Each plasmid was introduced into HM123 (*h⁻ leu1-32*) followed by 5 days incubation at 30°C. Ars2004 and vector serve as positive and negative controls, respectively.

Figure II-2

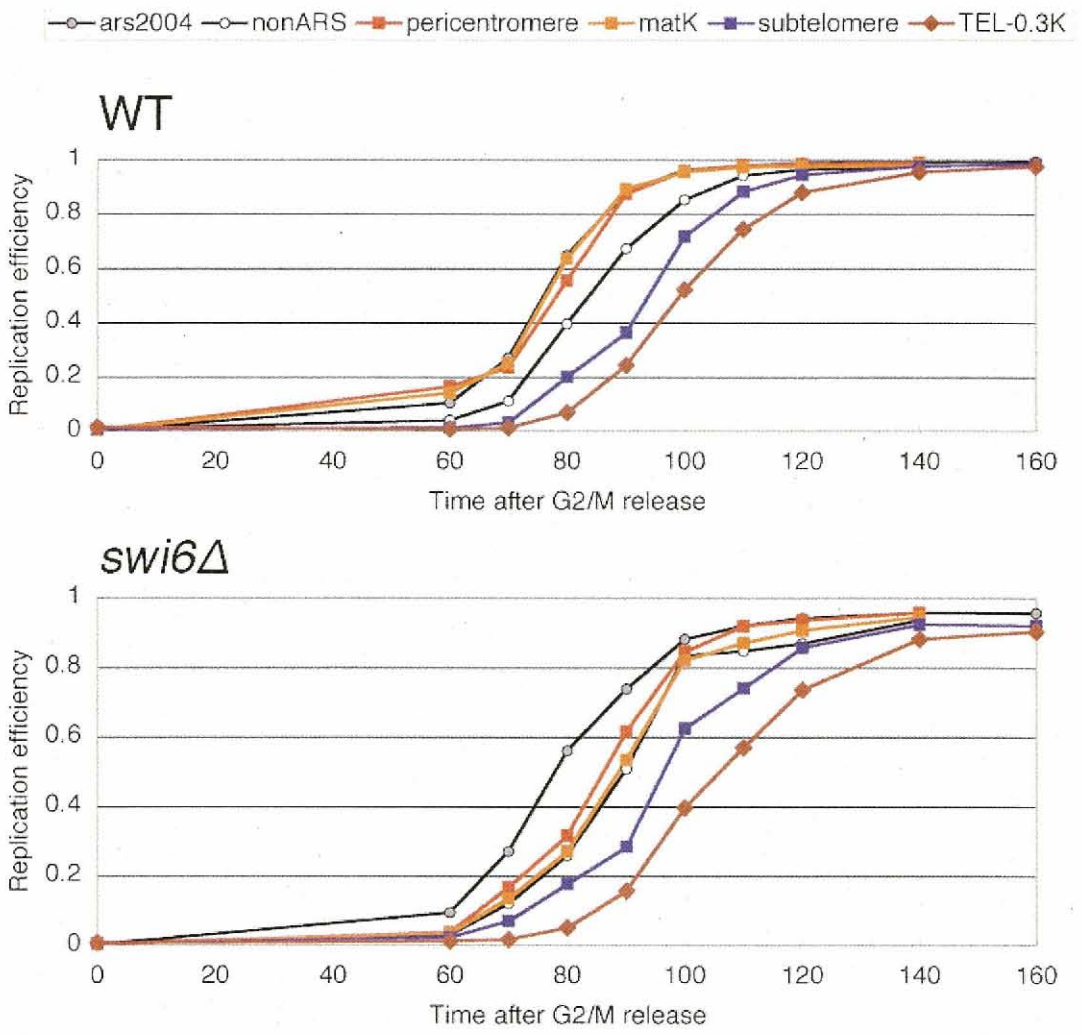

Fig. II-2. Early replication at the pericentromere and the *mat* locus depends on Swi6. Wild-type and *swi6Δ* cells carrying *cdc25-22* were arrested in G2/M phase at 36°C for 3 hr and then released at 25°C in the presence of BrdU. At the indicated time points, newly replicated DNA with heavy-light (HL) density was separated from unreplicated light-light (LL) DNA by CsCl density gradient centrifugation. Replication efficiency was determined by quantitative real-time PCR with the primers described in Fig. II-1A.

inserted at the silent *mat* locus (Fig. II-3B) in the presence of the mutant protein (Fig. II-3A), indicating that localization of Swi6 is impaired by the mutation. Strikingly, I observed delay in replication of the pericentromere and the silent *mat* locus in the mutant (Fig. II-3C), suggesting that H3K9me-dependent localization of Swi6 is required for early replication of these loci.

To examine whether the delay in replication of the pericentromere and *matK* in *swi6Δ* cells is caused by impaired initiation of replication, replication efficiency was measured in the presence of hydroxyurea (HU). In the wild type, *ars2004*, the pericentromere and *matK* replicated at efficiencies about ten times higher than the *nonARS* and the subtelomere (Fig. II-4A), consistent with efficient initiation at the pericentromere and the silent *mat* locus. In contrast, in *swi6Δ*, the replication efficiencies at the pericentromere and *matK* were reduced to the level of the *nonARS* locus, whereas *ars2004* replicated as efficiently as in the wild type (Fig. II-4A). These results suggest that Swi6 is required for initiation of replication at these heterochromatic loci. To examine more directly whether absence of Swi6 decreases initiation of replication at these loci, replication intermediates were analyzed by two-dimensional (2D) gel electrophoresis. In the wild type, the presence of bubble arcs at *ars2004*, the *dh* and *dg* repeats of the pericentromere and the *matK* locus indicates initiation of replication at these loci (Fig. II-4B, arrowheads). Strong Y arcs at the *dh* and *dg* repeats probably represent passive replication from neighboring repeats. In *swi6Δ* cells, the bubble arcs were reduced at the *dh* and *dg* repeats and the *matK* locus but not at *ars2004*, indicating reduced initiation of replication specifically at the pericentromere and the *mat* locus (Fig. II-4B). In addition, the Y arcs at the pericentromeric repeats were reduced, which is consistent with impaired initiation at the repeats (Fig. II-4B). These results confirm that Swi6 is required for efficient initiation of replication at the pericentromere and the silent *mat* locus.

Swi6 stimulates Sld3 loading at the pericentromeres and the silent *mat* locus

The initiation process consists of assembly of initiation factors at replication origins. In fission yeast, the factors assemble in a distinct order (Yabuuchi et al., 2006)(Fig. II-5A). To elucidate the mechanism by which Swi6 stimulates initiation of replication, we examined localization of replication factors at origins using chromatin immunoprecipitation (ChIP) analysis. I first examined Orc4 and Mcm6, components of pre-RCs, in wild type and

Figure II-3

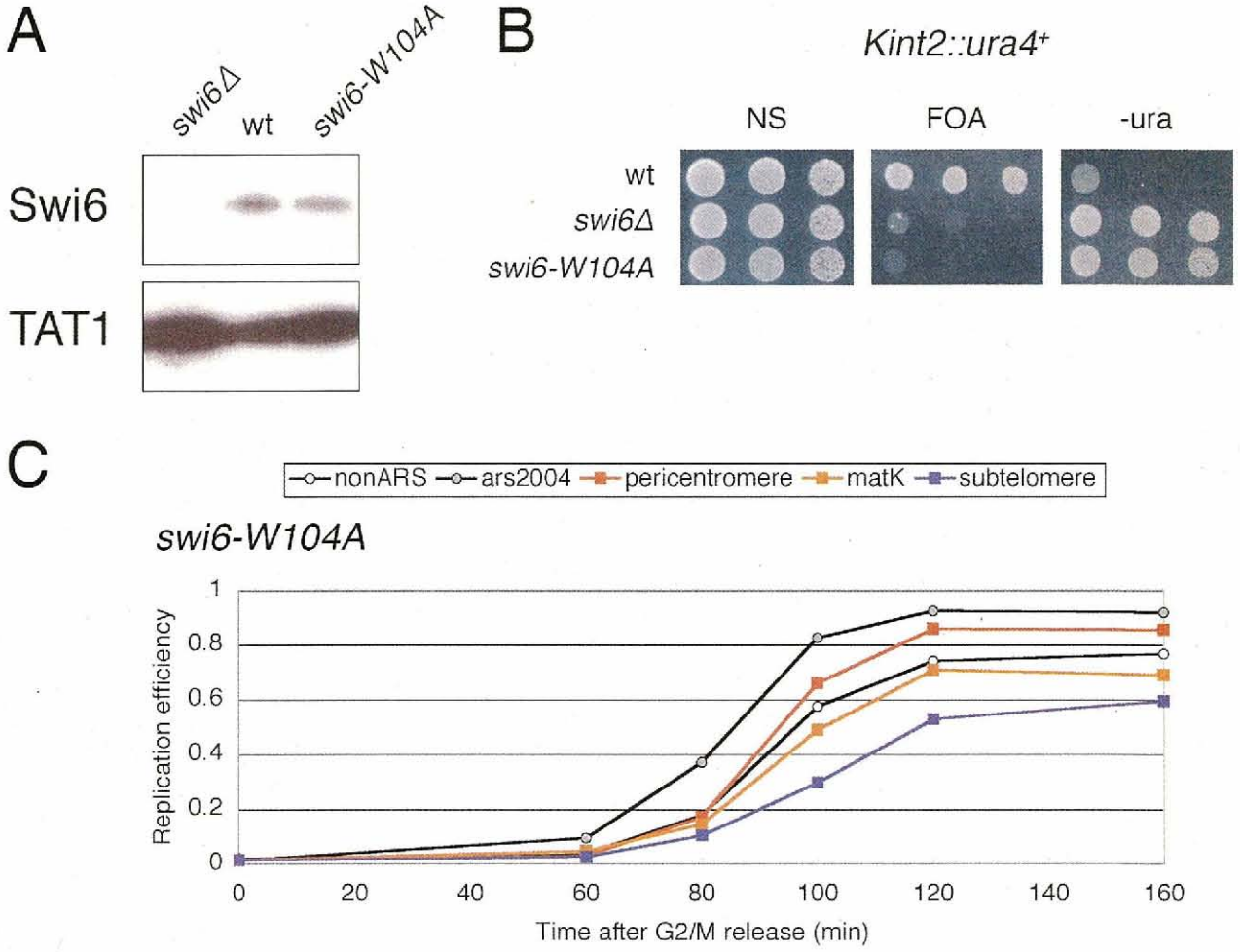

Fig. II-3. Swi6 promotes early replication at the pericentromere and the *mat* locus in a chromo-domain dependent manner. (A) The expression of Swi6-W104A was confirmed. Wild type (wt), *swi6Δ* or *swi6-W104A* cells were harvested and the cell extracts were analyzed by western blotting with anti-Swi6 (top) or anti-TAT1 (bottom) antibodies. TAT1 serves as a loading control. (B) The point mutation *swi6-W104A* impairs the silencing at the silent *mat* locus. Silencing of a *ura4*+ marker inserted at the silent *mat* locus was examined by growth on selective media. Ten-fold-diluted cultures of indicated strains were plated onto nonselective medium (NS), medium containing 5-FOA (FOA) and medium lacking uracil (-ura). (C) Chromo-domain of Swi6 is required for early replication at the pericentromere and the *mat* locus. Replication kinetics in *swi6-W104A* cells were analyzed as in Fig. II-2.

Figure II-4

A

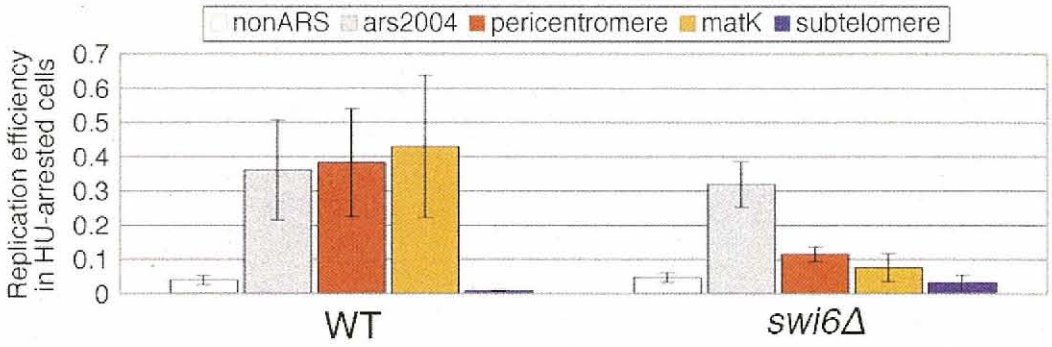

B

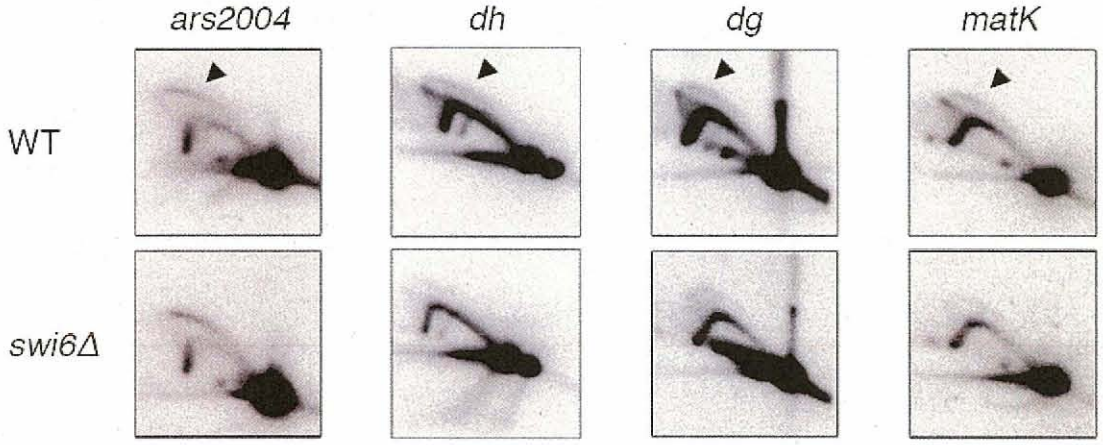

Fig. II-4. Swi6 promotes firing of origins in early S phase specifically at the pericentromere and the *mat* locus. (A) Replication efficiency was determined in wild-type and *swi6Δ* cells in the presence of HU (10 mM) at 100 min after release from G2/M synchronization. Error bars represent standard deviations. (B) Swi6 promotes initiation of replication at the pericentromere and the *mat* locus. Replication intermediates prepared from wild-type or *swi6Δ* cells with HU at 80 min after release from G2/M arrest were analyzed by neutral-neutral two-dimensional gel electrophoresis. Arrowheads indicate bubble arcs in wild-type samples.

Figure II-5

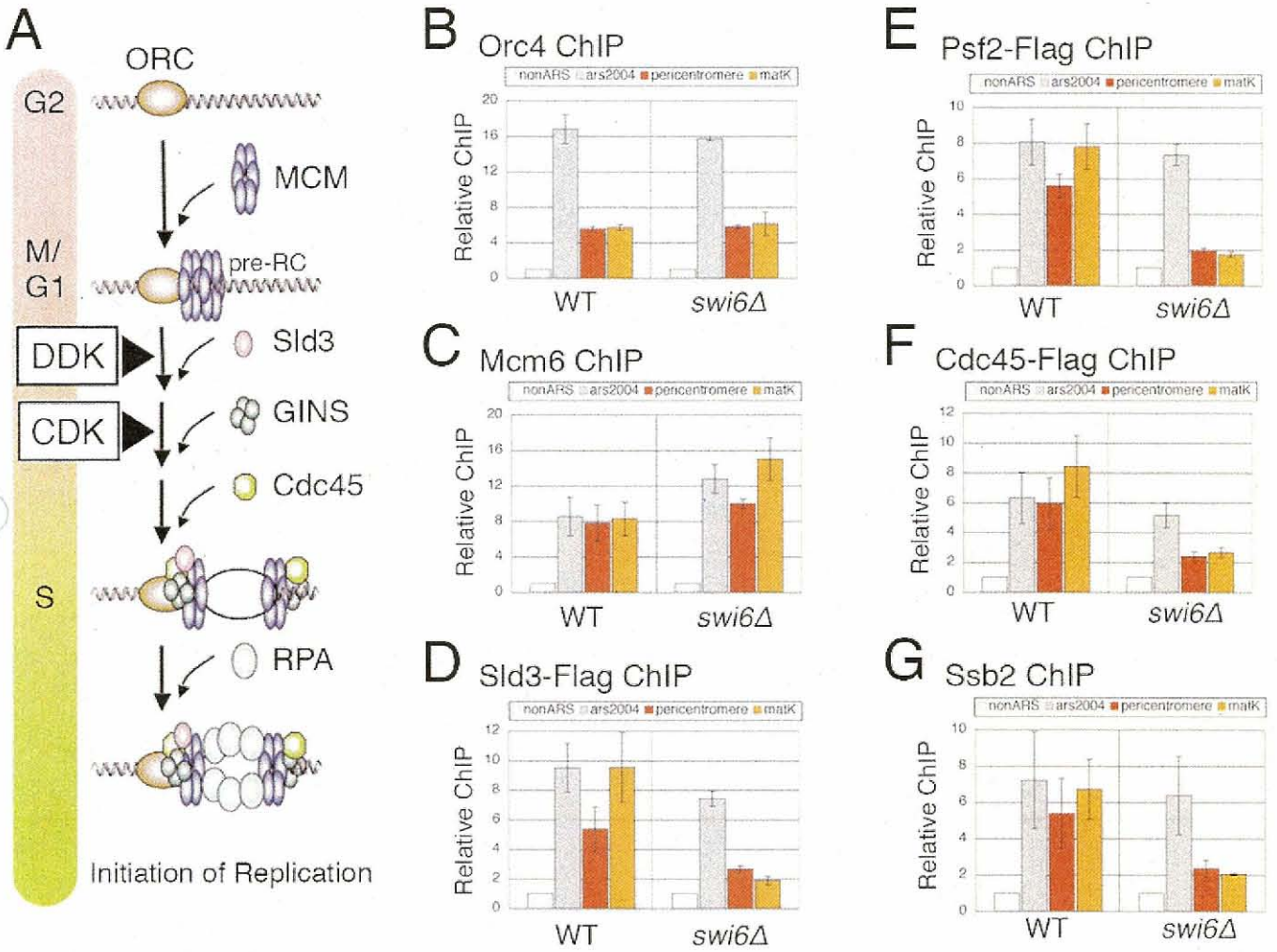

Fig. II-5. Swi6 stimulates loading of Sld3 at the pericentromere and the *mat* locus. (A) A model for replication initiation in fission yeast. ORC and MCM complexes bind to replication origins to form pre-replicative complexes (pre-RCs) in G1 phase. At the onset of S phase, Sld3 binds to origins in a DDK-dependent manner, and then the GINS complex is recruited in a CDK-dependent manner, followed by loading of Cdc45 before the single strand DNA binding protein (RPA) binds. (B-G) Localization of Sld3 to the pericentromere and the *mat* locus is impaired in *swi6Δ* cells. Localization of Orc4 (B), Mcm6 (C), Sld3-5Flag (D), Psf2-5Flag (E), Cdc45-5Flag (F) and Ssb2 (G) at euchromatic and heterochromatic loci was examined by ChIP using quantitative real-time PCR. Wild-type and *swi6Δ* cells, carrying psf2-5Flag or cdc45-5Flag, were arrested in early S phase by HU for 80 min after G2/M synchronization (B, C, E-G). Wild-type and *swi6Δ* cells, carrying sld3-5Flag, were arrested in early S phase by using *mcm5* mutant (Yamada et al., 2004) after G2/M synchronization (D). Recovery ratios of immunoprecipitated DNA to total DNA at the indicated loci were normalized to the value of nonARS locus. Error bars represent standard deviations.

swi6Δ cells arrested in early S phase by HU. Orc4-ChIP analysis in wild type revealed that the *ars2004*, pericentromere and *matK* fragments were enriched relative to the *nonARS* locus, indicating localization of ORC at these origins (Fig. II-5B). Absence of Swi6 did not affect localization of Orc4 (Fig. II-5B). Similarly, the preferential localization of Mcm6 at *ars2004*, pericentromere and *matK* was not decreased in *swi6Δ* cells (Fig. II-5C), indicating that Swi6 is not required for pre-RC formation at the pericentromere and the silent *mat* locus. In contrast, localization of Sld3 was decreased in *swi6Δ* cells at the pericentromere and *matK* but not at *ars2004* (Fig. II-5D). Consistent with this observation, localization of Psf2 (a component of GINS), Cdc45 and Ssb2 (a component of RPA), which depend on Sld3, was reduced at the pericentromere and the *matK* locus in *swi6Δ* (Figs. II-5E-G). These results strongly suggest that Swi6 stimulates loading of Sld3 onto origins in the pericentromere and the silent *mat* locus.

Physical interaction between Swi6 and Dfp1 is required for early replication at the pericentromeres and the silent *mat* locus

Then I addressed the molecular mechanism of the stimulation of Sld3-loading by Swi6. It has been reported that a C-terminal region of Dfp1, which contains a putative chromoshadow-domain binding (HP1-binding) motif (PxVxL/I/V), is involved in the interaction with Swi6 (Bailis et al., 2003). This interaction was thought to be separable from initiation activity of DDK, because overall DNA replication appeared to be normal in a *dfp1* mutant lacking the C-terminal region (Bailis et al., 2003). However, since DDK is required for loading of Sld3 onto replication origins (Yamada et al., 2004), I examined the possibility that the interaction is required for initiation of replication specifically at the pericentromere and the silent *mat* locus. To verify the interaction of Swi6 with Dfp1 *in vitro*, S-peptide tagged Dfp1 was mixed with GST-Swi6 or GST alone and pulled down with glutathione beads. Dfp1 was recovered with GST-Swi6 but not with GST alone, indicating that Dfp1 interacts directly with Swi6 (Fig. II-6B, lanes 6 and 10). I then tested whether the HP1-binding motif of Dfp1 is required for the interaction, by introducing amino acid changes in the motif (Fig. II-6A). Recovery of Dfp1-3A (carrying P447A, V449A and I451A substitutions) and Dfp1-2E (V448E and V449E) by pull-down assay was greatly reduced compared with wild type Dfp1 (Fig. II-6B, lanes 11 and 12), indicating that the motif is required for the interaction. To examine the effects of the substitutions on DNA replication *in vivo*, the endogenous *dfp1*$^{+}$

Figure II-6

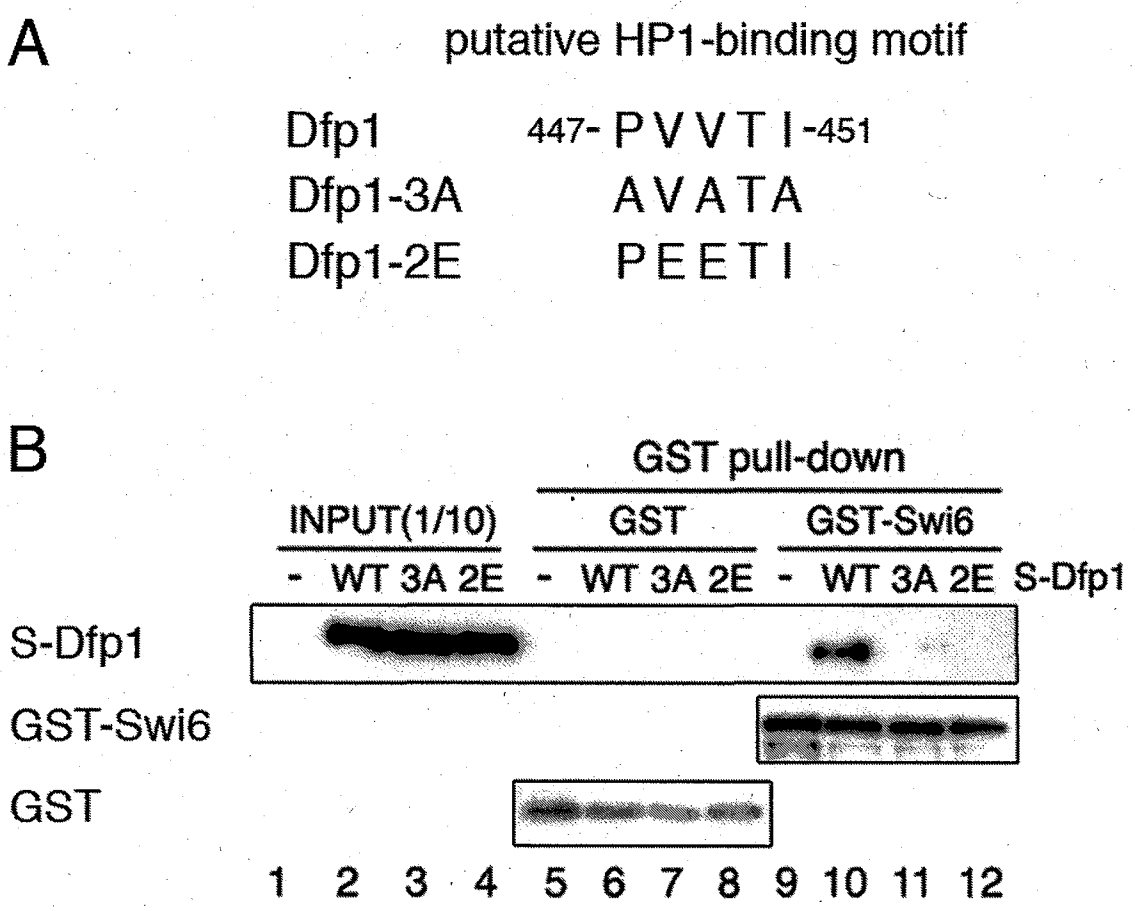

Fig. II-6. The HP1-binding motif in Dfp1 is required for efficient interaction with Swi6. (A) The amino acid sequence of the HP1-binding motif in the C-terminal region of Dfp1 and the substitutions in the motif (Dfp1-3A and Dfp1-2E) are shown. (B) The point mutations reduce the efficiency of interaction between Swi6 and Dfp1. S-peptide tagged Dfp1, Dfp1-3A and Dfp1-2E expressed *in vitro* were incubated with GST or GST-Swi6 in the presence of glutathione beads, and bead-bound proteins were analyzed by western blotting with anti-S and anti-GST antibodies.

Figure II-7

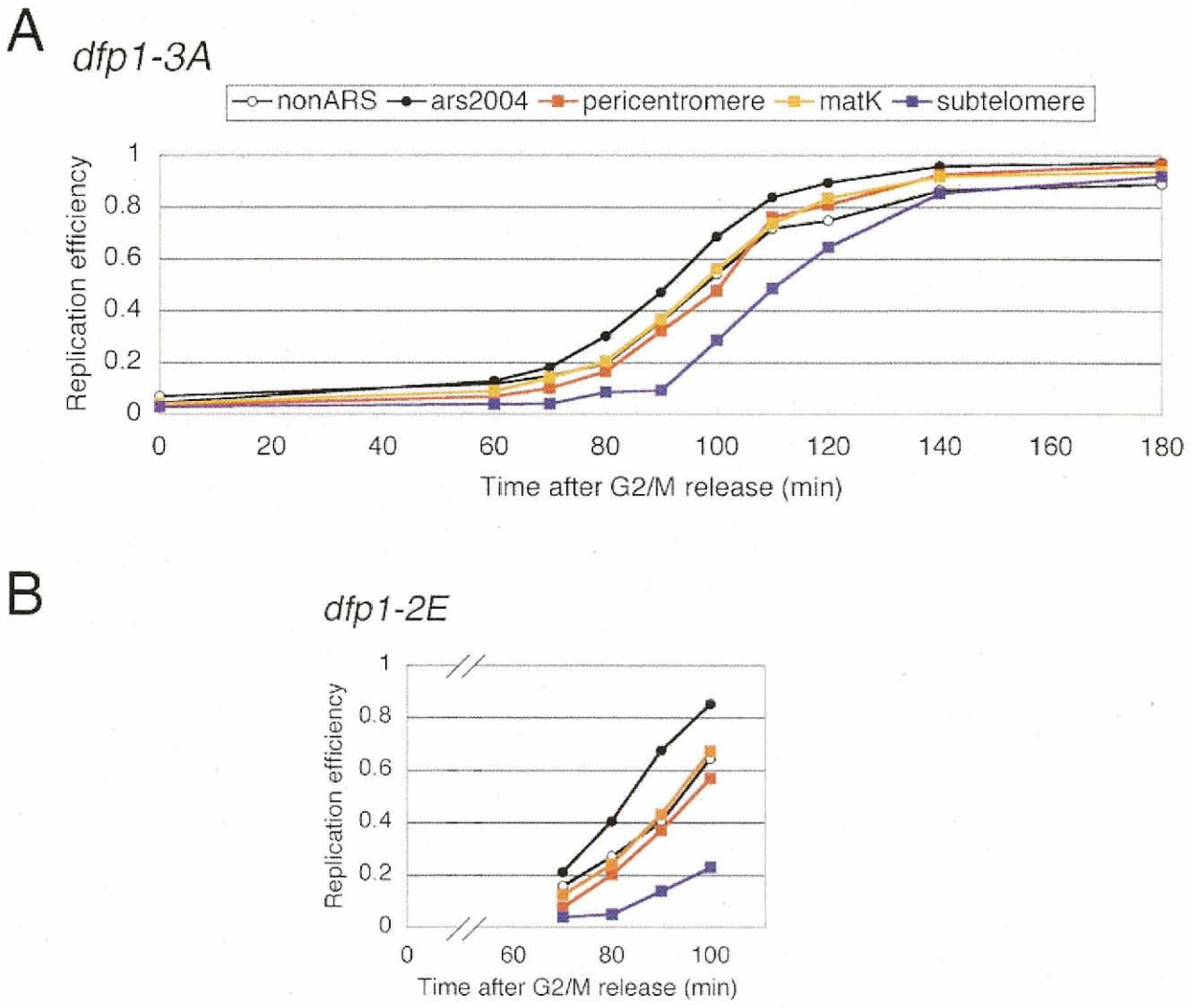

Fig. II-7. **Early replication of the pericentromere and the *mat* locus depends on the HP1-binding motif of Dfp1.** Replication kinetics in *dfp1-3A* (A) or *dfp1-2E* (B) cells were analyzed as described in Fig. II-2.

Figure II-8

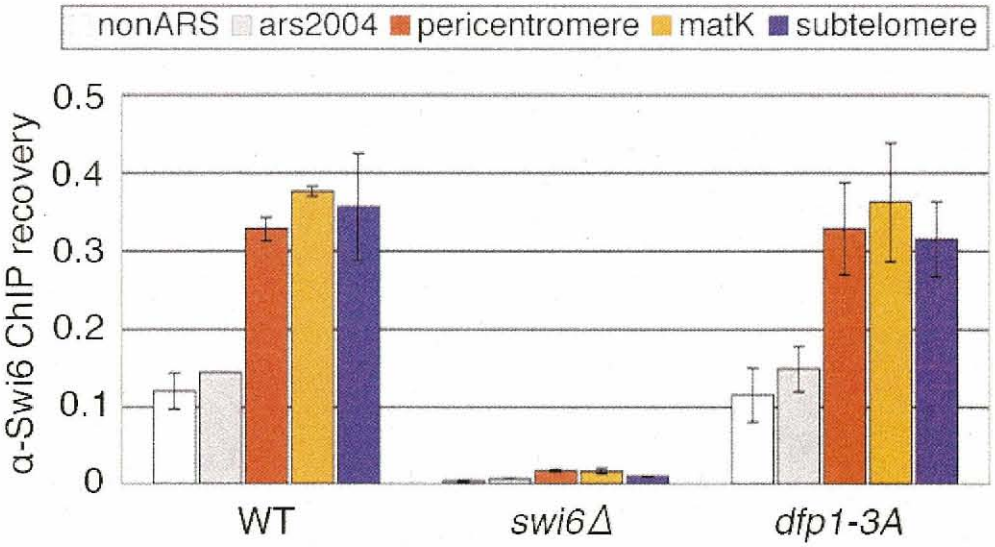

Fig. II-8. Swi6 localization at heterochromatin is maintained in the *dfp1-3A* mutant. The localization of Swi6 was analyzed by ChIP in wild type, *swi6Δ* and *dfp1-3A* cells arrested in early S phase by HU. Recovery ratios of immunoprecipitated DNA to total DNA at the indicated loci are shown. Error bars represent standard deviations.

gene was replaced with *dfp1-3A*. Replication of the pericentromere and *matK* in *dfp1-3A* cells was delayed to that of the *nonARS* locus, similar to the results observed in sw*i6Δ* cells (Fig. II-7A, compare with Fig. II-2). The *dfp1-2E* mutation caused similar delay in replication of the pericentromere and the *matK* (Fig. II-7B). Localization of Swi6 at heterochromatin was not significantly altered by the *dfp1-3A* mutation (Fig. II-8), suggesting that DDK functions downstream of Swi6 localization. These results show that the interaction of Swi6 with Dfp1 is required for early replication at the pericentromere and the silent *mat* locus. I attempted to determine localization of DDK by ChIP analysis in order to assess whether recruitment of DDK to these heterochromatic loci is dependent on Swi6. However, because of the low signal-noise ratio of immunoprecipitated DNA with S-4FLAG-Dfp1 or Dfp1-13Myc, I could not locate DDK at the pericentromere, the *matK* or even at the euchromatic origin *ars2004* (data not shown). Moreover, tagging C-terminal region by 13Myc caused defect in replication at the pericentromere locus (data not shown), suggesting that the C-terminal tag affects the interaction between Swi6 and Dfp1.

Forced recruitment of Dfp1 to the pericentromeres and the silent *mat* locus in the absence of Swi6 restores early replication of the loci

The results described above prompted me to examine whether forced localization of DDK at the pericentromere and the silent *mat* locus would restore early replication in the absence of Swi6. To localize Dfp1 to these loci in *swi6Δ* cells, Dfp1 fused at the C-terminus with two tandem copies of the chromo-domain (CD) of Swi6, which binds to H3K9me, was expressed from the native *dfp1*-promoter, because H3K9me remains in the pericentromere and at the specific sites within the silent *mat* region independently from Swi6 (Hall et al., 2002; Nakayama et al., 2001b; Sadaie et al., 2004). As shown in figure II-9A, early replication of the pericentromere and *matK* was restored in *swi6Δ dfp1-CFP-2CD* cells. As a control, expression of CFP-2CD without fusion to Dfp1 did not significantly affect replication of these loci (Fig. II-9A). Consistent with these results, I confirmed that bubble arcs were restored at the pericentromere and the silent *mat* locus in *swi6Δ* cells by expressing Dfp1-CFP-2CD, but not by expressing CFP-2CD (Fig. II-10). I also showed that tethering of Dfp1-3A-CFP-2CD to the pericentromere and the *mat* locus in *swi6Δ* cells restored early replication (Fig. II-9B), suggesting that delayed replication of these loci in *dfp1-3A* cells was caused by inefficient localization of DDK at these sites. From these results, I concluded that Swi6 activates

Figure II-9

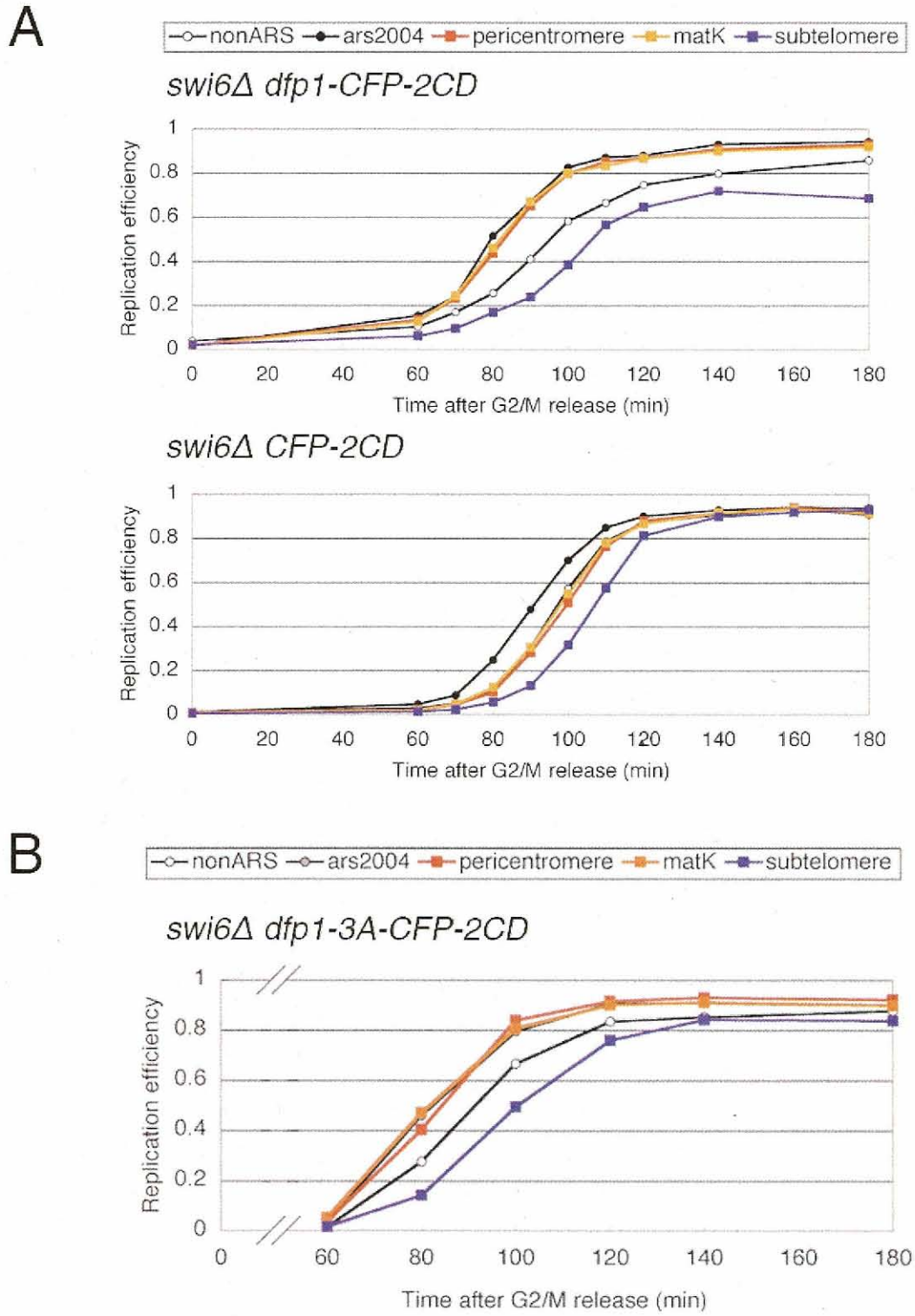

Fig. II-9. Tethering of Dfp1 restores early replication timing at the pericentromere and the *mat* locus in the absence of Swi6. (A, B) Dfp1-CFP-2CD or Dfp1-3A-CFP-2CD restores early replication timing at the pericentromere and the *mat* locus in the absence of Swi6. Dfp1 or Dfp1-3A was fused with CFP and two tandem copies of chromodomain (CD) of Swi6 and expressed from the native *dfp1*⁺ promoter in *swi6Δ* cells. Replication kinetics in *swi6Δ dfp1-CFP-2CD* and *swi6Δ CFP-2CD* cells (A) or *swi6Δ dfp1-3A-CFP-2CD* cells (B) were analyzed as in Fig. II-2.

Figure II-10

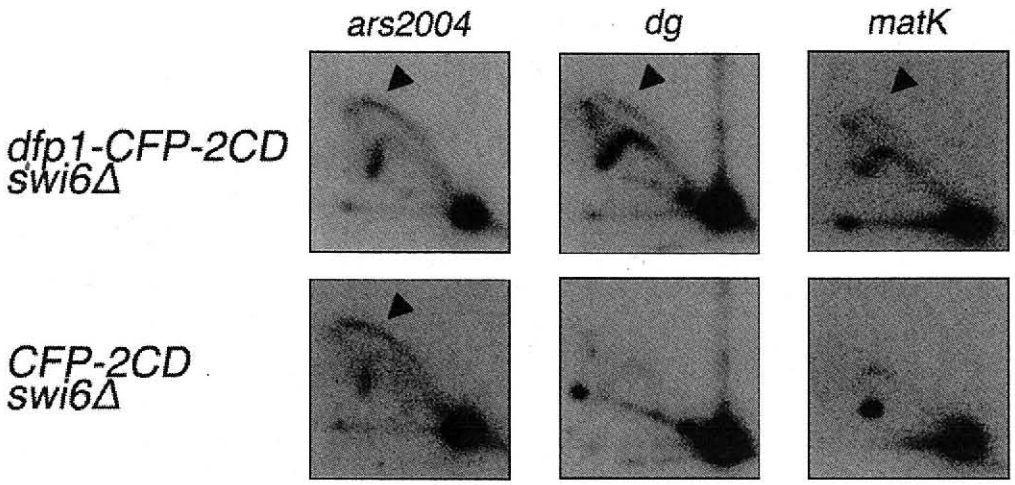

Fig. II-10. Expression of Dfp1-CFP-2CD restores initiation of replication at the peri-centromere and the *mat* locus in *swi6Δ* cells. Replication intermediates prepared from *swi6Δ* cells expressing Dfp1-CFP-2CD or CFP-2CD were analyzed as described in Fig. II-4B. Arrowheads indicate bubble arcs.

Figure II-11

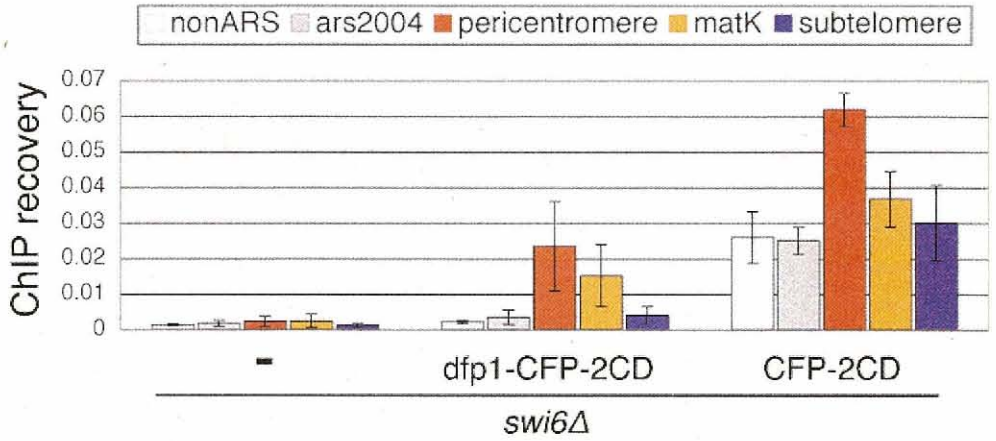

Fig. II-11. Dfp1-CFP-2CD localizes to the pericentromere and the *mat* locus in *swi6Δ* cells. ChIP analysis using anti-GFP antibody for CFP-tag was performed in *swi6Δ dfp1-CFP-2CD* and *swi6Δ CFP-2CD* cells as described in Fig. II-5B-G .

replication origins by recruiting DDK to heterochromatic loci. It should be noted that replication of the subtelomere was not significantly altered in *swi6Δ dfp1-CFP-2CD* cells (Fig. II-9A). ChIP analysis showed that Dfp1-CFP-2CD is localized at the pericentromere and *matK* locus, but not at the subtelomere (Fig. II-11). The absence of Dfp1-CFP-2CD from the subtelomere in *swi6Δ* is probably a result of decreased maintenance and spreading of H3K9me in the subtelomere in the absence of Swi6 (Cam et al., 2005)(Kanoh et al., 2005).

The H3K9me-dependent assembly of heterochromatin components in the absence of Swi6 is responsible for the delay of replication at the pericentromeres

The results suggest that access of DDK to the pericentromere and the silent *mat* locus, which is crucial for activation of replication origins in these loci, is hindered in *swi6Δ* cells. To test the possibility that remaining heterochromatin components that bind to H3K9me in the absence of Swi6 are responsible for the delay in replication, I examined the effects of deletion of *clr4*$^{+}$, a fission yeast homologue of *Su(var)3-9* histone methyltransferase, on replication in *swi6Δ* background, since localization of known heterochromatin components was abrogated in *clr4Δ* cells (Cam et al., 2005). In *swi6Δclr4Δ* cells, the pericentromere replicated in early S phase, supporting the notion that the remaining heterochromatin structures are responsible for the delay in replication (Fig. II-12). Interestingly, however, replication timing at the *matK* remained as late as the *nonARS* locus. I wondered whether pre-RC formation is maintained in the absence of heterochromatin assembly, because loss of *clr4* results in de-repression of transcription corresponding to non-coding RNA in heterochromatic loci (Cam et al., 2005), which might disturb pre-RC formation by removal of ORC complex (Mori and Shirahige, 2007). ChIP analysis was performed using extract from *swi6Δclr4Δ* cells taken at 60-minute intervals in the presence of HU after G2/M synchronization. At 0 min (G2/M phase), Orc4 but not Mcm6 signals were enriched at the *ars2004*, the pericentromere and the *matK* locus, suggesting ORC binding to these loci (Fig. II-13). Moreover, continuous localization of Orc4 and Mcm6 at the *ars2004*, as well as pericentromere and the *matK* locus, was observed from 60 min to 180 min after G2/M release (Fig. II-13), suggesting pre-RC formation in the absence of heterochromatin components. Since MCM leaves a replication origin after initiation of replication, accumulation of Mcm6 at the *matK* locus at 120 min and 180 min may result from inefficient initiation. From these results, in the absence of Swi6, H3K9me-dependent localization of other heterochromatin components suppress activation of

Figure II-12

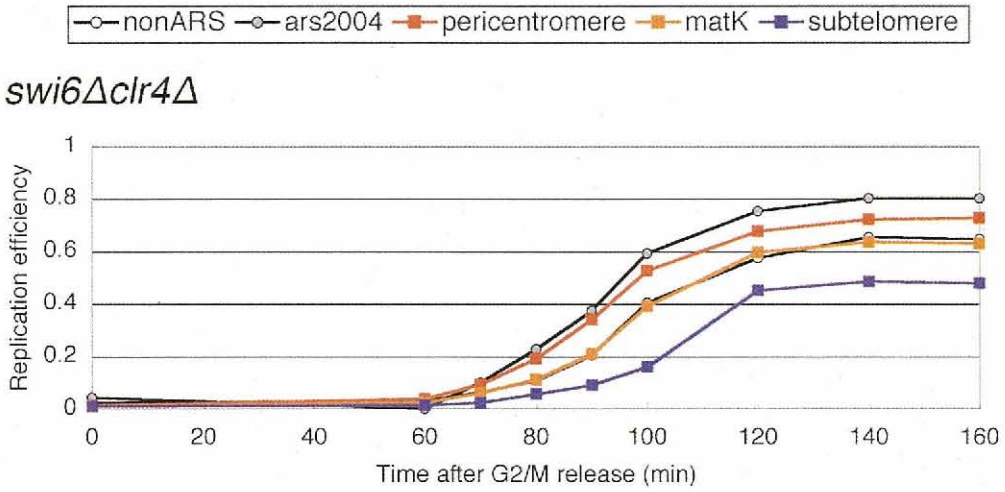

Fig. II-12. Deletion of the *clr4*⁺ in *swi6Δ* background restores early replication at the pericentromere but not at the *mat* locus. Replication kinetics of indicated loci in *swi6Δclr4Δ* double mutant cells were analyzed as described in Fig. II-2.

Figure II-13

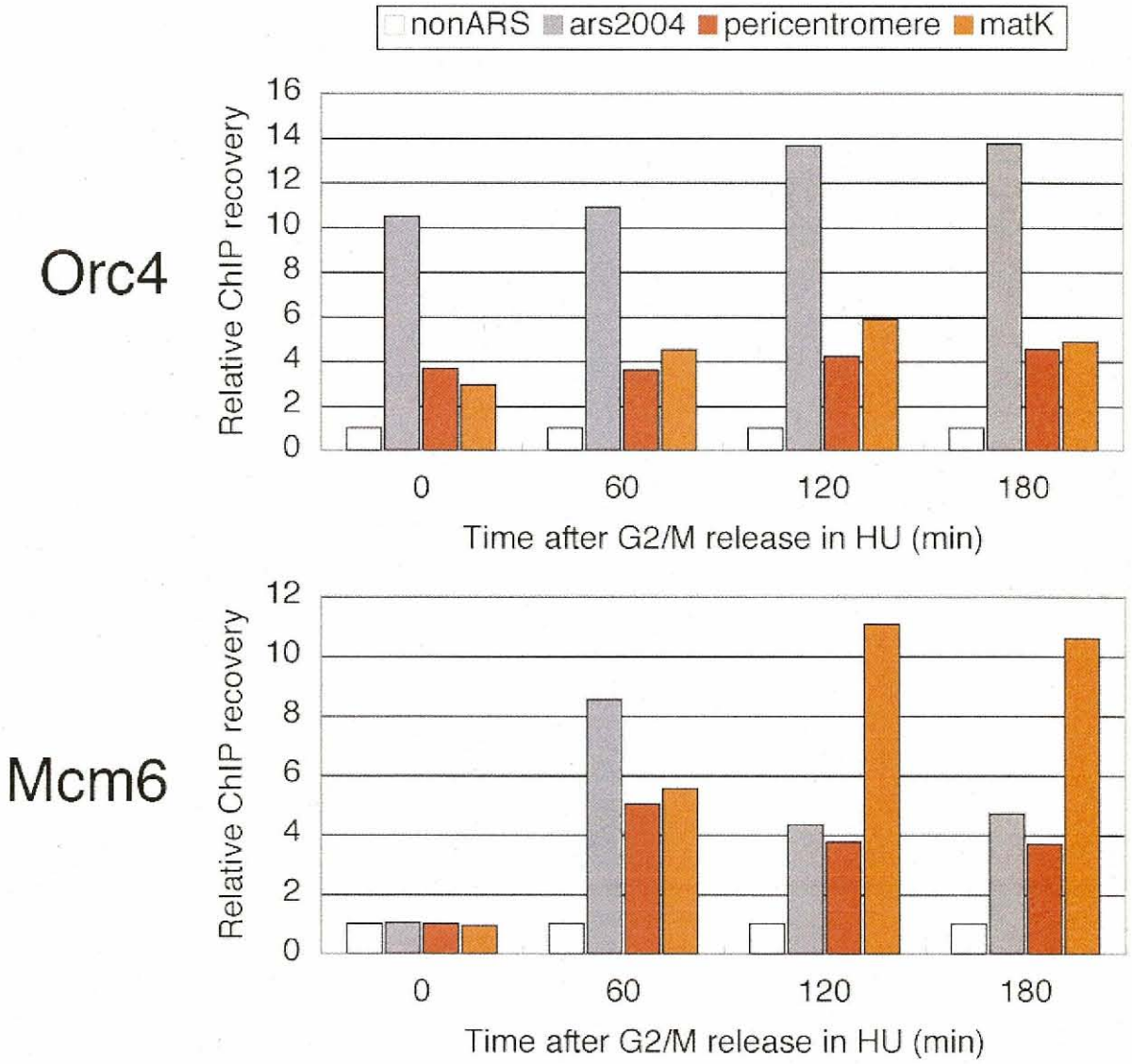

Fig. II-13. Pre-RC is formed at the pericentromere and the *mat* locus in the absence of heterochromatin assembly. The localization of Orc4 and Mcm6 was analyzed by ChIP in *swi6Δclr4Δ* cells. Samples were taken at 60-minute intervals after G2/M arrest. Recovery ratios of immunoprecipitated DNA to total DNA at the indicated loci were normalized to the value of nonARS locus.

pre-RCs at the pericentromere, whereas some other mechanism(s) may be responsible for the suppression at the silent *mat* locus. Both suppressive mechanisms are overcome by localization of Swi6 that recruits Dfp1 to the loci. In contrast to these loci, the subtelomeres replicated in very late in wild type, *swi6Δ* and *swi6Δclr4Δ* (Figs. II-2 and II-12). There seems to be distinct suppressing mechanism(s) specific to the subtelomeres, because it invalidates the positive effect of Swi6. These results suggest that replication origins are suppressed by different mechanisms at three heterochromatic loci.

Forced recruitment of Dfp1 to the subtelomeres accelerates replication timing

I questioned why the subtelomere replicates in late S phase regardless of Swi6 localization. Orc4 and Mcm6 were localized at the subtelomeric ARS in early S phase in wild type and *swi6Δ* cells, whereas Sld3, Psf2, Cdc45 or Ssb2 were not efficiently enriched at the subtelomeric ARS in either cell (Fig. II-14). Considering that DDK plays a pivotal role in replication of the pericentromere and the silent *mat* locus, it is possible that the subtelomeric region is highly inaccessible to DDK, resulting in late replication. I examined whether forced recruitment of DDK would accelerate replication in subtelomeric heterochromatin by expressing Dfp1-CFP-2CD or CFP-2CD in wild type cells, in which H3K9me is maintained at the subtelomere by a Swi6-dependent mechanism (Kanoh et al., 2005). Expression of CFP-2CD did not alter the replication kinetics of the subtelomere, as well as the TEL-0.3K, relative to *ars2004* and the *nonARS* locus, although replication of the pericentromere and *mat*K was slightly delayed (Fig. II-15), probably because CFP-2CD competes with Swi6 for binding to H3K9me. In contrast, expression of Dfp1-CFP-2CD accelerated replication of the subtelomere to be similar to that of the *nonARS* locus, whereas the replication kinetics of the pericentromere and *matK* were not significantly altered (Fig. II-15). Consistent with this result, replication timing of the TEL-0.3K was also accelerated to the similar extent of the subtelomere. These results suggest that subtelomeric origins are activated, at least partially, by tethering of DDK.

Figure II-14

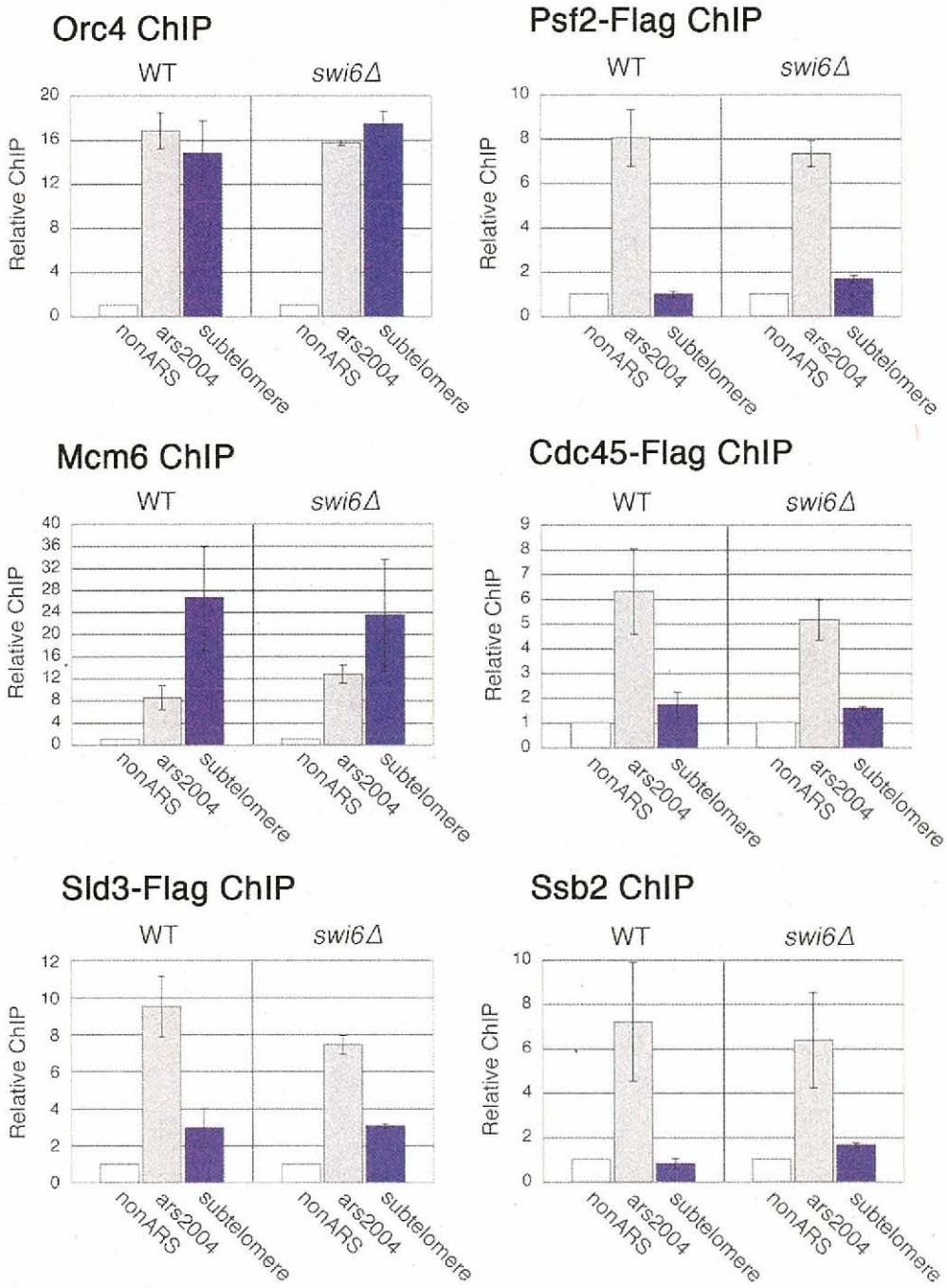

Fig. II-14. Initiation of replication at the subtelomeric ARS is inhibited after pre-RC formation in both wild type and *swi6Δ* cells. ChIP samples in Fig. II-5B-G were examined by quantitative real-time PCR using the subtelomeric primers shown in Fig. II-1A.

Figure II-15

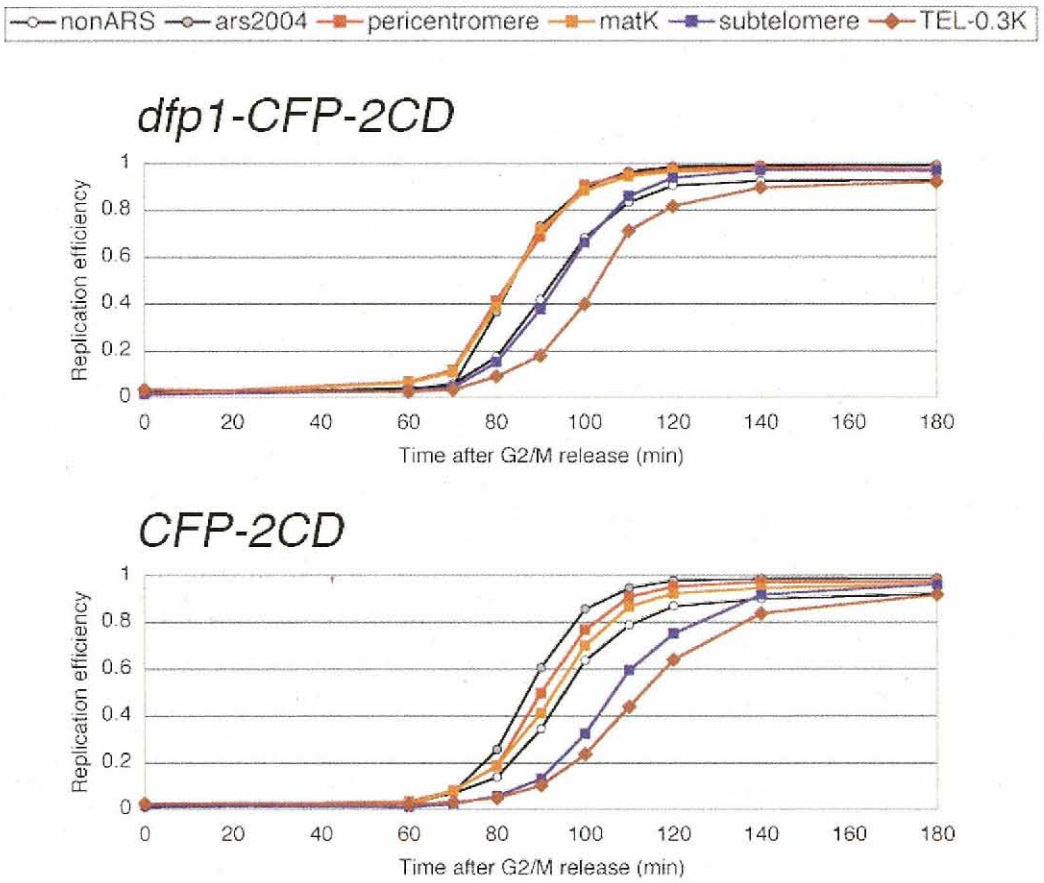

Fig. II-15. Expression of Dfp1-CFP-2CD in wild type cells accelerates replication timing at the subtelomere. Replication kinetics in *dfp1-CFP-2CD* and *CFP-2CD* cells were analyzed as in Fig. II-2.

DISCUSSION

The results presented here shed light on the dynamic nature of heterochromatin, providing the first example of a heterochromatin protein actively regulating initiation of DNA replication and the molecular evidences for the regulation of initiation by chromatin structures. I found that Sld3 loading and early firing of origins in the pericentromere and the silent *mat* locus are stimulated by Swi6 (Figs. II-2, 3C, 4 and 5D). Swi6 physically interacts with Dfp1 through the HP1-binding motif in Dfp1, which is required for early replication of the pericentromere and the silent *mat* locus (Figs. II-6B and 7). Furthermore, tethering Dfp1 or Dfp1-3A to the loci restored early replication in the absence of Swi6 (Figs. II-9 and 10).

Regulation of replication origins in the pericentromere and the silent *mat* locus

From the results in this study, I propose a model: Swi6 recruits DDK to pre-RCs in the heterochromatic pericentromere and the silent *mat* locus in early S phase and stimulates DDK-dependent assembly of the replication factor Sld3 (Fig. II-16). The underlying molecular mechanism is H3K9me-dependent localization of Swi6 and consequent Swi6-dependent localization of Dfp1.

The model presented here is compatible with the notion that H3K9me-dependent heterochromatin structures themselves are inaccessible to trans-acting factors, because replication is delayed in *dfp1-3A* and *swi6Δ* cells lacking the interaction of Dfp1 with Swi6 (Fig. II-16), and the delay in replication of the pericentromere was canceled in *swi6Δclr4Δ* cells (Fig. II-12). On the other hand, other mechanism(s) is responsible for the delay in replication of the silent *mat* locus in the absence of heterochromatin assembly (Fig. II-12). It was reported both the centromere and the *mat* locus preferentially localize adjacent to the spindle pole body (SPB) (Alfredsson-Timmins et al., 2007; Funabiki et al., 1993). Since subnuclear position has been proposed to be important for regulation of replication timing (Gilbert, 2002), and the deletion of *clr4* disrupts subnuclear localization of the *mat* locus (Alfredsson-Timmins et al., 2007) but not that of the centromere (Ekwall et al., 1996), localization adjacent to the SPB might be required for early replication of the pericentromere in the absence of heterochromatin assembly. The underlying molecular mechanism remains to be shown.

If the heterochromatin structure is intrinsically inaccessible to trans-acting factors,

Figure II-16

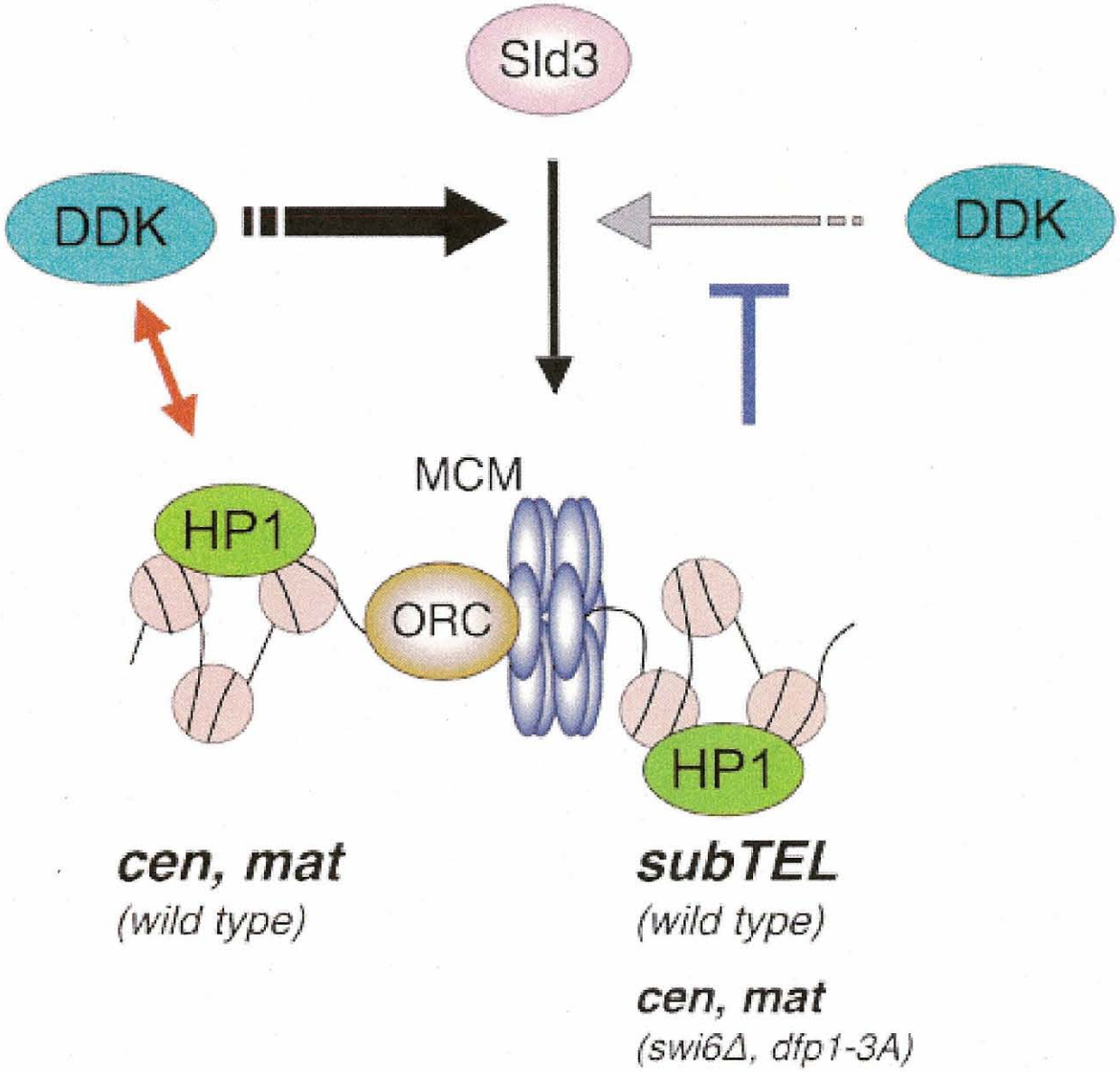

Fig. II-16. A model for regulation of replication origins in heterochromatic loci. Swi6/HP1 recruits DDK to the pericentromere and the *mat* locus through physical interaction, which promotes loading of Sld3 onto pre-RCs and early replication of the loci (left). The positive effect of Swi6 appears to be canceled in the subtelomeric region by unknown mechanism(s) (right). In *swi6Δ* and *dfp1-3A* mutant cells, remaining heterochromatin components and/or unknown mechanism(s) may prevent DDK localization in heterochromatin, resulting in late replication of the loci (right).

how other replication factors, such as MCM, GINS and Cdc45, are recruited to the origins in the pericentromere and the silent *mat* locus? It has shown recently that H3K9me and Swi6 localization are regulated in cell-cycle-dependent manner (Chen et al., 2008). The amount of H3K9me and Swi6 in the heterochromatic loci reduces in G1 phase of the cell cycle, which is the period of pre-RC formation. Thus, MCM may be loaded onto heterochromatic loci without the inhibitory effect of the heterochromatin structure. On the other hand, heterochromatin structure must be formed when Swi6 recruits DDK, thus it possibly inhibits recruitment of downstream factors. Since DDK has been proposed to phosphorylate the subunits of MCM complex (Masai et al., 2006), as well as Swi6 (Bailis et al., 2003), it is possible that the phosphorylation-dependent structural change of chromatin around origins allows recruitment of downstream factors. Structural change of origin chromatin by the effect of DDK phosphorylation is suggested in budding yeast (Geraghty et al., 2000).

Implication for regulation of replication in subtelomere

This study also suggests that the subtelomere region may possess another mechanism that counteracts the positive effect of Swi6 (Fig. II-16). Persistent suppression of replication and the resulting late replication may be involved in control of telomere length, as suggested in budding yeast (Bianchi and Shore, 2007). Suppressive chromatin structure has been proposed to be responsible for late replication of subtelomere in budding yeast (Gilbert, 2001b). However, my results are unfavorable for the involvement of H3K9me-dependent suppressive chromatin structure in replication control at fission yeast subtelomere; though it is still possible that telomere specific proteins and/or subnuclear localization have some role in regulation of telomeric replication. The involvement of Ku complex, which localize the telomere and regulate its subnuclear localization, in replication timing of telomere was reported in budding yeast (Cosgrove et al., 2002). Although the molecular mechanism for such suppression is unknown, tethering of DDK to the subtelomere partially overcomes the inhibitory effect (Fig. II-15). Therefore, DDK seems to be an important target even in regulation of subtelomeric replication origins.

Significance of early replication of the pericentromere and the *mat* locus

There are three consequences by activation of initiation: determination of replication timing of the locus; progression of replication fork in a specific direction from the locus; and

recruitment of factors depending on the process of initiation complex assembly. A plausible biological significance of regulation of replication timing has been proposed to be coupling with inheritance of chromatin structures during each cell cycle (Goren and Cedar, 2003). However, one could argue against this notion, because Swi6 remains at pericentromere and the silent *mat* locus after the delay of replication timing in *dfp1-3A* mutant. On the other hand, replication of the *mat1* locus in a specific direction is required for genomic imprinting at the *mat* locus (Dalgaard and Klar, 1999). Activation of the origin in the silent *mat* heterochromatin establishes the specific direction of replication fork at the *mat1* locus, although there seems to be redundant mechanism that blocks replication fork from the other side of the *mat1* locus to ensure fork direction (Dalgaard and Klar, 2001). Because the C terminus region of Dfp1 is required for localization of cohesin at the pericentromeric heterochromatin (Bailis et al., 2003), Swi6 and DDK seem to regulate both cohesin localization and initiation of DNA replication. It was proposed that cohesin is established at replication fork during S phase (Lengronne et al., 2006). To ensure cohesin establishment at the pericentromeric heterochromatin, DDK might participate in recruitment of cohesin immediately before initiation of replication, which guarantees temporal link between both pathways.

Control of the timing of heterochromatin replication may be important for regulation of gene expression during differentiation and development in higher eukaryotes, in which global regions of chromosomes form heterochromatin (Aladjem, 2007). The HP1-binding motif in Dfp1 does not appear to be conserved in Dbf4 homologues in other eukaryotes. However, their direct interaction needs to be examined experimentally, because HP1 has shown to interact with proteins through other domains such as chromo-domain (Pak et al., 1997). Thus, it is still attractive possibility that heterochromatin proteins participate in DNA replication through recruiting the regulatory kinase and/or other replication factors to origins in heterochromatic region.

MATERIALS AND METHODS

Yeast strains and genetics.

All *S. pombe* strains used are listed in Table II-1. Fission yeast strains were cultured in complete YE medium (0.5% yeast extract and 3% glucose) and Edinburgh minimal medium (Moreno et al., 1991). All solid media contain 2% agar. Transformation of *S. pombe* was performed by lithium acetate method (Forsburg, 2003).

Construction of Swi6 carrying chromo-domain mutant

To express Swi6-W104A mutant protein from the endogenous *swi6*$^+$ promoter, the *swi6*$^+$ coding sequence with its potential promoter and terminator regions was first cloned into pBluescript (pAL2pBK), and a *hyg*^{r} cassette was introduced into the pAL2pBK plasmid (pAL2pBK-H: a gift from Dr. J. Nakayama). The W104A mutation was introduced by site-directed mutagenesis using primers, 5'-CACTGGGATCGTCATAACCTTCGGCCTTCAAAAGGTATTCATAGCCTCCA-3' and 5'- CATCATAAGAGTCAGACGCTCTA-3'. The resultant fragment was used as primer for second PCR with 5'- AAATTTAAGCTTGCTAATGTACAAAAGCAGCAAC-3' and cloned into the *Afl*II-*Hind*III sites of pAL2pBK-H, generating pMH100. After confirmation of the sequence, pMH100 was cleaved with *Hpa*I for introduction into downstream of the *swi6* locus of HM1183 (*h*^{90} *cdc25-22 nmt1-TK*$^+$ *swi6Δ::kanMX6 his2 Kint2::ura4*$^+$), and the transformants were isolated using medium containing hygromycin.

Construction of Dfp1 carrying HP1-binding motif mutants

The point mutants *dfp1-3A* or *dfp1-2E* was constructed as below. The *dfp1-3A* or *dfp1-2E* mutation was introduced by site-directed mutagenesis using primers: 5'-GTAGTGCTGCTAGTGTTGCGGTGGCAACAGCTAATGGGAGAGATATCGCA-3' and 5'-AAGGATCCAATCTGGCCTTAAGGGACG-3' for *dfp1-3A*; or 5'-GTGCTGCTAGTGTTCCGGAGGAAACAATTAATGGGAGAGATATC-3' and 5'-AAGGATCCAATCTGGCCTTAAGGGACG-3' for *dfp1-2E*. The resultant fragments were used as primers for second PCR with 5'-AAGGATCCACTAGTATTGGCCGGTGT-3' and cloned into pBluescript to obtain pMH47 (pBS-*dfp1-3A*) and pMH48 (pBS-*dfp1-2E*), followed by confirmation of the sequences. A 0.2 kb 3'-UTR of *dfp1* was amplified using

primers, 5'-AAGGATCCACTAGTAATAGCCCGTGTCTTCAA-3' and 5'-AAGGATCCACTAGTCAGAAAATAAACCGTGAAAC-3', with *Bam*HI site and cloned into the *Bam*HI site of pBluescript to obtain pMH49. A *Spe*I fragment of pMH49 was incubated with T4 DNA polymerase to generate blunt end and cloned into the *Eco*RV site of pFA6a-kanMX6, resulting in pMH50. A *Bam*HI-*Spe*I fragment of pMH31 (a N terminus fragment of dfp1) and a *Spe*I-*Bam*HI fragement of pMH47 or pMH48 were cloned into *Bam*HI site of pMH50 to generate pMH51 or pMH52, respectively. Because C-terminal 13-Myc cassette caused defect in early replication of the pericentromere, the 13-Myc cassette and *ADH1* terminator of pMH51 or pMH52 were replaced with a potential terminator region of *dfp1*$^+$; C terminus fragment of *dfp1* was amplified using 5'-GACAGAGTCAAGAACCATC-3' and 5'-AAGGATCCACTAGTCAGAAAATAAACCGTGAAAC-3' as primers, followed by digestion with *Eco*RV and *Bam*HI, ant the resultant fragment was cloned into the *Eco*RV-*Bgl*II fragment of pMH51 or pMH52 to obtain pMH76 or pMH77, respectively. pMH76 or pMH77 was digested at the *Not*I sites for introduction into the *dfp1*$^+$ locus of HM683 (h^+ *nmt1-TK*$^+$), and the transformants were isolated using medium containing G418.

Construction of Dfp1 fused to chromodomain of Swi6

For construction of Dfp1-CFP-2CD or CFP-2CD, a plasmid carrying CFP open reading frame and a sequence encoding two copies of the chromo-domain of Swi6 (a gift from Dr. Y. Watanabe: pMH28)(Kawashima et al., 2007) was used. A 2.7 kb fragment containing *dfp1* ORF with its potential promoter or 1.0 kb fragment containing the potential promoter region was amplified using primers: 5'-AAAGGATCCGCGAGCTGATAATTCGCATC-3' and 5'-AAAGGATCCGCGGCCGCCTTAAGGGACGTTGAAC-3'; or 5'-AAAGGATCCGCGAGCTGATAATTCGCATC-3' and 5'-AAAGGATCCGCGGCCGCATGTGGTACAGCCACCTTAC-3', respectively, with *Bam*HI site at N-terminus and *Bam*HI-*Not*I sites at C-terminus. The resultant fragments were cloned into the *Bam*HI site of pBluescript to obtain pMH31 (pBS-Pdfp1-dfp1) or pMH37 (pBS-Pdfp1). A SphI-NotI fragment of pMH31 or pMH37 was cloned into pMH28, generating pMH32 or pMH39, in which the N-terminus of CFP is fused to the C-terminus of *dfp1*$^+$ or immediately adjacent to the *dfp1*$^+$ native promoter, respectively, with a *hyg*^{r} cassette. The pMH32 or pMH39 was cleaved with *Apa*I and integrated at the *lys1*$^+$ locus of HM664 (h^- *nmt1-TK*$^+$) or HM683 (h^+ *nmt1-TK*$^+$), respectively, and the transformants were isolated using

medium containing hygromycin.

BrdU incorporation.

Labeling of newly synthesized DNA with BrdU, separation of the heavy-light (HL) DNA from light-light (LL) DNA by CsCl density gradient centrifugation, and real-time PCR analysis were carried out as described in ***Part I***. Primers used for real-time PCR are listed in Table II-2.

Immunostaining

Yeast cell extracts were prepared as described previously (Ogawa et al., 1999) with some modification. *S. pombe* cells (1 x 10^8 cells) were washed twice with ice cold water and once with ice cold Lysis buffer (50 mM HEPES-KOH [pH 7.4], 140 mM NaCl, 1 mM EDTA, 0.1% Triton X-100, 0.1% sodium deoxycholate). The cell pellet was suspended in ice cold Lysis with protease inhibitor cocktail and PMSF and disrupted with glass beads by a bead beater (Micro Smash MS-100, TOMY). The broken cells were collected from the bottom of the tube through a puncture and sonicated four times for 10 sec. Supernatant after centrifugation was analyzed by SDS-PAGE followed by immunoblotting. Swi6 and Nda2/Tub1 (tubulin alpha 1/tubulin alpha 2) were detected by fluorography using rabbit anti-Swi6 (a gift from Dr. J. Nakayama) and mouse anti-TAT1 (a gift from Dr. K. Gull) antibodies, respectively, followed by reactions with HRP-conjugated antibodies (Jackson).

Construction of plasmids for *in vitro* translation

To express Dfp1, Dfp1-3A and Dfp1-2E by an *in vitro* translation system, expression plasmids were constructed as below. A fragment containing *dfp1* ORF was amplified with N-terminus *Nde*I site and C-terminus *Bam*HI site and cloned into the *Nde*I and *Bam*HI sites of pBluescript to obtain pBS-*dfp1*$^+$(a gift from Dr. H. Yabuuchi). The NdeI-BamHI fragment was cloned into pDONR201-FLAG-XCDC7 (a gift from Dr. T. Takahashi) carrying *att*L1 and *att*L2 for GATEWAY Cloning system to generate pMH55. To obtain pDONR plasmids carrying the point mutations of *dfp1*, a SpeI-EcoRV fragment of pMH47 (pBS-*dfp1-3A*) or pMH48 (pBS-*dfp1-2E*) was cloned into pMH55, resulting in pMH70 or pMH71, respectively. By using LR reaction, a *dfp1* fragment of pMH55, pMH70 or pMH71 was cloned into pCITE4a-DEST (a gift from Dr. T. Takahashi), which carries *att*R1 and *att*R2 at cloning site

of pCITE-4a (Novagen), to create pMH61, pMH72 or pMH73, respectively.

***In vitro* pull down assay.**

The binding of Dfp1 to Swi6 was analyzed essentially as described previously (Nakayama et al., 2001a). The N-terminally S-tagged Dfp1, Dfp1-3A and Dfp1-2E proteins were expressed from pMH61, pMH72 and pMH73, respectively, by using an *in vitro* translation system (Promega) and incubated with *E. coli* expressed GST-tagged Swi6 or GST (gifts from Dr. J. Nakayama) together with glutathione-Sepharose beads (GE Healthcare) in IP buffer-N50 (10 mM Tris-HCl [pH 8.0], 50 mM NaCl, 0.1% N-P40, 1 mM EDTA [pH 8.0]) for 2 hr at 4°C. The beads were washed three times with IP buffer-N50 and the bound proteins were analyzed by SDS-PAGE followed by immunoblotting. S-Dfp1 and GST-Swi6 were detected by fluorography using rabbit anti-S antibodies (Bethyl) and goat anti-GST antibodies (GE Healthcare), respectively, followed by reactions with HRP-conjugated antibodies (Jackson).

Chromatin immunoprecipitation.

Chromatin immunoprecipitation (ChIP) was performed essentially as described in ***Part I*** with rabbit anti-Orc4, rabbit anti-Mcm6, rabbit anti-Ssb2, mouse anti-Flag (M2 Monoclonal, Sigma), rabbit anti-Swi6 and rabbit anti-GFP (Living Colors Full-length A.v. Polyclonal Antibody, Clontech) antibodies. DNA prepared from whole-cell extracts or immunoprecipitated fractions was analyzed by real-time PCR using SYBR green I in a 7300 Real-Time PCR System (Applied Biosystems).

Two-dimensional gel electrophoresis.

Neutral-neutral two-dimensional gel electrophoresis analysis of replicating DNA was performed as described in ***Part I***. Relevant ARSs were used for southern hybridization probes after random prime labeling. For detection of pericentromeric origins, portions of the ARSs in the pericentromere (ars3.0K for *dg* and arsL for *dh*) (Smith et al., 1995) were cloned by PCR (pMH26 and pTN766: a gift from Dr. T. Nakagawa) to prevent cross hybridization between pericentromeric repeats and the silent *mat* locus.

Table II-1 ***S. pombe*** **strains used in this study**

Strain	Genotype	Figures II
HM123	h^- *leu1-32*	1B
HM664	h^- *ura4-D18::ura4⁺nmt1-TK⁺*	used for transformation
HM683	h^+ *ura4-D18::ura4⁺nmt1-TK⁺*	used for transformation
HM1182	h^{90} *cdc25-22 ura4-D18:: ura4⁺nmt1-TK⁺ his2 Kint2::ura4⁺*	2, 4A, 4B, 8
HM1183	h^{90} *cdc25-22 ura4-D18:: ura4⁺nmt1-TK⁺ his2 Kint2::ura4⁺ swi6Δ::kanMX6*	2, 4A, 4B, 8, 11
HM1418	h^- *ura4-D18::ura4⁺nmt1-TK⁺ lys1Δ::(dfp1⁺-CFP-2CD hphMX6)*	transformant
HM1420	h^{90} *cdc25-22 ura4-D18:: ura4⁺nmt1-TK⁺ his2 Kint2::ura4⁺ swi6Δ::kanMX6 lys1Δ::(dfp1⁺-CFP-2CD hphMX6)*	9A, **10**, **11**
HM1423	h^{90} *cdc25-22 ura4-D18:: ura4⁺nmt1-TK⁺ his2 Kint2::ura4⁺ lys1Δ::(dfp1⁺-CFP-2CD hphMX6)*	15
HM1460	h^- *ura4-D18::ura4⁺nmt1-TK⁺ lys1Δ::(CFP-2CD hphMX6)*	transformant
HM1467	h^{90} *cdc25-22 ura4-D18:: ura4⁺nmt1-TK⁺ his2 Kint2::ura4⁺ swi6Δ::kanMX6 lys1Δ::(CFP-2CD hphMX6)*	9A, **10**, **11**
HM1471	h^{90} *cdc25-22 ura4-D18:: ura4⁺nmt1-TK⁺ his2 Kint2::ura4⁺ lys1Δ::(CFP-2CD hphMX6)*	15
HM1482	h^{90} *cdc25-22 ura4-D18:: ura4⁺nmt1-TK⁺ his2 Kint2::ura4⁺ swi6Δ::kanMX6 clr4Δ::kanMX6*	12, 13
HM1588	h^{90} *cdc25-22 ura4-D18:: ura4⁺nmt1-TK⁺ Flag-cdc45::kanMX6 his2 Kint2::ura4⁺*	5C, **5F** **5G**, 14
HM1589	h^{90} *cdc25-22 ura4-D18:: ura4⁺nmt1-TK⁺ Flag-cdc45::kanMX6 his2 Kint2::ura4⁺ swi6Δ::kanMX6*	5C, 5F **5G**, 14
HM1590	h^{90} *cdc25-22 ura4-D18:: ura4⁺nmt1-TK⁺ psf2-5Flag::kanMX6 his2 Kint2::ura4⁺*	5B, 5E, 14
HM1591	h^{90} *cdc25-22 ura4-D18:: ura4⁺nmt1-TK⁺ psf2-5Flag::kanMX6 his2 Kint2::ura4⁺ swi6Δ::kanMX6*	5B, **5E**, 14
HM1826	h^+ *ura4-D18::ura4⁺nmt1-TK⁺ dfp1-3A::kanMX6*	transformant
HM1828	h^+ *ura4-D18::ura4⁺nmt1-TK⁺ dfp1-2E::kanMX6*	transformant
HM1841	h^{90} *cdc25-22 nda4-108 ura4-D18::ura4⁺nmt1-TK⁺ sld3-5Flag::kanMX6 his2 Kint2::ura4⁺*	5D, 14
HM1843	h^{90} *cdc25-22 nda4-108 ura4-D18::ura4⁺nmt1-TK⁺ sld3-5Flag::kanMX6 his2 Kint2::ura4⁺ swi6Δ::kanMX6*	5D, 14
HM1853	h^{90} *cdc25-22 ura4-D18::ura4⁺nmt1-TK⁺ dfp1-3A::kanMX6 his2 Kint2::ura4⁺*	7A, 8
HM1857	h^{90} *cdc25-22 ura4-D18::ura4⁺nmt1-TK⁺ dfp1-2E::kanMX6 his2 Kint2::ura4⁺*	7B
HM1899	h^+ *ura4-D18::ura4⁺nmt1-TK⁺ lys1Δ::(dfp1-3A-CFP-2CD hphMX6)*	transformant
HM1934	h^{90} *cdc25-22 ura4-D18::ura4+nmt1-TK⁺ his2 Kint2::ura4⁺ swi6Δ::kanMX6 lys1Δ::(dfp1-3A-CFP-2CD hphMX6)*	9B
HM1994	h^{90} *ura4-DS/E Kint2::ura4⁺ swi6Δ::kanMX6*	3A, 3B
HM2608	h^{90} *cdc25-22 ura4-D18::ura4+nmt1-TK⁺ his2 Kint2::ura4⁺ swi6Δ::kanMX6::(swi6-W104A hphMX6)*	3C
HM2613	h^{90} *ura4-DS/E Kint2::ura4⁺ swi6Δ::kanMX6::(swi6-W104A hphMX6)*	3A, 3B
TNF2518	h^{90} *ura4-DS/E Kint2::ura4⁺*	3A, 3B

Table II-2 **Primers used in this study**

Locus	Name	Sequence	Source
ars2004	ars2004-66-F	5'-CGGATCCGTAATCCCAACAA-3'	This study (Part I)
	ars2004-66-R	5'-TTTGCTTACATTTTCGGGAACTTA-3'	
nonARS	nonARS-70-F	5'-TACGCGACGAACCTTGCATAT-3'	This study (Part I)
	nonARS-70-R	5'-TTATCAGACCATGGAGCCCATT-3'	
dg (pericentromere)	dg-108-F	5'-TCCAAATGTCGCATGAACACTC-3'	This study (Part I)
	dg-108-R	5'-CTTTTTTGGGAATACATTGGGTTT-3'	
mat K locus	matK-108-F	5'-TCTTCCCTGCGTTGGACTTC-3'	This study (Part I)
	matK-108-R	5'-CACCCTACCATCCGTGTTACCT-3'	
subtelomere	TEL-59-F	5'-CAGAAGAGACTACAGAGGCGGTTT-3'	This study (Part I)
	TEL-59-R	5'-GGATGCCTTATCTGCGACCA-3'	
subtelomere	jk380 (TEL-0.3K-#1)	5'-TATTTCTTTATTCAACTTACCGCACTTC-3'	This study (Part I)
	jk381 (TEL-0.3K-#2)	5'-CAGTAGTGCAGTGTATTATGATAATTAAAATGG-3'	

CONCLUSION

In this thesis, I showed distribution of replication origins and their behavior in their chromatin contexts. Especially in heterochromatic region, I found intimate molecular link between heterochromatin structure and a replication regulator. The results provided the evidence that replication origins are distinctly regulated by the surrounding chromatin context.

In ***Part I***, by using the whole genome tiling chip and ChIP-qPCR, I found early and late origins tend to distribute separately on chromosome arm despite the random distribution of pre-RCs. On the other hand, I found replication origins are regulated differently in functional genomic loci; early origins accumulate in the pericentromere and the silent *mat* locus while late origins cluster in the subtelomeric heterochromatin, and pre-RC formation is suppressed at the kinetochore and the telomeric end.

In ***Part II***, I showed a heterochromatin protein, Swi6, stimulates early firing of origins in the pericentromere and the silent *mat* locus by recruiting a regulatory kinase, DDK, to the loci.

Replication origins in the pericentromere and the silent *mat* locus and maybe those in the subtelomere are regulated at the step of DDK loading. Interestingly, euchromatic late/potential origins are suppressed, at least in early S phase, at the step of Sld3 loading (Yabuuchi, 2008), suggesting that these origins are also regulated at the step of DDK loading. Euchromatic early origins are probably accessible to DDK, or alternatively, euchromatic origins may have distinct mechanism(s) to recruit DDK at specific period in S phase. Consequently, I propose that recruitment of DDK is a crucial step in the regulation of replication timing at all replication origins in fission yeast, although the mechanisms of recruitment may differ between chromatin regions. The biological significance of the regulation is one of the next attractive issues. I hope the knowledge obtained in this study will provide the clues to comprehend the mechanism for regulation of replication by chromatin structures in other systems.

ACKNOWLEDGEMENTS

My heartfelt appreciation goes to Professor Hisao Masukata whose comments and suggestions were of inestimable value for my study. I am also indebted to Drs. Takuro Nakagawa and Tatsuro Takahashi whose comments made enormous contribution to this study. I also deeply appreciate to Drs. Katsuhiko Shirahige, Yuki Katou and Takehiko Itoh for great contribution to the tiling chip analysis. I would also like to express my gratitude to Drs. Jun-ichi Nakayama for critical discussion and providing materials, Yoshinori Watanabe, Junko Kanoh and Keith Gull for providing materials, and Kanji Furuya for valuable advice on two-dimensional gel electrophoresis. I would also like to thank all of the members of Prof. Masukata's laboratory for the supports. Especially I am very grateful to Dr. Yoshiki Yamada, Dr. Hayato Yabuuchi and Mr. Masayoshi Fukuura for providing materials and helpful discussions. I am a Research Fellow of the Japan Society for the Promotion of Science and ***Part II*** of my research is supported by a grant-in-aid for JSPS fellows.

Finally, I wish to express my sincere appreciation to my parents and my wife for their moral support and warm encouragement during the course of this study.

REFERENCES

Aggarwal, B.D. and Calvi, B.R. (2004) Chromatin regulates origin activity in Drosophila follicle cells. *Nature*, **430**, 372-376.

Ahmed, S., Saini, S., Arora, S. and Singh, J. (2001) Chromodomain protein Swi6-mediated role of DNA polymerase alpha in establishment of silencing in fission Yeast. *J. Biol. Chem.*, **276**, 47814-47821.

Aladjem, M.I. (2007) Replication in context: dynamic regulation of DNA replication patterns in metazoans. *Nat. Rev. Genet.*, **8**, 588-600.

Alfredsson-Timmins, J., Henningson, F. and Bjerling, P. (2007) The Clr4 methyltransferase determines the subnuclear localization of the mating-type region in fission yeast. *J. Cell Sci.*, **120**, 1935-1943.

Aparicio, J.G., Viggiani, C.J., Gibson, D.G. and Aparicio, O.M. (2004) The Rpd3-Sin3 histone deacetylase regulates replication timing and enables intra-S origin control in Saccharomyces cerevisiae. *Mol. Cell. Biol.*, **24**, 4769-4780.

Arcangioli, B. (1998) A site- and strand-specific DNA break confers asymmetric switching potential in fission yeast. *EMBO J.*, **17**, 4503-4510.

Bailis, J.M., Bernard, P., Antonelli, R., Allshire, R.C. and Forsburg, S.L. (2003) Hsk1-Dfp1 is required for heterochromatin-mediated cohesion at centromeres. *Nat. Cell. Biol.*, **5**, 1111-1116.

Bell, S.P. and Dutta, A. (2002) DNA replication in eukaryotic cells. *Annu. Rev. Biochem.*, **71**, 333-374.

Bianchi, A. and Shore, D. (2007) Early replication of short telomeres in budding yeast. *Cell*, **128**, 1051-1062.

Bickmore, W.A. and Carothers, A.D. (1995) Factors affecting the timing and imprinting of replication on a mammalian chromosome. *J. Cell Sci.*, **108 (Pt 8)**, 2801-2809.

Brewer, B.J. and Fangman, W.L. (1987) The localization of replication origins on ARS plasmids in S. cerevisiae. *Cell*, **51**, 463-471.

Cam, H.P., Sugiyama, T., Chen, E.S., Chen, X., FitzGerald, P.C. and Grewal, S.I. (2005) Comprehensive analysis of heterochromatin- and RNAi-mediated epigenetic control of the fission yeast genome. *Nat. Genet.*, **37**, 809-819.

Chang, Y.C. (2000) Residuals analysis of the generalized linear models for longitudinal data. *Stat. Med.*, **19**, 1277-1293.

Chen, E.S., Zhang, K., Nicolas, E., Cam, H.P., Zofall, M. and Grewal, S.I. (2008) Cell cycle control of centromeric repeat transcription and heterochromatin assembly. *Nature*, **451**, 734-737.

Chuang, R.Y. and Kelly, T.J. (1999) The fission yeast homologue of Orc4p binds to replication origin DNA via multiple AT-hooks. *Proc. Natl. Acad. Sci. U. S. A.*, **96**, 2656-2661.

Clyne, R.K. and Kelly, T.J. (1995) Genetic analysis of an ARS element from the fission yeast Schizosaccharomyces pombe. *EMBO J.*, **14**, 6348-6357.

Cosgrove, A.J., Nieduszynski, C.A. and Donaldson, A.D. (2002) Ku complex controls the replication time of DNA in telomere regions. *Genes Dev.*, **16**, 2485-2490.

Dai, J., Chuang, R.Y. and Kelly, T.J. (2005) DNA replication origins in the Schizosaccharomyces pombe genome. *Proc. Natl. Acad. Sci. U. S. A.*, **102**, 337-342.

Dalgaard, J.Z. and Klar, A.J. (1999) Orientation of DNA replication establishes mating-type switching pattern in S. pombe. *Nature*, **400**, 181-184.

Dalgaard, J.Z. and Klar, A.J. (2001) A DNA replication-arrest site RTS1 regulates imprinting by determining the direction of replication at mat1 in S. pombe. *Genes Dev.*, **15**, 2060-2068.

Danis, E., Brodolin, K., Menut, S., Maiorano, D., Girard-Reydet, C. and Mechali, M. (2004) Specification of a DNA replication origin by a transcription complex. *Nat. Cell Biol.*, **6**, 721-730.

Diffley, J.F. (2004) Regulation of early events in chromosome replication. *Curr. Biol.*, **14**, R778-R786.

Diffley, J.F., Cocker, J.H., Dowell, S.J. and Rowley, A. (1994) Two steps in the assembly of complexes at yeast replication origins in vivo. *Cell*, **78**, 303-316.

Dubey, D.D., Kim, S.M., Todorov, I.T. and Huberman, J.A. (1996) Large, complex modular structure of a fission yeast DNA replication origin. *Curr. Biol.*, **6**, 467-473.

Dubey, D.D., Zhu, J., Carlson, D.L., Sharma, K. and Huberman, J.A. (1994) Three ARS elements contribute to the ura4 replication origin region in the fission yeast, Schizosaccharomyces pombe. *EMBO J.*, **13**, 3638-3647.

Ekwall, K., Nimmo, E.R., Javerzat, J.P., Borgstrom, B., Egel, R., Cranston, G. and Allshire, R. (1996) Mutations in the fission yeast silencing factors clr4+ and rik1+ disrupt the localisation of the chromo domain protein Swi6p and impair centromere function. *J. Cell Sci.*, **109 (Pt 11)**, 2637-2648.

Feng, W., Collingwood, D., Boeck, M.E., Fox, L.A., Alvino, G.M., Fangman, W.L., Raghuraman, M.K. and Brewer, B.J. (2006) Genomic mapping of single-stranded DNA in hydroxyurea-challenged yeasts identifies origins of replication. *Nat. Cell Biol.*, **8**, 148-155.

Forsburg, S.L. (2003) Introduction of DNA into S. pombe cells. *Curr. Protoc. Mol. Biol.*, **Chapter 13**, Unit 13.17.

Funabiki, H., Hagan, I., Uzawa, S. and Yanagida, M. (1993) Cell cycle-dependent specific positioning and clustering of centromeres and telomeres in fission yeast. *J. Cell Biol.*, **121**, 961-976.

Geraghty, D.S., Ding, M., Heintz, N.H. and Pederson, D.S. (2000) Premature structural changes at replication origins in a yeast minichromosome maintenance (MCM) mutant. *J. Biol. Chem.*, **275**, 18011-18021.

Gilbert, D.M. (2001a) Making sense of eukaryotic DNA replication origins. *Science*, **294**, 96-100.

Gilbert, D.M. (2001b) Nuclear position leaves its mark on replication timing. *J. Cell Biol.*, **152**, F11-15.

Gilbert, D.M. (2002) Replication timing and transcriptional control: beyond cause and effect. *Curr. Opin. Cell Biol.*, **14**, 377-383.

Gomez, M. and Antequera, F. (1999) Organization of DNA replication origins in the fission yeast genome. *EMBO J.*, **18**, 5683-5690.

Goren, A. and Cedar, H. (2003) Replicating by the clock. *Nat. Rev. Mol. Cell Biol.*, **4**, 25-32.

Grewal, S.I. and Jia, S. (2007) Heterochromatin revisited. *Nat. Rev. Genet.*, **8**, 35-46.

Guenatri, M., Bailly, D., Maison, C. and Almouzni, G. (2004) Mouse centric and pericentric satellite repeats form distinct functional heterochromatin. *J. Cell Biol.*, **166**, 493-505.

Hall, I.M., Shankaranarayana, G.D., Noma, K., Ayoub, N., Cohen, A. and Grewal, S.I. (2002) Establishment and maintenance of a heterochromatin domain. *Science*, **297**, 2232-2237.

Hayashi, M., Katou, Y., Itoh, T., Tazumi, A., Yamada, Y., Takahashi, T., Nakagawa, T., Shirahige, K. and Masukata, H. (2007) Genome-wide localization of pre-RC sites and identification of replication origins in fission yeast. *EMBO J.*, **26**, 1327-1339.

Heichinger, C., Penkett, C.J., Bahler, J. and Nurse, P. (2006) Genome-wide characterization of fission yeast DNA replication origins. *EMBO J.*, **25**, 5171-5179.

Hiratani, I., Leskovar, A. and Gilbert, D.M. (2004) Differentiation-induced replication-timing changes are restricted to AT-rich/long interspersed nuclear element (LINE)-rich isochores. *Proc. Natl. Acad. Sci. USA*, **101**, 16861-16866.

Hollo, G., Kereso, J., Praznovszky, T., Cserpan, I., Fodor, K., Katona, R., Csonka, E., Fatyol, K., Szeles, A., Szalay, A.A. and Hadlaczky, G. (1996) Evidence for a megareplicon covering megabases of centromeric chromosome segments. *Chromosome Res.*, **4**, 240-247.

Jacobs, S.A. and Khorasanizadeh, S. (2002) Structure of HP1 chromodomain bound to a lysine 9-methylated histone H3 tail. *Science*, **295**, 2080-2083.

Jeon, Y., Bekiranov, S., Karnani, N., Kapranov, P., Ghosh, S., MacAlpine, D., Lee, C., Hwang, D.S., Gingeras, T.R. and Dutta, A. (2005) Temporal profile of replication of human chromosomes. *Proc. Natl. Acad. Sci. U. S. A.*, **102**, 6419-6424.

Kanoh, J., Sadaie, M., Urano, T. and Ishikawa, F. (2005) Telomere binding protein Taz1 establishes Swi6 heterochromatin independently of RNAi at telomeres. *Curr. Biol.*, **15**, 1808-1819.

Katou, Y., Kanoh, Y., Bando, M., Noguchi, H., Tanaka, H., Ashikari, T., Sugimoto, K. and Shirahige, K. (2003) S-phase checkpoint proteins Tof1 and Mrc1 form a stable replication-pausing complex. *Nature*, **424**, 1078-1083.

Kawashima, S.A., Tsukahara, T., Langegger, M., Hauf, S., Kitajima, T.S. and Watanabe, Y. (2007) Shugoshin enables tension-generating attachment of kinetochores by loading Aurora to centromeres. *Genes Dev.*, **21**, 420-435.

Kim, S.M., Dubey, D.D. and Huberman, J.A. (2003) Early-replicating heterochromatin. *Genes Dev.*, **17**, 330-335.

Kim, S.M. and Huberman, J.A. (2001) Regulation of replication timing in fission yeast. *EMBO J.*, **20**, 6115-6126.

Labib, K. and Diffley, J.F. (2001) Is the MCM2-7 complex the eukaryotic DNA replication fork helicase? *Curr. Opin. Genet. Dev.*, **11**, 64-70.

Lengronne, A., McIntyre, J., Katou, Y., Kanoh, Y., Hopfner, K.P., Shirahige, K. and Uhlmann, F. (2006) Establishment of sister chromatid cohesion at the S. cerevisiae replication fork. *Mol. Cell*, **23**, 787-799.

MacAlpine, D.M. and Bell, S.P. (2005) A genomic view of eukaryotic DNA replication. *Chromosome Res.*, **13**, 309-326.

MacAlpine, D.M., Rodriguez, H.K. and Bell, S.P. (2004) Coordination of replication and transcription along a Drosophila chromosome. *Genes Dev.*, **18**, 3094-3105.

Machida, Y.J., Hamlin, J.L. and Dutta, A. (2005) Right place, right time, and only once: replication initiation in metazoans. *Cell*, **123**, 13-24.

Maison, C. and Almouzni, G. (2004) HP1 and the dynamics of heterochromatin maintenance. *Nat. Rev. Mol. Cell. Biol.*, **5**, 296-304.

Masai, H., Taniyama, C., Ogino, K., Matsui, E., Kakusho, N., Matsumoto, S., Kim, J.M., Ishii, A., Tanaka, T., Kobayashi, T., Tamai, K., Ohtani, K. and Arai, K. (2006) Phosphorylation of MCM4 by Cdc7 kinase facilitates its interaction with Cdc45 on the chromatin. *J. Biol. Chem.*, **281**, 39249-39261.

Maundrell, K. (1993) Thiamine-repressible expression vectors pREP and pRIP for fission

yeast. *Gene*, **123**, 127-130.

Moreno, S., Klar, A. and Nurse, P. (1991) Molecular genetic analysis of fission yeast Schizosaccharomyces pombe. *Methods Enzymol.*, **194**, 795-823.

Mori, S. and Shirahige, K. (2007) Perturbation of the activity of replication origin by meiosis-specific transcription. *J. Biol. Chem.*, **282**, 4447-4452.

Nakayama, J., Allshire, R.C., Klar, A.J. and Grewal, S.I. (2001a) A role for DNA polymerase alpha in epigenetic control of transcriptional silencing in fission yeast. *EMBO J.*, **20**, 2857-2866.

Nakayama, J., Klar, A.J. and Grewal, S.I. (2000) A chromodomain protein, Swi6, performs imprinting functions in fission yeast during mitosis and meiosis. *Cell*, **101**, 307-317.

Nakayama, J., Rice, J.C., Strahl, B.D., Allis, C.D. and Grewal, S.I. (2001b) Role of histone H3 lysine 9 methylation in epigenetic control of heterochromatin assembly. *Science*, **292**, 110-113.

Ogawa, Y., Takahashi, T. and Masukata, H. (1999) Association of fission yeast Orp1 and Mcm6 proteins with chromosomal replication origins. *Mol. Cell. Biol.*, **19**, 7228-7236.

Okuno, Y., Okazaki, T. and Masukata, H. (1997) Identification of a predominant replication origin in fission yeast. *Nucleic Acids Res.*, **25**, 530-537.

Okuno, Y., Satoh, H., Sekiguchi, M. and Masukata, H. (1999) Clustered adenine/thymine stretches are essential for function of a fission yeast replication origin. *Mol. Cell. Biol.*, **19**, 6699-6709.

Olsson, T., Ekwall, K. and Ruusala, T. (1993) The silent P mating type locus in fission yeast contains two autonomously replicating sequences. *Nucleic Acids Res.*, **21**, 855-861.

Pak, D.T., Pflumm, M., Chesnokov, I., Huang, D.W., Kellum, R., Marr, J., Romanowski, P. and Botchan, M.R. (1997) Association of the origin recognition complex with heterochromatin and HP1 in higher eukaryotes. *Cell*, **91**, 311-323.

Patel, P.K., Arcangioli, B., Baker, S.P., Bensimon, A. and Rhind, N. (2006) DNA replication origins fire stochastically in fission yeast. *Mol. Biol. Cell*, **17**, 308-316.

Pidoux, A.L. and Allshire, R.C. (2004) Kinetochore and heterochromatin domains of the fission yeast centromere. *Chromosome Res.*, **12**, 521-534.

Prasanth, S.G., Prasanth, K.V., Siddiqui, K., Spector, D.L. and Stillman, B. (2004) Human Orc2 localizes to centrosomes, centromeres and heterochromatin during chromosome inheritance. *EMBO J.*, **23**, 2651-2663.

Raghuraman, M.K., Winzeler, E.A., Collingwood, D., Hunt, S., Wodicka, L., Conway, A., Lockhart, D.J., Davis, R.W., Brewer, B.J. and Fangman, W.L. (2001) Replication dynamics of the yeast genome. *Science*, **294**, 115-121.

Remus, D., Beall, E.L. and Botchan, M.R. (2004) DNA topology, not DNA sequence, is a critical determinant for Drosophila ORC-DNA binding. *EMBO J.*, **23**, 897-907.

Sadaie, M., Iida, T., Urano, T. and Nakayama, J. (2004) A chromodomain protein, Chp1, is required for the establishment of heterochromatin in fission yeast. *EMBO J.*, **23**, 3825-3835.

Sanchez, J.A., Kim, S.M. and Huberman, J.A. (1998) Ribosomal DNA replication in the fission yeast, Schizosaccharomyces pombe. *Exp. Cell Res.*, **238**, 220-230.

Santocanale, C. and Diffley, J.F. (1998) A Mec1- and Rad53-dependent checkpoint controls late-firing origins of DNA replication. *Nature*, **395**, 615-618.

Sasaki, T. and Gilbert, D.M. (2007) The many faces of the origin recognition complex. *Curr. Opin. Cell Biol.*, **19**, 337-343.

Schubeler, D., Scalzo, D., Kooperberg, C., van Steensel, B., Delrow, J. and Groudine, M. (2002) Genome-wide DNA replication profile for *Drosophila melanogaster*: a link

between transcription and replication timing. *Nat. Genet.*, **32**, 438-442.

Schwaiger, M. and Schubeler, D. (2006) A question of timing: emerging links between transcription and replication. *Curr. Opin. Genet. Dev.*, **16**, 177-183.

Sclafani, R.A. and Holzen, T.M. (2007) Cell cycle regulation of DNA replication. *Annu. Rev. Genet.*, **41**, 237-280.

Segurado, M., de Luis, A. and Antequera, F. (2003) Genome-wide distribution of DNA replication origins at A+T-rich islands in *Schizosaccharomyces pombe*. *EMBO Rep.*, **4**, 1048-1053.

Segurado, M., Gomez, M. and Antequera, F. (2002) Increased recombination intermediates and homologous integration hot spots at DNA replication origins. *Mol. Cell*, **10**, 907-916.

Shechter, D., Costanzo, V. and Gautier, J. (2004) ATR and ATM regulate the timing of DNA replication origin firing. *Nat. Cell Biol.*, **6**, 648-655.

Shirahige, K., Hori, Y., Shiraishi, K., Yamashita, M., Takahashi, K., Obuse, C., Tsurimoto, T. and Yoshikawa, H. (1998) Regulation of DNA-replication origins during cell-cycle progression. *Nature*, **395**, 618-621.

Smith, J.G., Caddle, M.S., Bulboaca, G.H., Wohlgemuth, J.G., Baum, M., Clarke, L. and Calos, M.P. (1995) Replication of centromere II of *Schizosaccharomyces pombe*. *Mol. Cell Biol.*, **15**, 5165-5172.

Stevenson, J.B. and Gottschling, D.E. (1999) Telomeric chromatin modulates replication timing near chromosome ends. *Genes Dev.*, **13**, 146-151.

Takahashi, K., Murakami, S., Chikashige, Y., Funabiki, H., Niwa, O. and Yanagida, M. (1992) A low copy number central sequence with strict symmetry and unusual chromatin structure in fission yeast centromere. *Mol. Biol. Cell*, **3**, 819-835.

Takahashi, T., Ohara, E., Nishitani, H. and Masukata, H. (2003) Multiple ORC-binding sites are required for efficient MCM loading and origin firing in fission yeast. *EMBO J.*, **22**, 964-974.

Takebayashi, S., Sugimura, K., Saito, T., Sato, C., Fukushima, Y., Taguchi, H. and Okumura, K. (2005) Regulation of replication at the R/G chromosomal band boundary and pericentromeric heterochromatin of mammalian cells. *Exp. Cell Res.*, **304**, 162-174.

Vashee, S., Cvetic, C., Lu, W., Simancek, P., Kelly, T.J. and Walter, J.C. (2003) Sequence-independent DNA binding and replication initiation by the human origin recognition complex. *Genes Dev.*, **17**, 1894-1908.

Weinreich, M., Palacios DeBeer, M.A. and Fox, C.A. (2004) The activities of eukaryotic replication origins in chromatin. *Biochim. Biophys. Acta.*, **1677**, 142-157.

White, E.J., Emanuelsson, O., Scalzo, D., Royce, T., Kosak, S., Oakeley, E.J., Weissman, S., Gerstein, M., Groudine, M., Snyder, M. and Schubeler, D. (2004) DNA replication-timing analysis of human chromosome 22 at high resolution and different developmental states. *Proc. Natl. Acad. Sci. USA*, **101**, 17771-17776.

Wohlgemuth, J.G., Bulboaca, G.H., Moghadam, M., Caddle, M.S. and Calos, M.P. (1994) Physical mapping of origins of replication in the fission yeast Schizosaccharomyces pombe. *Mol. Biol. Cell*, **5**, 839-849.

Wood, V., Gwilliam, R., Rajandream, M.A., Lyne, M., Lyne, R., Stewart, A., Sgouros, J., Peat, N., Hayles, J., Baker, S., Basham, D., Bowman, S., Brooks, K., Brown, D., Brown, S., Chillingworth, T., Churcher, C., Collins, M., Connor, R., Cronin, A., Davis, P., Feltwell, T., Fraser, A., Gentles, S., Goble, A., Hamlin, N., Harris, D., Hidalgo, J., Hodgson, G., Holroyd, S., Hornsby, T., Howarth, S., Huckle, E.J., Hunt, S., Jagels, K., James, K., Jones, L., Jones, M., Leather, S., McDonald, S., McLean, J., Mooney, P.,

Moule, S., Mungall, K., Murphy, L., Niblett, D., Odell, C., Oliver, K., O'Neil, S., Pearson, D., Quail, M.A., Rabbinowitsch, E., Rutherford, K., Rutter, S., Saunders, D., Seeger, K., Sharp, S., Skelton, J., Simmonds, M., Squares, R., Squares, S., Stevens, K., Taylor, K., Taylor, R.G., Tivey, A., Walsh, S., Warren, T., Whitehead, S., Woodward, J., Volckaert, G., Aert, R., Robben, J., Grymonprez, B., Weltjens, I., Vanstreels, E., Rieger, M., Schafer, M., Muller-Auer, S., Gabel, C., Fuchs, M., Dusterhoft, A., Fritzc, C., Holzer, E., Moestl, D., Hilbert, H., Borzym, K., Langer, I., Beck, A., Lehrach, H., Reinhardt, R., Pohl, T.M., Eger, P., Zimmermann, W., Wedler, H., Wambutt, R., Purnelle, B., Goffeau, A., Cadieu, E., Dreano, S., Gloux, S., Lelaure, V., Mottier, S., Galibert, F., Aves, S.J., Xiang, Z., Hunt, C., Moore, K., Hurst, S.M., Lucas, M., Rochet, M., Gaillardin, C., Tallada, V.A., Garzon, A., Thode, G., Daga, R.R., Cruzado, L., Jimenez, J., Sanchez, M., del Rey, F., Benito, J., Dominguez, A., Revuelta, J.L., Moreno, S., Armstrong, J., Forsburg, S.L., Cerutti, L., Lowe, T., McCombie, W.R., Paulsen, I., Potashkin, J., Shpakovski, G.V., Ussery, D., Barrell, B.G. and Nurse, P. (2002) The genome sequence of Schizosaccharomyces pombe. *Nature*, **415**, 871-880.

Woodfine, K., Fiegler, H., Beare, D.M., Collins, J.E., McCann, O.T., Young, B.D., Debernardi, S., Mott, R., Dunham, I. and Carter, N.P. (2004) Replication timing of the human genome. *Hum. Mol. Genet.*, **13**, 191-202.

Wyrick, J.J., Aparicio, J.G., Chen, T., Barnett, J.D., Jennings, E.G., Young, R.A., Bell, S.P. and Aparicio, O.M. (2001) Genome-wide distribution of ORC and MCM proteins in *S. cerevisiae*: high-resolution mapping of replication origins. *Science*, **294**, 2357-2360.

Wyrick, J.J., Holstege, F.C., Jennings, E.G., Causton, H.C., Shore, D., Grunstein, M., Lander, E.S. and Young, R.A. (1999) Chromosomal landscape of nucleosome-dependent gene expression and silencing in yeast. *Nature*, **402**, 418-421.

Yabuuchi, H. (2008) Initiation complex formation and its regulation for DNA replication in fission yeast. *PhD thesis, Osaka University, Toyonaka, Osaka.*

Yabuuchi, H., Yamada, Y., Uchida, T., Sunathvanichkul, T., Nakagawa, T. and Masukata, H. (2006) Ordered assembly of Sld3, GINS and Cdc45 is distinctly regulated by DDK and CDK for activation of replication origins. *EMBO J.*, **25**, 4663-4674.

Yamada, Y., Nakagawa, T. and Masukata, H. (2004) A novel intermediate in initiation complex assembly for fission yeast DNA replication. *Mol. Biol. Cell*, **15**, 3740-3750.

Zofall, M. and Grewal, S.I. (2006) Swi6/HP1 recruits a JmjC domain protein to facilitate transcription of heterochromatic repeats. *Mol. Cell*, **22**, 681-692.

Supplementary Table S1 *S. pombe* origins of replication identified in this study

Chromosome I												
Ori Number	Class	Cds1 Suppression	Bioinfo Number (Segurado *et al.*)	ORIs Number (Heichinger *et al.*)	ORF Microarray Number (Feng *et al.*)		ARS/2D-gel Number (Segurado *et al.*)	Map Position (bp)		Orc4 localization	5' Gene/ORF	3' Gene/ORF
					wt (HU)	Δcds1 (HU)		Orc1	Mcm6			
1001	L	Yes						15375.5	15375.5	+	SPAC212.07c	SPAC212.06c
1002	L	Yes						51625.5	*	+	SPAC977.09c	SPAC977.10
1003	L	Yes						54625.5	55375.5	+	SPAC977.10	SPAC977.11
1004	L	Yes	1011					63375.5	62875.5	+	SPAC977.14c	SPAC977.15
1005	L	Yes	1012					71125.5	*	+	SPAC977.17	SPAPJ695.01c
1006	L	Yes						75375.5	75375.5	+		
1007	L	Yes	1013					80125.5	*	+	SPAPJ695.01c	ght3/SPAC1F8.01
1008	L	Yes	1014			1001		85625.5	*	+	ght3/SPAC1F8.01	SPAC1F8.02c
1009	L	Yes						89125.5	88625.5	+	SPAC1F8.02c	str3/SPAC1F8.03c
1010	L			1001				95125.5	96375.5	+	SPAC1F8.04c	isp3/SPAC1F8.05
1011	E		1015	1002		1002	AT1015	113875.5	113875.5	+	SPAC11D3.03c	SPAC11D3.04c
1012	L							151125.5	150875.5	+	SPAC5H10.02c	SPAC5H10.03
1013	L					1004		167125.5	166375.5	-	gmh1/SPAC5H10.11	SPAC5H10.12c
1014	E							191125.5	191125.5	+	SPAC13G6.08	SPAC13G6.09
1015	E		1018	1004	1002	1005		200125.5	200625.5	+	SPAC24B11.02	aps1/SPAC24B11.03
1016	L	Yes						239375.5	240875.5	+	rps2601/SPAC806.03c	SPAC806.04c
1017	L	Yes	1020			1006		244875.5	245125.5	-	SPAC806.04c	SPAC806.05
1018	L	Yes	1021			1007		295375.5	295375.5	-	SPAC1F5.02	SPAC18B11.11
1019	L	Yes	1022					303125.5	303125.5	+	tup11/SPAC18B11.10	SPAC18B11.09c
1020	E		1025	1008	1003	1009		365625.5	365625.5	+	SPAC630.09c	SPAC630.10
1021	L	Yes	1026					411125.5	411375.5	+	cuf1/SPAC31A2.11c	SPAC31A2.12
1022	E		1027	1010		1010		441625.5	441625.5	+	rad32/SPAC13C5.07	fep1/SPAC23E2.01
1023	L							457875.5	457125.5	+	ste7/SPAC23E2.03c	SPAC24H6.13
1024	E							465125.5	465125.5	+	uba3/SPAC24H6.12c	SPAC24H6.11c
1025	E		1028	1011		1011		474375.5	474375.5	+	gef1/SPAC24H6.09	SPAC24H6.08
1026	E		1029	1012		1012		490375.5	490625.5	+	SPAC24H6.02c	SPAPB21F2.01
1027	E		1030	1014	1004	1014		563625.5	563625.5	+	SPAC2F7.14c	rsm24/SPAC2F7.15
1028	L				1005			593375.5	593125.5	+	SPAC3H8.03	SPAC3H8.04
1029	L	Yes	1031	1015				608625.5	609125.5	+	SPAC3H8.09c	spc20/SPAC3H8.10
1030	L	Yes	1032	1016		1015		651125.5	650875.5	+	SPAC1D4.07c	SPAC1D4.08
1031	E		1033	1018/1019	1007	1016	ORI 12	715125.5	715875.5	+	sxa2/SPAC1296.03c	SPAC1296.04
1032	L							741125.5	739875.5	+	SPAC22G7.05	ura1/SPAC22G7.06c
1033	L							750875.5	750125.5	+	SPAC22G7.07c	ppk8/SPAC22G7.08
1034	L		1034					762375.5	*	+	SPAC4G8.03c	SPAC4G8.15c
1035	L							766125.5	765875.5	+		
1036	L							785625.5	784625.5	+	atp10/SPAC4G8.11c	SPAC4G8.12c
1037	L		1035	1020	1008	1017		794875.5	794875.5	+	SPAC16C9.02c	SPAC16C9.03
1038	E			1021	1009	1018		845375.5	*	+	SPAC521.02	SPAC521.03
1039	E							894375.5	893875.5	-	SPAC23G3.12c	SPAC22H12.01c
1040	E		1039	1024	1010	1020		902875.5	903375.5	+	SPAC22H12.05c	rpc19/SPAC1687.01
1041	L	Yes						939375.5	939125.5	+	ssl3/SPAC1687.18c	SPAC1687.19c
1042	E		1040	1025	1011	1021		966125.5	966875.5	+	byr4/SPAC222.10c	hem13/SPAC222.11
1043	L		1041			1022	AT1041	1028625.5	1028125.5	+	fap2/SPAC139.04c	SPAC139.05
1044	E		1042	1028				1080125.5	1080375.5	+	plb1/SPAC1A6.04c	SPAC1A6.05c
1045	E				1013	1023		1084125.5	1084375.5	-	meu31/SPAC1A6.06c	SPAC1A6.07
1046	E		1043	1029	1013	1023		1091125.5	1091375.5	+	lag1/SPAC1A6.09c	SPAC30D11.15c
1047	E		1044	1030			ars1	1097125.5	1097125.5	+	hus5/SPAC30D11.13	rpl3802/SPAC30D11.12
1048	L		1045			1024		1148875.5	1148875.5	+	SPAC56F8.12	SPAC56F8.13
1049	E		1046	1032		1025		1157375.5	1157625.5	+	esc1/SPAC56F8.16	psc2/SPAC22A12.01c
1050	E							1163375.5	1162875.5	-	csn4/SPAC22A12.03c	rps2201/SPAC22A12.04c
1051	E			1033	1014	1026		1191875.5	1192125.5	+	SPAC22A12.17c	SPAC4C5.01
1052	E		1047	1034				1197375.5	1197125.5	+	ryh1/SPAC4C5.02c	SPAC4C5.03
1053	E					1027		1226375.5	1226375.5	+	psm3/SPAC10F6.09c	SPAC10F6.10
1054	E		1048	1035	1015	1028		1255875.5	1255875.5	+	cut6/SPAC56E4.04c	SPAC56E4.05
1055	E		1049	1036	1016	1029		1275875.5	1276125.5	+	csn2/SPAPB17E12.04c	rpl3703/SPAPB17E12.05
1056	L	Yes	1050					1360625.5	1360625.5	+	fin1/SPAC19E9.02	pas1/SPAC19E9.03
1057	E		1052	1041	1019	1034		1445125.5	1445125.5	+	SPAC3A12.13c	cam1/SPAC3A12.14
1058	E		1053	1043	1020	1035		1477625.5	1477625.5	+	SPAC9.07c	SPAC9.08c

1059	L				1021	1036		1499875.5	*	+	SPAC5D6.09c	mes1/SPAC5D6.08c
1060	E		1055	1046				1510125.5	1509875.5	+	SPAC5D6.04	SPAC5D6.02c
1061	E	Yes#		1047	1022	1038		1574125.5	1575125.5	+	SPAC23H4.19	rbx1/SPAC23H4.18c
1062	L	Yes						1600375.5	1600125.5	+	gln1/SPAC23H4.06	SPAC23H4.05c
1063	E		1056	1049				*	*	+	msc1/SPAC343.11c	rds1/SPA343.12
1064	E				1024	1039		1667375.5	1667625.5	+		
1065	E		1057	1050		1040		1709125.5	1709125.5	+	SPAC664.02c	SPAC664.03
1066	E			1051				1719625.5	1719625.5	+	SPAC664.08c	ggt1/SPAC664.09
1067	L		1059					1766125.5	1768125.5	+	ulp2/SPAC17A5.07c	SPAC17A5.08
1068	L							1823875.5	*	-	psu1/SPAC1002.13c	SPAC1002.20
1069	E		1061	1054		1043		1834875.5	1835125.5	+	SPAC1002.18	SPAC1002.21
1070	L	Yes			1028	1045		1892625.5	*	+	SPAPB1A10.14	SPAPB1A10.15
1071	L	Yes	1062		1028	1045		1894875.5	1895625.5	+	SPAPB1A10.15	sdh2/SPAC140.01
1072	L							1947375.5	1947125.5	+	SPAC3H1.08c	SPAC3H1.09c
1073	L	Yes	1063					1954875.5	1954875.5	+	SPAC3H1.10	SPAC3H1.11
1074	L	Yes						*	1959375.5	+		
1075	E		1064	1056	1030	1047		1975875.5	1975875.5	+	rpl3001/SPAC9G1.03c	oxa101/SPAC9G1.04
1076	L	Yes				1048		2026125.5	2026125.5	+	ddb1/SPAC17H9.10c	SPAC17H9.11
1077	L		1065	1057		1049		2042875.5	2042875.5	+	snu13/SPAC607.03c	SPAC607.04
1078	L	Yes	1067	1059				2097125.5	2096875.5	+	obr1/SPAC3C7.14c	SPAC25A8.03c
1079	L	Yes	1068	1061		1051		2141375.5	2141125.5	+	pnk1/SPAC23C11.04c	SPAC23C11.05
1080	E		1069		1032	1052		2195375.5	2195125.5	+	hsl4/SPAC1783.04c	hrp1/SPAC1783.05
1081	E		1070	1063	1033	1053	ORI 18/ORI J	2228875.5	2228875.5	+	SPAC18G6.05c	SPAC18G6.06
1082	L							2233125.5	2233125.5	+	mra1/SPAC18G6.07c	SPAC18G6.09c
1083	E		1073	1066	1034	1054		2250625.5	2250625.5	+	byr3/SPAC13D6.02c	SPAC13D6.03c
1084	L			1067				2263875.5	2264125.5	-	SPAC4G9.06c	B8647-3/SPAC4G9.07
1085	E					1055		2274625.5	2274375.5	+	arg11/SPAC4G9.09c	arg3/SPAC4G9.10
1086	E		1074	1068		1055		2280875.5	2280875.5	+	vps26/SPAC4G9.13c	SPAC4G9.14
1087	L	Yes			1035	1056		2305125.5	2305625.5	+	mac1/SPAC13G7.04c	SPAC13G7.05
1088	L	Yes	1077	1072	1036	1057		2340375.5	2340625.5	+	SPAC6C3.08	SPAC6C3.09
1089	L							2363375.5	2363875.5	+	SPAC17G8.11c	SPAC17G8.12

1090	L	Yes	1079					2406875.5	2407125.5	+	sck1/SPAC1B9.02c	SPAC1B9.03c
1091	L	Yes						2417125.5	2418625.5	+	SPAC6B12.03c	SPAC6B12.04c
1092	E		1080	1075			rip1	2439375.5	2439375.5	+	SPAC6B12.14c	cpc2/SPAC6B12.15
1093	E		1081	1075	1037	1059		2442875.5	2442875.5	+	cpc2/SPAC6B12.15	meu26/SPAC6B12.16
1094	E		1082	1076				2452875.5	2452625.5	+	SPAC32A11.02c	phx1/SPAC32A11.03c
1095	E			1076				2457125.5	2458125.5	+	phx1/SPAC32A11.03c	trp2/SPAC19A8.15
1096	L							2510125.5	2511125.5	-	gly1/SPAC23H3.09c	ssr2/SPAC23H3.10
1097	L	Yes				1061		2526375.5	2526375.5	+	SPAC25H1.01c	jmj1/SPAC25H1.02
1098	L	Yes						2528625.5	2528625.5	+	jmj1/SPAC25H1.02	mug66/SPAC25H1.03
1099	E			1078		1062		2579125.5	2579375.5	+	prs1/SPAC4A8.14	cdc3/SPAC4A8.15c
1100	L					1063		2601125.5	2601375.5	+	SPAC823.11	SPAC823.12
1101	L				1039	1064		2615875.5	2615625.5	-	SPAC7D4.13c	SPAC7D4.12c
1102	L		1085	1079				2618875.5	2618625.5	-	SPAC7D4.12c	sec39/SPAC7D4.11c
1103	L	Yes#	1086	1080	1040	1065		2644125.5	2644125.5	+	itr1/SPAC4F8.15	hcs1/SPAC4F8.14c
1104	L	Yes	1088	1081		1066		2668625.5	*	-	hxk2/SPAC4F8.07c	SPAC4F8.06
1105	E	Yes#	1090	1082	1042	1067		2720625.5	2720625.5	+	SPAPB2B4.04c	vma5/SPAPB2B4.05
1106	E		1092	1084	1043	1068		2762625.5	2762625.5	+	SPAC6F6.13c	ypt5/SPAC6F6.15
1107	E			1086	1045	1069		2804375.5	2804375.5	+	SPAC1B05.16c	crm1/SPAC1B2.01
1108	L	Yes				1072		2875625.5	2876125.5	+	SPACUNK4.17	SPACUNK4.19
1109	L	Yes	1094	1089		1072		2883875.5	2883625.5	+	SPACUNK4.15	SPACUNK4.14
1110	E							2938875.5	2938625.5	+	SPAC2E1P3.05c	SPAPB2C8.01
1111	E		1095	1091				2960625.5	2961125.5	+	SPAPB24D3.07c	SPAPB24D3.08c
1112	E				1050	1074		2978125.5	2978125.5	+	agl1/SPAPB24D3.10c	SPAPB1A11.01
1113	E				1050	1074		*	2980625.5	+	SPAPB1A11.01	SPAPB1A11.02
1114	E			1092	1050	1074		2984125.5	2984125.5	+	SPAPB1A11.02	SPAPB1A11.03
1115	E		1096	1093	1051	1075		3010875.5	3010875.5	+	maf1/SPAC31G5.12c	SPAC31G5.21
1116	E		1097	1094	1051	1075		3023625.5	3022875.5	+	SPAC31G5.18c	SPAC31G5.19
1117	E							3032125.5	3034125.5	+	SPAC1786.01c	SPAC1786.04
1118	E							3053875.5	3053625.5	+	SPAC24C9.06c	bgs2/SPAC24C9.07c
1119	E		1098	1095	1052	1076	ORI 76	3060875.5	3061125.5	+	bgs2/SPAC24C9.07c	SPAC24C9.08
1120	L							3071125.5	*	-	SPAC24C9.11	SPAC24C9.12c

1121	E		1099	1096	1054	1078		3127875.5	3127875.5	+	srb8/SPAC688.08	SPAC688.09
1122	E		1100	1097		1079		3145375.5	3145375.5	+	SPAC688.14	bet5/SPAC3G9.16c
1123	L	Yes						3159375.5	3159375.5	+	peg1/SPAC3G9.12	SPAC3G9.11c
1124	E		1101	1098	1055	1080		3185375.5	3185375.5	+	SPAC3G9.01	SPAC1486.01
1125	E		1104	1101				3301625.5	3301625.5	+	eme1/SPAPB1E7.06c	SPAPB1E7.07
1126	E		1105	1102	1058	1085	pARS767	3321875.5	3321875.5	+	rps602/SPAPB1E7.12	mns1/SPAC2E1P5.01c
1127	E		1106	1103	1059	1087		3405625.5	3405875.5	+	apc5/SPAC959.09c	SPAP32A8.02
1128	E		1107	1104	1060			3411375.5	3411375.5	+	SPAP32A8.03c	rpl501/SPAC3H5.12c
1129	E		1109	1107	1062	1090	ORI c27	3499125.5	3499125.5	+	rps502/SPAC328.10c	SPAC16E8.01
1130	E		1110		1063	1091		3542125.5	3542125.5	-	SPAC1B1.02c	kap95/SPAC1B1.03c
1131	E		1111	1109				3549625.5	3549625.5	+	SPAC1B1.04c	bsu1/SPAC17A2.01
1132	E		1112	1110				3571375.5	3570625.5	+	SPAC17A2.15	csx1/SPAC17A2.09c
1133	E		1114	1110				3577625.5	3577875.5	+	SPAC17A2.10c	SPAC17A2.11
1134	E							*	*	+	SPAC17A2.11	SPAC17A2.12
1135	E							3592875.5	3593375.5	+	SPAC17G6.02c	SPAC17G6.03
1136	E					1092		3611375.5	3612625.5	+	SPAC17G6.11c	cul1/SPAC17G6.12
1137	E		1115	1112	1065	1093		3635625.5	3635625.5	+	SPAC1142.04	ctr5/SPAC1142.05
1138	E'							3646125.5	3647125.5	+	cgs1/SPAC8C9.03	SPAC8C9.04
1139	E		1116	1114	1066	1094		3701375.5	3701625.5	+	rnde6/SPAC15A10.10	ubr11/SPAC15A10.11
1140	E							3746875.5	3749875.5	+	rpl1002/SPAP7G5.05	SPAP7G5.06
1141	E			1117/1118		1096		3753625.5	3753625.5	+	SPAP7G5.06	centromere
1142	E			1122	1069	1097		3841125.5	3841375.5	+	SPAC4H3.07c	SPAC4H3.08
1143	E		1124	1123				3853375.5	3853375.5	+	SPAC4H3.12c	SPAC4H3.13
1144	E		1125/1126	1126	1071	1098		3878875.5	3879375.5	+	pma1/SPAC1071.10c	SPAC1071.11
1145	E							3882875.5	*	+		
1146	E		1127	1127				3898625.5	3898875.5	+	SPAC926.07c	SPAC926.08c
1147	E		1128	1128	1072	1099		3954125.5	3953875.5	+	SPAC2F3.14c	isk1/SPAC2F3.15
1148	E			1129	1174	1100		3992875.5	3992875.5	+	SPAPB15E9.01c	SPAPB15E9.02c
1149	E		1129		1174	1100		3995875.5	3995875.5	+	SPAPB15E9.02c	Tf2-5/SPAPB15E9.03c
1150	L							4010625.5	4010125.5	+	SPAC27E2.03c	SPAC27E2.11c
1151	E		1130	1130	1075	1101		4020125.5	4020375.5	+	SPAC27E2.06c	pvg2/SPAC27E2.07

1152	E		1131	1131	1076	1102	ORI 19	4073125.5	4072375.5	+	SPAC19G12.13c	its3/SPAC19G12.14
1153	E		1132	1132	1077	1103		4089125.5	4089125.5	+	mnl1/SPAC23A1.04c	SPAC23A1.05
1154	E		1133	1133	1078	1104		4137375.5	4137375.5	+	bgl2/SPAC26H5.08c	SPAC26H5.09c
1155	E							4141125.5	4141125.5	+	SPAC26H5.09c	tif51/SPAC26H5.10c
1156	E				1079	1105		4154625.5	4154625.5	+	SPAC26H5.13c	SPAC25B8.01
1157	L							4178125.5	*	-	SPAC25B8.11	SPAC25B8.12c
1158	L							4180875.5	4180625.5	+	SPAC25B8.12c	isp7/SPAC25B8.13c
1159	E		1134	1134	1081	1106		4185875.5	4185875.5	+	isp7/SPAC25B8.13c	mal2/SPAC25B8.14
1160	E			1135				4197625.5	4197875.5	+	SPAC683.03	SPAC683.02c
1161	E				1082	1107		4232625.5	4232625.5	+	SPAC1F7.06	flp1/SPAC1F7.07c
1162	E							4240125.5	4239875.5	+	flo1/SPAC1F7.08	SPAC1F7.09c
1163	E		1135	1136			pcr1	4255125.5	4255125.5	+	pcr1/SPAC21E11.03c	ppr1/SPAC21E11.04
1164	E		1136	1137	1083	1108		4275625.5	4275625.5	+	SPAC2C4.07c	SPAC2C4.08
1165	E		1137	1138	1084	1110		4326625.5	4326875.5	+	SPAC27F1.05c	SPAC27F1.10
1166	L	Yes	1138		1085	1111		4365875.5	4366625.5	+	SPAC23D3.12	SPAC23D3.13c
1167	L					1112		4387375.5	*	+	SPAC1527.03	sec72/SPAC30.01c
1168	L	Yes'	1139	1139	1086	1113		4415625.5	4415875.5	+	SPAC29E6.06c	SPAC29E6.07
1169	E'	Yes		1140		1114		4439625.5	4439875.5	+	SPAC9E9.17c	leu2/SPAC9E9.03
1170	L	Yes	1140			1115		4451375.5	4451375.5	+	ypt2/SPAC9E9.07c	rad26/SPAC9E9.08
1171	L	Yes						4459625.5	4457375.5	+	SPAC9E9.09c	cbh1/SPAC9E9.10c
1172	L	Yes						4468875.5	4468375.5	+	SPAC9E9.12c	wos2/SPAC9E9.13
1173	E			1141		1116		4484625.5	4484625.5	+	stm1/SPAC17C9.10	tim13/SPAC17C9.09c
1174	E		1141	1144		1118		4534125.5	4534125.5	+	SPAC27D7.11c	but1/SPAC27D7.12
1175	L	Yes	1142					4605375.5	4605375.5	+	SPAC12B10.15c	SPAC1093.01
1176	L		1143	1149		1120		4653375.5	4653625.5	+	SPAC144.01	SPAC144.02
1177	L	Yes		1150	1090	1121		4674875.5	4675125.5	+	gwt1/SPAC144.10c	rps1102/SPAC144.11
1178	E		1145	1152	1091	1123		4740375.5	4740375.5	+	SPAC458.04c	pik3/SPAC458.05
1179	E	Yes	1146	1153	1092	1124		4779625.5	4779625.5	+	SPAC11H11.02c	SPAC11H11.03c
1180	E'					1125		4803875.5	4803875.5	+	SPAC22F8.08	rrp16/SPAC22F8.09
1181	E			1155		1127		4845625.5	4845125.5	+	atg13/SPAC4F10.07c	SPAC4F10.08
1182	E		1147	1156				4853375.5	4853625.5	+	SPAC4F10.10c	spn1/SPAC4F10.11

1183	E'	Yes	1148		1094	1128		4883125.5	4882875.5	+	SPAC19B12.02c	bgs3/SPAC19B12.03
1184	L							4912375.5	4913125.5	+	rpn502/SPAPB8E5.02c	mae1/SPAPB8E5.03
1185	E			1158		1129		4917375.5	4917625.5	+	SPAPB8E5.04c	mfm1/SPAPB8E5.05
1186	E		1149	1160				4964125.5	4964125.5	+	vht1/SPAC1B3.16c	clr2/SPAC1B3.17
1187	L							4985625.5	4984875.5	+	SPAC1952.09c	SPAC1952.10c
1188	E		1152	1162	1096	1132	ORI 22	5025375.5	5025375.5	+	SPAC22E12.03c	ccs1/SPAC22E12.04
1189	L		1154	1164		1134		5098125.5	5097375.5	+	rpl3002/SPAC1250.05	atl1/SPAC1250.04c
1190	E		1155	1166	1098	1136		5156625.5	5157375.5	+	SPAC26F1.12c	SPAC26F1.11/dubious
1191	E			1167				5178625.5	5178625.5	+	SPAC26F1.05	etr1/SPAC26F1.04c
1192	L				1100	1137		5190375.5	5190375.5	+	SPAPJ691.02	SPAPJ691.03
1193	E		1156	1168	1101	1138		5234125.5	5234625.5	+	mek1/SPAC14C4.03	B22918-2/SPAC14C4.04
1194	L	Yes	1158					5272375.5	5272375.5	+	adg1/SPAPJ760.03c	SPAC2H10.01
1195	L	Yes	1159	1170		1140		5322875.5	5323125.5	+	hsp9/SPAP8A3.04c	SPAP8A3.05
1196	E		1160	1171	1103	1142		5394125.5	5393875.5	+	SPAC3G6.07	erv1/SPAC3G6.08
1197	E		1162	1173		1144		5449125.5	5449625.5	+	SPAC1039.01	SPAC1039.02
1198	E'							5470375.5	5470375.5	-	isp5/SPAC1039.09	mmf2/SPAC922.01
1199	E		1163	1174	1104	1145		5477125.5	5476875.5	+	SPAC1039.11c	SPAC922.03
1200	E'		1164	1175				5483375.5	5482625.5	-	SPAC922.04	SPAC922.05c
1201	L							5487625.5	5487375.5	-	SPAC922.06	SPAC922.07c
1202	L	Yes	1166	1176		1146		5502625.5	5502875.5	+	mel1/SPAC869.07c	SPAC869.06c
1203	L	Yes	1167	1176				*	5506625.5	+	SPAC869.06c	SPAC869.05c
1204	L	Yes						5510875.5	*	+	SPAC869.05c	SPAC869.04
1205	L	Yes						5517875.5	5516125.5	+	SPAC869.03c	SPAC869.02c
1206	L	Yes	1168					5521875.5	*	+	SPAC869.02c	SPAC869.01
1207	L	Yes	1169		1105	1147		5529875.5	*	+	SPAC186.01	SPAC186.02c

Chromosome II

Ori Number	Class	Cds1 Suppression	Bioinfo Number (Segurado *et al.*)	ORIs Number (Heichinger *et al.*)	ORF Microarray Number (Feng *et al.*)		ARS/2D-gel Number (Segurado *et al.*)	Map Position (bp)		Orc4 localization	5' Gene/ORF	3' Gene/ORF
					wt (HU)	Δcds1 (HU)		Orc1	Mcm6			
2001	L	Yes						*	31375.5	+	SPBC1348.10c	SPBC1348.11
2002	L	Yes						38125.5	38125.5	+	SPBC1348.13	SPBC1348.14c
2003	L	Yes						53125.5	53125.5	+	grt1/SPBPB8B6.04c	SPBPB8B6.05c
2004	L	Yes						63375.5	61875.5	+	SPBPB21E7.02c	SPBPB21E7.04c
2005	L	Yes						66875.5	*	+	SPBPB21E7.05	SPBPB21E7.06
2006	L							69875.5	*	+	SPBPB21E7.06	aes1/SPBPB21E7.07
2007	L	Yes						74375.5	74375.5	+	SPBPB21E7.08	SPBPB21E7.09
2008	L							78125.5	*	+	SPBPB21E7.09	SPBPB21E7.10
2009	E				2001	2001		81875.5	81375.5	+	SPBPB21E7.10	SPBPB10D8.01
2010	L		2001					86875.5	*	+	SPBPB10D8.02c	SPBPB10D8.03
2011	E'		2002	2001				90875.5	91375.5	+	SPBPB10D8.03	SPBPB10D8.04c
2012	L		2006			2002		104625.5	*	+	SPBPB10D8.07c	SPBC359.01
2013	E		2007					112125.5	111875.5	+	air2/SPBC359.02	SPBC359.03c
2014	L		2008	2002				*	117625.5	+	SPBC359.03c	SPBC359.04c
2015	L		2010					132375.5	132625.5	+	SPBC359.06	SPBC1683.01
2016	E		2011	2003				142375.5	142125.5	+	SPBC1683.03c	SPBC1683.04
2017	E		2012	2004	2002	2003		152125.5	152125.5	+	SPBC1683.05	SPBC1683.06c
2018	L	Yes	2013		2003	2004		201875.5	202125.5	+	fbp1/SPBC660.04c	SPBC660.05
2019	L	Yes	2014					204375.5	*	+	SPBC660.05	SPBC660.06
2020	L							228875.5	228875.5	+	SPBC660.15	SPBC660.16
2021	E		2015	2005	2004	2005		259125.5	259125.5	+	clr3/SPBC800.03	rpl4301/rpl37a-1
2022	E		2016	2006				278625.5	278625.5	+	SPBC800.11	SPBC800.12c
2023	E					2006		282375.5	282375.5	+	SPBC800.13	SPBC1773.01
2024	E							324125.5	*	+	SPBC1773.17c	car1/SPBP26C9.02c
2025	E		2018	2009				326625.5	326625.5	+	car1/SPBP26C9.02c	SPBP26C9.03c
2026	E		2019	2009				333375.5	333375.5	+	SPBP26C9.03c	SPBC1271.15c
2027	E					2008		354875.5	357375.5	+	SPBC1271.09	SPBC1271.08c
2028	L	Yes	2023	2013				454625.5	454625.5	-	SPBC428.06c	meu6/SPBC428.07
2029	L				2008	2011		485375.5	484875.5	+	alp6/SPBC902.01c	ctf18/SPBC902.02c
2030	E			2014	2009	2012		*	518625.5	+	rps27/SPBC1685.10	rlp1/SPBC1685.11
2031	E		2024	2015				521125.5	*	+	rlp1/SPBC1685.11	SPBC1685.12c
2032	E							523625.5	523125.5	+		
2033	E				2010			529375.5	529625.5	+	SPBC1685.13	SPBC1685.14c

2034	E		2025	2016				571125.5	570625.5	+	SPBC354.09c	SPBC354.10
2035	E			2017				593375.5	592875.5	+	tea4/wsh3	wtf2/SPBC1706.02c
2036	E		2026	2018	2012	2014	AT2026	604125.5	604125.5	+	rpl803/rpkD4	rps1701/SPBC839.05c
2037	E				2013	2016		670125.5	670375.5	+	SPBC947.05c	SPBC947.04
2038	E		2028	2021				674875.5	675125.5	+	SPBC947.04	SPBC947.03c
2039	E			2023		2017		717875.5	717625.5	+	ubc4/SPBC119.02	SPBC119.03
2040	E					2017		721875.5	*	–	mei3/SPBC119.04	csh3/SPBC119.05c
2041	E							724125.5	723875.5	+	csh3/SPBC119.05c	sco1/SPBC119.06
2042	E		2029	2024	2014	2018		746375.5	746125.5	+	SPBC119.18	rti1/SPBC119.14
2043	E							833875.5	833875.5	+	SPBC530.15c	SPBC36.01c
2044	E							838625.5	*	+	SPBC36.01c	SPBC36.02c
2045	E		2031	2027				*	841375.5	+	SPBC36.02c	SPBC36.03c
2046	E				2017	2021		844625.5	843875.5	+		
2047	E		2032	2027	2017	2021		848125.5	848125.5	+	SPBC36.03c	cys11/SPBC36.04
2048	L	Yes	2033					890875.5	892875.5	+	pmp1/SPBC713.11c	erg1/SPBC713.12
2049	L	Yes	2035					949625.5	949625.5	+	gap1/SPBC646.12c	sds23/SPBC646.13
2050	L	Yes	2036	2030		2023		958125.5	958125.5	+	SPBC846.15c	SPBC846.16
2051	L	Yes						962875.5	962875.5	+	dic1/SPBC855.01c	SPBP35G2.02
2052	E			2033		2025		1055875.5	1055875.5	-	gtr1/SPBC337.13c	rpb4/SPBC337.14
2053	L	Yes				2026		1079125.5	1080875.5	+	SPBC1734.10c	SPBC1734.11
2054	E		2038	2034	2019	2027		1106375.5	1106625.5	+	cyp3/SPBC1709.04c	sks2/SPBC1709.05
2055	E		2039	2035	2020	2028		1142845.5	1142625.5	+	skp1/SPBC409.05	uch2/SPBC409.06
2056	E							1148625.5	1148875.5	+	wis1/SPBC409.07c	SPBC409.08
2057	E			2038	2023	2029		1244875.5	1245125.5	+	gyp10/SPBC651.03c	SPBC651.04
2058	E		2041	2039			AT2041	1255875.5	1255625.5	+	rpc1/SPBC651.08c	SPBC651.09c
2059	E		2042/2043	2040				1267375.5	1266125.5	+	cwl1/SPBC31A8.01c	SPBC31A8.02
2060	E			2041				1269625.5	*	+	SPBC31A8.02	but2/SPBC3D6.02
2061	E		2044	2042	2024	2030	ORI c7	1278375.5	1278875.5	+	mad1/SPBC3D6.04c	ptp4/SPBC3D6.05
2062	E		2046	2044	2025	2031		1313625.5	1313625.5	+	sol1/SPBC30B4.04c	kap109/SPBC30B4.05
2063	E							1352125.5	1351125.5	+	SPBC27B12.14	SPBC27B12.12c
2064	L							1386875.5	*	–	hht2/SPBC8D2.04	sfi1/SPBC8D2.05c

2065	E			2045	2026	2032		1389875.5	1390125.5	+	SPBC8D2.16c	SPBC8D2.17
2066	E		2047	2047				1444625.5	1444375.5	+	SPBP22H7.05c	SPBP22H7.06
2067	E		2048	2048	2028	2034		1457625.5	1457625.5	+	nep2/SPBC32H8.02c	bem46/SPBC32H8.03
2068	L							1462375.5	1462375.5	+	SPBC32H8.05	SPBC32H8.06
2069	L	Yes				2035		1500875.5	1501125.5	+	SPBC11B10.08	cdc2/SPBC11B10.09
2070	E		2049	2050	2029	2036	ars2004	1546625.5	1546375.5	+	SPBC83.18c	atf1/SPBC29B5.01
2071	E				2030		ars2003	1557125.5	1556875.5	+	isp4/SPBC29B5.02c	rpl26/SPBC29B5.03c
2072	E		2051	2051	2031		ars2002	1589875.5	1590125.5	+	kap1/SPBC28F2.10c	SPBC28F2.11
2073	E			2053				1656875.5	1656875.5	+	SPBC21B10.09	SPBC21B10.08c
2074	E			2054				1667625.5	1668375.5	+	nrf1/SPBC21B10.04c	SPBC21B10.03c
2075	E'							1683375.5	1683125.5	+	ubp11/SPBC1902.04c	ran1/SPBC19C2.05
2076	E			2055	2033	2038		1707875.5	1708375.5	+	SPBC2F12.15c	gua1/SPBC2F12.14c
2077	E			2056	2033	2038		1718875.5	1718375.5	+	SPBC2F12.12c	rep2/SPBC2F12.11c
2078	E				2034	2039		1752125.5	1750625.5	+	SPBC1D7.03	scr1/SPBC1D7.02c
2079	E			2058	2035	2040		1780375.5	1780125.5	+	sce3/SPBC18H10.04c	SPBC18H10.05
2080	E			2059	2036	2041		1807625.5	1806875.5	+	SPBC18H10.18c	SPBC18H10.19
2081	L	Yes	2062	2060		2042		1869875.5	1869875.5	+	mug142/SPBC3H7.09	SPBC3H7.08c
2082	E				2037			1894625.5	1894625.5	-	spo14/SPBP16F5.01c	mcs2/SPBP16F5.02
2083	E			2061		2044		1943375.5	1943875.5	+	pab2/SPBC16E9.12c	ksp1/SPBC16E9.13
2084	E			2062	2039			1954625.5	1955125.5	+	SPBC16E9.16c	rem1/SPBC16E9.17c
2085	E			2063	2039			1965625.5	1965875.5	+	SPBC1E8.03c	Tf2-10-pseudo/SPBC1E8.04
2086	E		2063	2064	2040	2046		2025625.5	2024875.5	+	SPBP23A10.11c	SPBP23A10.12
2087	E		2065	2066	2041	2047		2053625.5	2053875.5	-	SPBC29A3.07c	pof4/SPBC29A3.08
2088	L		2066	2067		2048		2071875.5	2071625.5	-	SPBC29A3.16	gef3/SPBC29A3.17
2089	L	Yes	2067					2106375.5	2108625.5	-	nil1/SPBC23G7.04c	sui1/SPBC23G7.05
2090	L	Yes						2112625.5	2112375.5	+	SPBC23G7.07c	rga7/SPBC23G7.08c
2091	E	Yes	2068	2068	2042	2049	pARS758/ORI 75	2119625.5	2119375.5	+	matmc_2/SPBC23G7.09	SPBC23G7.10c
2092	E		2069/2070	2069		2050		*	2131125.5	+	rpp202/SPBC23G7.15c	matmi_1/SPBC1711.01c
2093	E							2134125.5	2134375.5	+		
2094	E		2071	2070				2139625.5	2139125.5	+	matmc_1/SPBC1711.02	SPBC1711.03
2095	E			2072				2178875.5	2178875.5	+	nup85/SPBC17G9.04c	cyp6/SPBC17G9.05

2096	E		2072	2073	2044	2051	" AT2072	2188625.5	2187625.5	+	csx2/SPBC17G9.08c	tif213/SPBC17G9.09
2097	E		2073	2075	2045	2054		2247875.5	2247875.5	+	SPBC15C4.04c	SPBC15C4.05
2098	L	Yes			2046	2055		2267125.5	2267625.5	+	SPBC21H7.06c	his5/SPBC21H7.07c
2099	E		2074	2076	2047	2056		2320625.5	2320875.5	+	trx2/SPBC12D12.07c	ned8/SPBC24C6.01c
2100	L	Yes				2057		2340125.5	2341125.5	+	SPBC24C6.09c	SPBC24C6.10c
2101	L	Yes	2075					2412875.5	2412375.5	+	mex67/SPBC1921.03c	SPBC1921.04c
2102	E		2076	2080	2049	2059		2445375.5	2445125.5	+	ucp3/SPBC21D10.05c	fmx1/SPBC12C2.13c
2103	E			2081				2525375.5	2525375.5	+	SPBC365.14c	alp4/SPBC365.15
2104	E							2532875.5	2532875.5	+	alp4/SPBC365.15	SPBC365.16
2105	E		2078	2082				2554875.5	2554875.5	+	SPBC29A10.07	SPBC29A10.08
2106	L	Yes	2080		2052	2063	AT2080	2582875.5	2583125.5	+	SPBC2G5.02c	SPBC2G5.03
2107	E		2081	2083				2595625.5	2595625.5	+	rpc25/SPBC2G5.07c	SPBC25B2.01
2108	L							2614625.5	"	+	SPBC25B2.08	SPBC25B2.09c
2109	L	Yes						2649875.5	2650125.5	+	SPBC6B1.08c	SPBC6B1.12c
2110	E		2084	2087		2066		2704875.5	2703625.5	+	mrpl39/SPBC4F6.08c	str1/SPBC4F6.09
2111	E		2085	2088				2740625.5	2740375.5	+	SPBC336.02	efc25/SPBC336.03
2112	E		2086	2091	2055	2068	tug1	2793125.5	2792375.5	+	gpx1/SPBC32F12.03c	tug1/SPBC32F12.04
2113	E		2087	2092			rum1	2801375.5	2801375.5	+	duo1/SPBC32F12.08c	rum1/SPBC32F12.09
2114	L	Yes	2088			2069	pARS745	2829875.5	2830125.5	+	SPBC19C7.04c	SPBC19C7.05
2115	E	Yes	2089	2093		2070	pARS772	2903125.5	2902375.5	+	SPBP4H10.14c	SPBP4H10.15
2116	L	Yes						2911875.5	"	-	SPBP4H10.18c	SPBP4H10.19c
2117	E		2091	2094	2057	2071		2941125.5	2940875.5	+	ubp9/SPBC1703.12	SPBC1703.13c
2118	E		2092	2095	2058	2072		2988875.5	2988625.5	+	SPBC2D10.11c	rhp23/SPBC2D10.12
2119	L		2094	2096		2073		3054125.5	3053875.5	+	SPBC13E7.06	SPBC13E7.07
2120	L	Yes	2095	2098	2060	2075		3099875.5	3099375.5	+	zuo1/SPBC30D10.01	rap1/SPBC1778.02
2121	L	Yes						3163375.5	3163875.5	+	SPBC609.01	ptn1/SPBC609.02
2122	E		2097	2100		2078		3177875.5	3177875.5	+	dis2/SPBC776.02c	SPBC776.03
2123	E		2100	2102		2080		3288875.5	3289125.5	+	SPBC20F10.02c	SPBC20F10.03
2124	E			2103		2082		3339125.5	3339625.5	+	SPBC17D1.05	dbp3/SPBC17D1.06
2125	E		2102	2104		2083		3363375.5	3363125.5	+	SPBC11C11.12	rpl1807/SPBC11C11.07
2126	L	Yes	2103				pARS727	3381125.5	3381125.5	+	SPBC3B8.08	dsd1/SPBC3B8.07c

2127	L		2104					3410125.5	3410125.5	+	ptr2/SPBC13A2.04c	SPBC4B4.01c
2128	E		2105	2106	2063	2084		3423875.5	3424125.5	+	smg1/SPBC4B4.05	vps25/SPBC4B4.06
2129	E			2107	2064	2085		3468375.5	3468375.5	+	SPBC2G2.16	SPBC2G2.17c
2130	E		2107	2108				3489875.5	3489625.5	+	zfs1/SPBC1718.07c	SPBPB7E8.01
2131	E							3493125.5	3493125.5	+		
2132	L							3503875.5	3504125.5	-	SPBPB7E8.02	SPBC1105.01
2133	E				2065	2086		3512875.5	3511875.5	+	mrpl16/SPBC1105.03c	cbp1/SPBC1105.04c
2134	E			2109				3515125.5	3515125.5	+	cbp1/SPBC1105.04c	exg1/SPBC1105.05
2135	E	Yes'	2108	2110	2066	2087		3558375.5	3558375.5	+	SPBC887.09c	mcs4/SPBC887.10
2136	E				2067	2088		3599125.5	3599125.5	+	dna2/SPBC16D10.04c	mok13/SPBC16D10.05
2137	E		2110	2111				3607125.5	3607375.5	+	mok13/SPBC16D10.05	SPBC16D10.06
2138	E		2111	2112	2068	2089		3636875.5	3636875.5	+	SPBP8B7.01c	SPBP8B7.02
2139	L	Yes						3703125.5	3705125.5	+	puc1/SPBC19F5.01c	SPBC19F5.02c
2140	E	Yes	2114	2115		2092		3722875.5	3722375.5	+	mcm7/SPBC25D12.03c	suc22/SPBC25D12.04
2141	E		2115	2117	2069	2093		3765125.5	3764375.5	+	sar1/SPBC31F10.08c	SPBC31F10.07
2142	L							3779375.5	3779375.5	+	hip1/SPBC31F10.13c	hip3/SPBC31F10.14c
2143	L			2118	2070	2094		3804125.5	3804125.5	-	SPBC21C3.02c	SPBC21C3.03
2144	E			2119				3816875.5	3817125.5	+	SPBC21C3.10c	SPBC21C3.11
2145	E		2116	2121	2071	2095		3840875.5	3840875.5	+	SPBC23E6.01c	SPBC23E6.02
2146	E		2119	2123	2072	2098		3917875.5	3918125.5	+	SPBC1604.09c	imp1/SPBC1604.08c
2147	E							3928125.5	3928625.5	+	SPBC1604.04	SPBC1604.03c
2148	E		2120	2124	2073	2099		3940125.5	3940875.5	+	SPBC1677.03c	thi2/SPBC26H8.01
2149	L	Yes						3976125.5	3977375.5	+	dis3/SPBC26H8.10	SPBC26H8.11c
2150	L	Yes						3985875.5	3986875.5	+	SPBC26H8.12	ste11/SPBC32C12.02
2151	E		2123	2125	2076	2101		4021125.5	4021375.5	-	nup120/SPBC3B9.16c	isa2/SPBC3B9.17
2152	L			2126				4033375.5	4032125.5	+	gil11/SPBC215.04	gpd1/SPBC215.05
2153	L							4035625.5	4035125.5	+		
2154	L	Yes	2125		2078	2104		4109375.5	4109375.5	+	SPBC56F2.06	SPBC56F2.05c
2155	L				2079			4131125.5	4131125.5	+	cnp3/SPBC1861.01c	abp2/SPBC1861.02
2156	L		2128	2129	2081	2107		4204875.5	4204875.5	+	alg6/SPBC342.01c	SPBC342.02
2157	E			2130				4228125.5	4228125.5	+	SPBC16G5.07c	trp4/SPBC16G5.08

2158	E	Yes*		2131	2082	2108		4238625.5	4238625.5	+	top3/SPBC16G5.12c	SPBC16G5.13
2159	L	Yes				2109		4253625.5	4253875.5	+	erg24/SPBC16G5.18	SPBC16G5.19
2160	L	Yes	2129	2132		2110		4294125.5	4294625.5	+	rsm25/SPBC16A3.04	lyn1/SPBC16A3.03c
2161	L	Yes						4345875.5	4346125.5	+	rpt1/SPBC16C6.07c	qcr6/SPBC16C6.08c
2162	E		2130	2133	2083	2111		4361875.5	4362125.5	-	SPBC244.02c	sid4/SPBC244.01c
2163	L	Yes				2113		4413125.5	4414125.5	+	SPBC1289.13c	SPBC1289.14
2164	L		2131	2135	2084	2114		4421875.5	4421875.5	+	Tf2-11/SPBC1289.17	SPBC1289.15
2165	L							4427875.5	4427875.5	+	SPBC1289.15	SPBC1289.16c
2166	E		2132	2136				4442375.5	4442125.5	+	SPBC8E4.03	SPBC8E4.02c
2167	L		2133	2137		2115		4453125.5	4453375.5	+	pho1/SPBP4G3.02	SPBP4G3.03
2168	L					2115		4456125.5	*	+	SPBP4G3.03	SPBPB2B2.01
2169	L							4458875.5	*	-		

Chromosome III

Ori Number	Class	Cds1 Suppression	Bioinfo Number (Segurado *et al.*)	ORIs Number (Heichinger *et al.*)	ORF Microarray Number (Feng *et al.*)		ARS/2D-gel Number (Segurado *et al.*)	Map Position (bp)		Orc4 localization	5' Gene/ORF	3' Gene/ORF
					wt (HU)	Δcds1 (HU)		Orc1	Mcm6			
3001	E		3002	3001	3001	3001		35375.5	35375.5	+	SPCP20C8.03	SPCC1884.01
3002	E		3003	3004		3003		76375.5	76625.5	+	SPCC757.12	SPCC757.13
3003	E		3005	3007	3003	3004	ars3002/3004	123875.5	122875.5	+	SPCC330.07c	alg11/SPCC330.08
3004	E			3008				188125.5	189125.5	+	fft2/SPCC1235.05c	sif1/SPCC1235.06
3005	E		3006	3009	3004	3006		206875.5	207875.5	+	ght8/SPCC1235.13	ght5/SPCC1235.14
3006	E		3007	3010				232125.5	231875.5	+	SPCC548.08c	ght1/SPCC548.07c
3007	E		3009	3012		3007		254125.5	253875.5	+	SPCC794.04c	SPCC794.8
3008	E			3013				279375.5	278125.5	-	mae2/SPCC794.12c	SPCC794.15
3009	E		3010	3014		3008		286375.5	286625.5	+	SPCC553.10	spb70/pol12
3010	E			3015	3006			305875.5	305875.5	-	SPCC553.03	SPCC553.02
3011	E							347625.5	347625.5	+	dis1/SPCC736.14	SPCC736.15
3012	E		3012	3017	3008	3010		370125.5	370375.5	+	SPCC594.07c	qcr9/SPCC1682.01
3013	E		3013	3018	3009	3011		398125.5	398125.5	+	ubp16/SPCC1682.12c	SPCC1682.13
3014	E		3015	3020				505625.5	505625.5	+	SPCC970.06	rpl3601/SPCC970.05
3015	E		3016	3021	3011	3013		518625.5	518875.5	+	rad16/SPCC970.01	prp11/SPCC10H11.01
3016	E		3017	3024				565625.5	565625.5	+	sap1/SPCC1672.02c	SPCC1672.03c
3017	E		3018	3025	3012	3014		575125.5	575125.5	+	asp1/SPCC1672.06c	SPCC1672.07
3018	E			3026				605625.5	605375.5	-	ung1/SPCC1183.06	SPCC1183.07
3019	E		3019	3028	3014	3015		643125.5	643125.5	+	taf72/SPCC5E4.03c	cut1/SPCC5E4.04
3020	E		3020	3029		3016		666125.5	666125.5	+	pin1/SPCC16C4.03	SPCC16C4.04
3021	E		3021	3030	3015	3017		720125.5	720125.5	+	SPCC18B5.02c	wee1/SPCC18B5.03
3022	E		3022	3031	3016	3018		764125.5	764125.5	+	oca2/SPCC1020.10	SPCC1020.09
3023	E		3023					826875.5	827875.5	+	SPCC1393.13	SPCC2H8.02
3024	E				3018	3020		847875.5	847875.5	-	SPCC63.06	SPCC63.07
3025	E		3024	3033				853625.5	853625.5	+	ppk36/SPCC63.08c	SPCC63.10c
3026	E		3025	3035	3019	3022		936375.5	936875.5	+	SPCC24B10.19c	SPCC24B10.20
3027	E		3026	3036	3020	3023		966375.5	967875.5	+	SPCC1795.13	SPCC1795.12c
3028	E							971125.5	971375.5	+		
3029	E			3037				986125.5	985875.5	+	SPCC1795.07	map2/SPCC1795.06
3030	L	Yes	3027	3038		3025		1039625.5	1039625.5	+	SPCC1259.02c	rpa12/SPCC1259.03
3031	E			3041				1066125.5	1065875.5	+	meu27/SPCC1259.14c	centromere
3032	E			3042	3021	3026		1141875.5	1142125.5	+	centromere	SPCC4B3.18
3033	E		3039	3044	3024	3028		1254125.5	1254125.5	+	snd1/SPCC645.08c	mrpl37/SPCC645.09
3034	E		3040	3045	3025	3030		1324125.5	1323875.5	+	rpl3402/SPCC1322.15	SPCC1322.16
3035	E			3046	3026	3031		1343375.5	1343375.5	+	SPCC338.18	rad21/SPCC338.17c
3036	E		3042	3047	3027	3032		1371875.5	1371125.5	+	SPCC338.02	ags1/SPCC1281.01
3037	E							*	1373875.5	+		
3038	E				3028	3033		1393625.5	*	-	rsc7/SPCC1281.05	SPCC1281.06c
3039	E			3048				1396875.5	1396875.5	+	SPCC1281.06c	SPCC1281.07c
3040	E		3043	3049			AT3043	1411125.5	1411375.5	+	SPCC622.07	hta1/SPCC622.08c
3041	E		3044	3050		3034	AT3044	1417875.5	1417875.5	+	SPCC622.10c	SPCC622.11
3042	E		3045	3051	3029	3035		1449125.5	1449125.5	+	SPCC61.04c	SPCC61.05
3043	E		3046	3052	3031	3036		1511875.5	1511875.5	+	dcr1/SPCC584.10c	SPCC584.11c
3044	E					3037		1524875.5	1524875.5	+	SPCC584.15c	SPCC584.16c
3045	E		3047	3053		3037		1532625.5	1532125.5	+	SPCC584.01c	cuf2/SPCC584.02
3046	E			3054		3038		1556375.5	1556375.5	+	SPCC162.12	SPCC162.11c

3047	E			3055		3039		1576875.5	1576625.5	+	ent1/SPCC162.07	SPCC162.06c
3048	E		3048	3056				1595375.5	1595125.5	+	SPCC13B11.02c	SPCC13B11.03c
3049	E		3049	3057	3032	3040		1609875.5	1609875.5	+	SPCC777.06c	SPCC777.07
3050	E							1672875.5	1672875.5	+	dad5/SPCC417.02	SPCC417.03
3051	E							1675875.5	1675625.5	+	SPCC417.04	chr2/SPCC417.05c
3052	E							1680625.5	1680625.5	+	ppk35/SPCC417.06c	mto1/SPCC417.07c
3053	E		3051	3059	3035	3041		1687125.5	1685125.5	+	mto1/SPCC417.07c	tef3/SPCC417.08
3054	E		3052	3060	3035	3041		1690125.5	1690625.5	+	tef3/SPCC417.08	SPCC417.09c
3055	E		3053	3061	3036	3042	AT3053	1720125.5	*	+	SPCC191.08	gst1/SPCC191.09c
3056	E				3036	3042		*	1723375.5	+	SPCC191.10	inv1/SPCC191.11
3057	E		3054	3062				1728625.5	1728875.5	+	SPCC1450.01c	SPCC1450.02
3058	E			3063	3037	3043		1754625.5	1754875.5	+	cek1/SPCC1450.11c	SPCC1450.12
3059	E							1815375.5	1814625.5	+	cgs2/SPCC285.09c	SPCC285.10c
3060	E		3055	3064	3038	3044	ORI c11	1823125.5	1823125.5	+	SPCC285.13c	SPCC285.14
3061	E		3056	3065			nmt1	1838375.5	1838625.5	+	SPCC1223.01	nmt1/SPCC1223.02
3062	E		3057	3065	3039	3045	AT3057	1845375.5	1845375.5	+	gut2/SPCC1223.03c	SPCC1223.04c
3063	E							1861375.5	1860625.5	+	SPCC1223.09	SPCC1223.10c
3064	E		3058	3066		3046		1868125.5	1868375.5	+	ptc2/SPCC1223.11	meu10/SPCC1223.12c
3065	E							1878625.5	1879125.5	-	SPCC297.01	ssp1/SPCC297.03
3066	E				3040	3047		1922625.5	1923625.5	+	SPCC74.09	sly1/SPCC74.01
3067	E		3059	3068	3040	3047		1930125.5	1929875.5	+	SPCC74.02c	ssp2/SPCC74.03c
3068	E							1937375.5	1936125.5	+	ssp2/SPCC74.03c	SPCC74.04
3069	E			3069	3041	3048		1969375.5	1969625.5	+	SPCC18.06c	rpc53/SPCC18.07
3070	E		3060	3072	3042	3049		2036375.5	2036375.5	+	SPCC1739.04c	set5/SPCC1739.05
3071	E							*	*	+	set5/SPCC1739.05	SPCC1739.06c
3072	E							2042625.5	*	+	SPCC1739.07	SPCC1739.08c
3073	E							2046375.5	2046625.5	+	SPCC1739.08c	cox13/SPCC1739.09c
3074	E				3043	3050		2064375.5	2064625.5	+	npp106/SPCC1739.14	wtf21/SPCC1739.15
3075	E			3073				2068625.5	2068625.5	+	wtf21/SPCC1739.15	amt1/SPCPB1C11.01
3076	E							2072375.5	2072875.5	+	amt1/SPCPB1C11.01	SPCPB1C11.02
3077	L							2076375.5	2076625.5	+	SPCPB1C11.02	SPCPB1C11.03

3078	E		3062	3074	3044	3051	pARS744	2108375.5	2108375.5	+	ksg1/SPCC576.15c	wtf22/SPCC576.16c
3079	E		3064	3077	3047	3053		2201875.5	2201875.5	+	SPCC830.09c	SPCC830.10
3080	E							2258375.5	2258625.5	+	bgs4/SPCC1840.02c	sal3/SPCC1840.03
3081	E		3065	3079	3049	3054		2277125.5	2277125.5	+	SPCC1840.09	lsm8/SPCC1840.10
3082	E			3080		3055		2300875.5	2301375.5	+	alr1/SPCC965.08c	SPCC965.09
3083	L	Yes	3066					2309625.5	2309625.5	+	SPCC965.12	SPCC965.13
3084	E		3068	3083	3051	3058		2383625.5	2383375.5	+	SPCC1827.03c	SPCC1827.04

Legend and Comments

Ori number: Replication origins identified as pre-RC sites in this study; the first digit indicates the chromosome number (1-3).
Class: Activity of origins determined by BrdU incorporation in the presence of HU (see online materials); E, Early origin (red column); L, Late and/or inefficient origin (blue column).
Cds1 suppression: Origins suppressed by Cds1-dependent checkpoint in the presence of HU (see online materials).
Bioinfo Number: AT-rich island number (Segurado et al., 2003).
ORIs Number: Origins defined by the increase in DNA content (Heichinger et al., 2006). Location of each ORI was compared with our origins by its peak and flanking ORF position.
ORF Microarray Number: Origins defined by the increase in ssDNA content in the presence of HU (Feng et al., 2006). 5-kb deviation, which corresponds to fork movement in the presence of HU, from the original peak position was allowed.
ARS/2D-gel Number: Name of ARS or origins identified by ARS analyses and 2D-gel analyses (summarized in Segurado et al., 2003).
Map Position: The peak position of Orc1 and Mcm6 signals (see online materials).
Orc4 localization: A "+" and "-" indicates that significant signal of Orc4 was detected or not, respectively (see online materials).
5' Gene/ORF, 3' Gene/ORF: The name of the 5' gene/ORF or 3' gene/ORF flanking the region containing the pre-RC site.

#: A significant but faint signal of BrdU was detected.
*: A peak was not programatically picked up, although significant localization of Orc1 or Mcm6 was detected.